CHARACTERIZATION OF NOVEL SMALL REGULATORY RNAs IN *Borrelia burgdorferi* AND THEIR ROLE IN LYME DISEASE PATHOGENESIS

A Dissertation

by

DIANA NATALIE MEDINA

Submitted to the Office of Graduate and Professional Studies of
Texas A&M University
in partial fulfillment of the requirements for the degree of

DOCTOR OF PHILOSOPHY

Chair of Committee, Jon T. Skare
Committee Members, James Samuel
Helene Andrews-Polymenis
Joseph A. Sorg
Head of Department, David Threadgill

December 2019

Major Subject: Genetics

ABSTRACT

The causative agent of Lyme disease *Borrelia burgdorferi,* is maintained in nature in an enzootic cycle involving a tick vector and a mammalian host. In order to cycle between two vastly different hosts*, B. burgdorferi* tightly regulates its gene expression by sensing environmental cues. In bacteria, small regulatory RNAs (sRNAs) have emerged as post-transcriptional regulators of genes associated in different cell processes such as chemotaxis, metabolism and virulence. The sRNAs bind to transcripts and affect their translation and/or stability, thus, modulating and fine-tuning gene expression. Recently, in *B. burgdorferi,* a repertoire of sRNAs has been identified and a significant number of them are differentially expressed at temperatures *in vitro* that mimic the tick vector or mammalian host, suggesting a potential role in the enzootic cycle.

In this work, we tested the role of seven putative sRNAs of *B. burgdorferi* in the experimental mouse model of infection. Of those, two were further examined in more detail. The genetic inactivation of the sRNA in between the gene *bbd04* and the pseudogene *bbd05a* of linear plasmid 17 (lp17), designated SR0725, was dispensable for borrelial mouse infection. However, the genetic inactivation of the sRNA between the genes *bbd18* and *bbd21* of linear plasmid 17 (lp17)*,* denoted SR0736, resulted in an attenuated phenotype in the mouse model. RNA-seq studies revealed 19 dysregulated transcripts in the sRNA mutant strain compared to the parent. Global proteomics and western blot analysis revealed two proteins were significantly less abundant in the sRNA mutant than in the parent. Taken together,

this study describes a novel *trans*-acting sRNA potentially involved in post-transcriptional regulation of multiple genes by stabilizing transcripts and/or targeting mRNAs for degradation in *B. burgdorferi.* Our work highlights the importance of a *trans*-acting sRNA for optimum infection in the Lyme disease spirochetal bacterium, *Borrelia burgdorferi.*

DEDICATION

To my parents, for their endless love, support, encouragement and sacrifices.

ACKNOWLEDGEMENTS

First and foremost, I would like to express my deepest gratitude to my committee chair Dr. Jon T. Skare for all his support, guidance and patience throughout the years. Thank you for being an excellent mentor. I could have not asked for a better PhD advisor and for this, I will always be grateful. I will like to thank my committee members, Dr. James Samuel, Dr. Helene Andrews-Polymenis and Dr. Joseph A. Sorg for their valuable insights and guidance throughout the course of my PhD. Thank you to Dr. Meghan Lybecker, Dr. Hyde, Dr. Linden Hu, Dr. Tao Lin, Dr. Steve Norris and Dr. Erin Troy for their guidance, suggestions and collaboration in my PhD project. Thank you to Dr. Dana Shaw and Dr. Jenny Hyde for initially training me in *Borrelia burgdorferi* work and for being role models and mentors. I wish to extend my gratitude to excellent undergraduate students that were critical in my research progress, Lauren Weise, Parmida Tehranchi and Kristen Sanchez. Thanks to the Skare lab former and present members for their help in experimental design, suggestions, helpful critiques and for being my lab family.

Thank you to the Interdisciplinary Graduate Program in Genetics at Texas A&M University for all their help with the steps necessary to progress and culminate my PhD. I will also like to acknowledge the TAMUS AGEP program and Isah Juranek for providing me with professional development opportunities and tools that made the PhD road smoother. Thank you to my colleagues and faculty of the Microbial Pathogenesis and Immunology department for their support. I wish to give thanks to the administrative staff, Paula McCarver, Monica Ocon, LeeAnn Nichols

and Norma Jones, for being so helpful and assisting me in multiple ways throughout my graduate student life.

I would like to thank my parents, Ana Maldonado Ceja and Ulises Medina Pérez, for being my biggest cheerleaders during my PhD and for teaching me the value of education. I express my sincere and wholehearted thanks to my husband Sergio J. Pérez Ruiz, for his love and support throughout my PhD. Thank you my love for being my rock and for always believing in me even when I didn't believe in myself. This would have not been possible without you by my side.

Finally, I would like to thank my closest friends Alicia Hernández, Nathalie Ayala and Lumariz Hernández for their words of encouragement in moments of crisis. Thank you to my graduate school buddies Carolina Mantilla Rojas, Sara Talmage, Selene Howe, Wilmarie Marrero Ortiz, Keishla Ortiz López, Dona Kanavy and Leah Saputra for being my support system and making my time at Texas A&M University a wonderful experience.

CONTRIBUTORS AND FUNDING SOURCES

Contributors

This work was supported by a dissertation committee consisting of Professor Jon. T Skare [advisor, committee chair], Professors James Samuel and Helene Andrews-Polymenis from the Department of Microbial Pathogenesis and Immunology, and Professor Joseph A. Sorg from the Department of Biology.

The RNA-seq experiment found in Chapter III was performed by Texas A&M Institute for Genome Sciences & Society (TIGSS). The University of Texas Southwestern Proteomics core performed the Tandem Mass Tags (TMT) experiment in Chapter III. Tn-seq experiment was done by Dr. Linden Hu from Tufts University for Chapter III. The small RNA library in *Borrelia burgdorferi* was performed by Dr. Meghan Lybecker in University of Colorado, Colorado Springs for Chapter III.

All other work conducted for the dissertation was completed by the student independently.

Funding Sources

This work was supported in part by a Graduate Diversity Excellence Fellowship from Texas A&M University, as well as a Genetics Fellow Award from the Program in Genetics at Texas A&M University. This work was funded by Public Health Service Grants R01-AI042345, R21-AI123672 and R01-AI131656 (to JTS).

NOMENCLATURE

CDC	Centers for Disease Control and Prevention
EM	Erythema Migrans
PLDS	Post-Treatment Lyme Disease Syndrome
ORFs	Open Reading Frames
TCS	Two Component System
DMC	Dialysis Membrane Chamber
sRNA	Small regulatory RNA
RBS	Ribosomal Binding Site
IG	Intergenic
Tn	Transposon
TMT	Tandem Mass Tags

TABLE OF CONTENTS

LIST OF FIGURES

LIST OF TABLES

CHAPTER I

INTRODUCTION AND LITERATURE REVIEW

Discovery of Lyme disease

In 1975, in Lyme, Connecticut, USA, fifty-one residents, composed of adults and children, displayed a similar type of arthritis (1). Initially, the children were misdiagnosed with juvenile rheumatoid arthritis (1). Approximately one quarter of the patients had developed an expanding, annular skin lesion weeks before the onset of arthritis (1). Similar skin lesions had been reported previously in Europe and thought to be transmitted by an infectious agent through the bite of the sheep tick, *Ixodes ricinus* (1). After substantial investigations by infectious disease specialists, public health officials, microbiologists, and entomologists, the cause of a seasonal arthritis was found associated with a spirochetal bacterium from the North American deer tick, *Ixodes scapularis* in 1982 (2). Subsequent studies recovered Lyme disease-associated spirochetes from skin, blood, and cerebrospinal fluid specimens (3,4). DNA-DNA hybridizations determined the causative agent of Lyme disease to be a new species within the genus *Borrelia* and was named *Borrelia burgdorferi,* after its co-discover Willy Burgdorfer (5).

Lyme Disease is the most common vector-borne disease in North America and Europe (6). Lyme disease spirochetes are widely distributed in temperate regions of the Northern hemisphere, specifically in North America, Europe, and Asia, in which infected wildlife and ticks are prevalent (7,8). Approximately 30,000 cases are confirmed to the Centers for Disease Control and Prevention (CDC) each year

in the United States, but it is believed that the number of diagnosed cases is as high as 329,000 cases (9–11). Thus, Lyme disease is a significant public health issue.

Lyme disease causing spirochetes

The causative agent of Lyme disease, *Borrelia burgdorferi,* belongs to the bacterial phylum Spirochaetes (7,12). Long, serpentine morphology with inner and outer membrane surrounding periplasmic flagella is the signature feature of the phylum (13). Members of the phylum are found to live in marine sediments, soil, guts of arthropods and vertebrates as obligate parasites (7,14). The genus *Borrelia* is member of the family Spirochaetaceae, this genus include two major phylogenetic groups of pathogenic bacteria, the etiological agents of Relapsing Fever (RF) and Lyme Disease (14,15). Phylogenetic analyses have led to the division of Lyme disease spirochetes into multiple species, collectively known as *Borrelia burgdorferi sensu lato* (*s.l.*) (7). From the *sensu lato (s.l.)* complex of 21 genospecies, 18 are named spirochetes and 3 remain unnamed (16,17). Three genospecies predominate as human pathogens causing Lyme borreliosis (LB), notably *Borrelia burgdorferi sensu stricto* (*s.s.*) in the United States and Western Europe, as well as *Borrelia garinii* and *Borrelia azfelii* in Eurasia (6,7).

Manifestation and Treatment of Lyme disease

Spirochetes are deposited into the dermis of the host together with the saliva of an infected tick during the blood meal (7,12). Infection rarely occurs during the first 24 hours of tick feeding, but becomes increasingly likely after the tick has been

attached from 36 to 48 hours or longer to the host (7). The tick remains attached to the host during feeding for approximately 4-5 days (7). Thus, early removal of ticks is generally seen as an effective means to limit Lyme borreliosis.

Lyme disease is a multi-stage disorder which consists of stage 1, a localized infection to the dermis, followed by days or weeks by stage 2, a disseminated infection, followed by month to years later by stage 3, a persistent, chronic, and difficult to treat disease (18,19). In localized infection, after the incubation period of 3-32 days, a painless, expanding skin lesion termed Erythema Migrans (EM) develops in 70-80% of cases in North America, near to the area of the tick bite (18,20). Often the EM develops a clearing as it enlarges giving it a “bulls eye” appearance, but in many instances the lesion is in the form of a red band. The identification of the EM is an important sign that allows for rapid diagnosis of Lyme disease in endemic areas but, unfortunately, this feature is not seen in all patients (17,18). The expansion of the EM lesion is presumed to be associated with the migration of spirochetes in an outward direction from the tick bite site (21). Antibiotic therapy at the early stages of infection, e.g., when a patient is displaying EM, is highly effective (18,19).

In the U.S., EM is frequently accompanied by flu-like symptoms, such as malaise and fatigue, headache, mild stiff neck, arthralgias, myalgias, and fever (18,20). Within days to weeks after initial tick bite, the infection progresses to the second stage characterized by disseminated disease (19,22). Dissemination of *B. burgdorferi* occurs via the bloodstream, lymphatic system, and tissue invasion (7,22). During this phase, *B. burgdorferi* binds to host proteins and adheres via

interactions with integrins, proteoglycans, or glycoproteins on host cells or tissue matrices (7,20,23). This initial site of colonization likely serves as a base for replication and subsequent dissemination of *B. burgdorferi* to deeper tissues. The result of this event may lead to secondary annular skin lesions, musculoskeletal, cardiac, and neurologic symptoms (19,24). Asymptomatic infection may occur, but at this stage is not common (20,25).

If left untreated, Lyme disease can progress to a persistent or chronic phase. Late manifestations of Lyme disease include debilitating neurological symptoms, chronic fatigue, and what has been designated as “treatment resistant” Lyme arthritis (20,26–29). A small percentage of patients, approximately 10%, develop post-treatment Lyme disease syndrome (PLDS), in which symptoms can persist for months or years even following oral and intravenous antibiotic therapy for 2 or 3 months (30,31).

The recommended treatment for Lyme disease includes doxycycline, amoxicillin, or cefuroxime axetil, for 14-21 days for early or disseminated infection (32). For hospitalized individuals or patients with PLDS, a combination of oral and intravenous antibiotics is recommended (32). Currently, there is no available vaccine against Lyme disease. As such, the best line of defense against Lyme disease is to prevent the initial *B. burgdorferi* infection by rapid removal of the tick, or if presumed to be infected, to receive antibiotic treatment soon after transmission.

The enzootic life cycle of *B. burgdorferi*

In nature, *B. burgdorferi* is maintained in an enzootic cycle between a tick vector and a vertebrate host (7,12). *B. burgdorferi* is transmitted by four hard-bodied ticks from the *Ixodes ricinus* complex: *I. scapularis* and *I. pacificus* in eastern and western North America, respectively, *I. ricinus* in Europe, and *I. persulcatus* (the tiaga tick) in Asia (7). The tick has four stages: egg, larva, nymph and adult. After hatching, the tick takes three blood meals, one as a larva, a second as a nymph and the third as an adult. *I. scapularis* life span generally last 2 years (18). Larvae feed on diverse species of vertebrates, usually small mammals or birds for the first blood meal (7). The white-footed mouse, *Peromyscus leucopus,* is considered to be the main reservoir in the northeastern United States (7). Rodents and birds are the main reservoirs in Europe for *B. afzelii* and *B. garinii,* respectively (7).

The tick larvae hatch uninfected, i.e., no transovarial transmission occurs, and the larvae must acquire *B. burgdorferi* from the blood of an infected reservoir host (7)(Fig. 1). Once *Borrelia* is acquired by an *Ixodes* larval tick, the infection is maintained throughout its life (7) (Fig. 1). After molting into a nymph, the tick will seek another blood meal, whereby *B. burgdorferi* can be transmitted (Fig. 1). The blood meal triggers *B. burgdorferi* to replicate, escape the tick midgut to the hemocoel, and exit through the salivary glands into the mammalian host, completing the enzootic cycle (7,13) (Fig. 1). Humans typically get infected in late spring and early summer months by nymph ticks harboring *B. burgdorferi* (7) (Fig. 1). It is believed that the nymphal stage is the most relevant vector for Lyme disease in humans, since they need a blood meal to molt into an adult, and their small in size,

which means they often go unnoticed. Humans are dead-end host and not part of the natural enzootic cycle (7). Finally, adult tick feed preferentially on large mammals like deer, which do get infected by *B. burgdorferi* but clear the infection, presumably due to potent innate immune killing mechanism, including complement resistance. Deer do serve an important role in the lifecycle as they are the site where adult ticks mate to propagate more *Ixodes* species (7,33).

B. burgdorferi segmented genome and metabolic limitations

In 1997, the *B. burgdorferi* strain B31, originally isolated from a tick collected in Shelter Island, New York, was sequenced (34). It revealed a complex genome consisting of 910,725 base pair linear chromosome and up to 23 circular and linear plasmids, ranging in size from 5 to 56 kb, which contained approximately 600 kilobases of additional genetic material (34,35). Interestingly, the linear replicons have covalently closed telomeres (36). To date, 28 complete and draft genome sequences of Lyme disease spirochetes have been placed in the public database (37,38). The strain B31 genome has a low G+C content (~28%) with most of the housekeeping genes encoded on the chromosome (34). Of all the open reading frames (ORFs) predicted in *B. burgdorferi*, lipoproteins represents 7.8% of the genome (34). A significant number of the lipoproteins are plasmid encoded (34,35). Certain lipoproteins differentially expressed during the enzootic cycle contribute to the pathogenesis of *B. burgdorferi* (7,12,23,39–41).

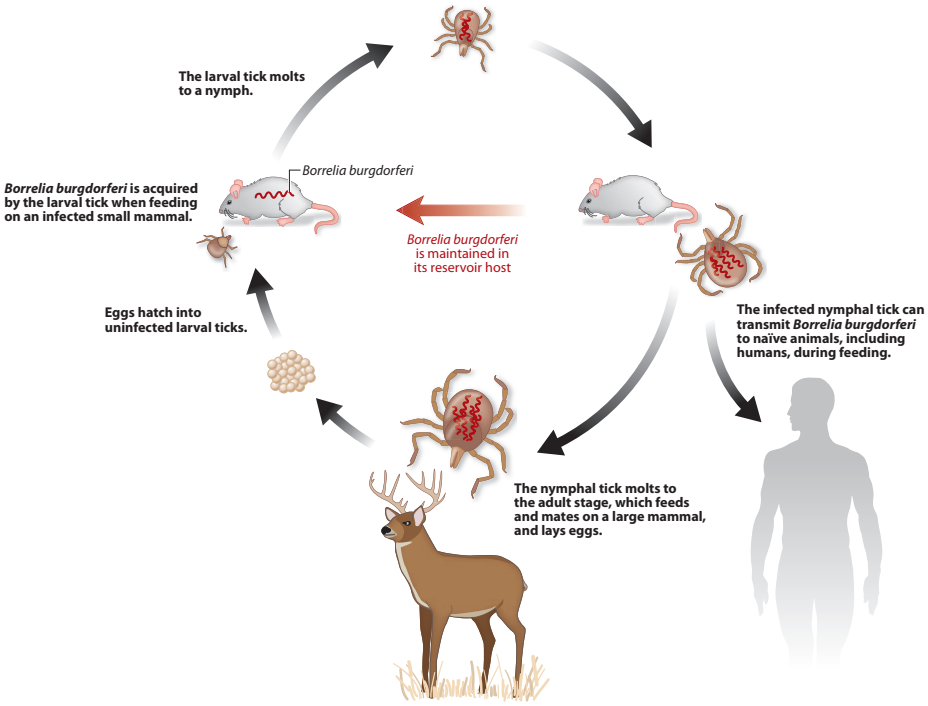

Figure 1. A schematic representation of the *Borrelia burgdorferi* enzootic cycle from Brisson *et al*., 2012. *B. burgdorferi* cycles between ticks of the *Ixodes* genus and a variety of warm-blooded vertebrate hosts. Larvae ticks can become infected with the bacterium when feeding on an infected reservoir. The larva tick molts into nymph and lie dormant through the winter months. Humans are accidental, dead end hosts that typically become infected by the bite of an infected nymph during the spring and summer months. Reprinted with permission from Annual Review of Genetics. Copyright date of August 13, 2019.

B. burgdorferi has limited metabolic capabilities. It lacks machinery for synthesizing nucleotides, amino acids, and fatty acids, reflecting its lifestyle as an obligate parasite (34). Cultivation of *B. burgdorferi in vitro* is achieved by growing in rich undefined media, termed BSK-II (42). Interestingly*, B. burgdorferi* does not seem to require iron and does not encode orthologues for any known iron-requiring metalloproteins (34,43). In addition, it lacks genes encoding enzymes for the tricarboxylic acid cycle and oxidative phosphorylation, deriving energy instead from the fermentation of sugars to lactic acid via the Embden–Meyerhof pathway (32,37). Given these limitations, *B. burgdorferi* survives by scavenging nutrients and metabolites from its hosts.

Cellular architecture of *B. burgdorferi*, motility, and chemotaxis

B. burgdorferi cells are long in length, approximately 10-20 μm and thin in diameter, around 0.3 μm (22,46). *B. burgdorferi* is organized as a Gram-negative organism with an inner and outer membrane (47). One major difference from *B. burgdorferi* outer membrane distinct then a traditional Gram-negative organism is the lack of lipopolysaccharides (LPS) (48). Instead, *B. burgdorferi* has an abundance of diverse outer surface exposed lipoproteins within its outer membrane (23,49). During the initial exposure in the mammal, *B. burgdorferi* lipoproteins are recognized by Toll-like receptor 2 (TLR2) and activate the host immune response in concert with Myd88 (50,51).

In regard to motility, spirochetes are unique in that they contain subsurface flagella, or endoflagella, that mediate their movement. In *B. burgdorferi*, 7-11

endoflagella are present in each cell and are attached to each cell pole, forming molecular ribbons that wrap clockwise around the protoplasmic cylinder (52). Not only do the endoflagella provide motility to *B. burgdorferi*, but they also provide the spirochete with its helical or planar flat-wave morphology (46,53).

Borrelial cells swimming in a single direction is achieved by one endoflagella in one pole moving clockwise and the second endoflagella in the opposite pole moving counterclockwise (22). Reversal of swimming occurs when both endoflagella change direction of rotation (22). When both endoflagella move in a counterclockwise or clockwise rotation, this results in a flex state, similar to the tumble pattern in other bacteria (22).

Motility is essential for *B. burgdorferi* pathogenesis throughout the enzootic cycle. When an infected tick begins feeding on a host, *B. burgdorferi* uses biphasic migration to escape the tick midgut (54). First, the spirochetes move by adhering to the midgut epithelial cells and second, they penetrate the cell junctions to access the hemocoel in a process that requires their endoplasmic flagella (54). After the spirochetes are in the hemocoel, they traffic to the salivary glands and are subsequently deposited in the dermis of the new host (7,55). *B. burgdorferi* uses motility in the mammalian host to disseminate from the site of the tick bite to colonize distant tissue sites such as joints, heart, and lymph nodes (7,22). *B. burgdorferi* disseminate through the extracellular matrices, via the bloodstream and the lymphatic system, resulting in a systemic infection and subsequent disease (22,24,56).

The movement towards a beneficial chemical stimulus or the movement away from a harmful stimulus, is an important chemotactic response in bacteria towards finding the optimum conditions for its survival. The flagellar motors found at both cell poles coordinate the rotation that enables the spirochete to run or flex in response to chemotactic cues (57). Chemotaxis and motility genes represent approximately 6% of the *B. burgdorferi* genome (57). In *B. burgdorferi,* chemotaxis is regulated by a two-component signal transduction pathway that utilizes a membrane-bound chemoreceptor and a methyl-accepting chemotaxis protein (MCP), which interacts with coupling protein CheW and histidine kinase CheA, to form a complex that senses environmental cues (22,46,57). CheA autophosphorylates and transfers its phosphate to three response regulators, CheY1, CheY2 and CheY3 (CheY-P) (34,58). CheY3 is considered the key chemotactic response regulator in *B. burgdorferi* and is needed for full virulence (58,59). CheY3-P interacts with the motor switch proteins of *B. burgdorferi* and controls the rotational direction of the flagellar motors (58,59). Levels of CheY3-P leads to different motility patterns, low concentration of CheY3-P initiates a run motility, meanwhile high CheY3-P concentrations causes *B. burgdorferi* to flex (22).

CheX dephosphorylates CheY-P rapidly reducing CheY-P concentrations (60). CheX is enhanced by forming a complex with CheD (61). Additional genes have been found to be associated with motility and chemotaxis. The hypothetical protein BB0569 has sequence similarity to MCPs, localizes at the cell poles and is essential for chemotaxis (62). In addition, the carbon storage regulator CsrA, is involved in post-transcriptional regulation of flagellar genes (63,64). In contrast to

enteric bacteria, which contain only single copies of the chemotaxis machinery components, *B. burgdorferi* harbors genes for two CheAs, two CheRs, two CheBs, three CheYs and three CheWs (34,46,65).

Differential gene expression in the mammalian host and during tick feeding

B. burgdorferi lives in two distinct and different milieus, the arthropod vector and the mammalian host. The spirochete senses and responds to environmental cues such as temperature, pH, dissolved gases, as well as unidentified host factors, to modulate its gene expression to promote its survival within its hosts (66–76). *B. burgdorferi* encodes three sigma factors: RpoD, RpoS and RpoN (34). Of these, RpoS appears to function in a regulatory role as both a repressor and an activator of gene expression (7,12,77,78). In addition, *B. burgdorferi* encodes two sets of two-component systems (TCS); the first is composed of the sensor histidine kinase Hk2 and the response regulator Rrp2 (79–82). These proteins are required for gene expression that promotes mammalian infection (12,34,76,81,83–85). Although the factors that activate Hk2 remains unclear (77), Rrp2 is activated by phosphorylation (Rrp2-P) and acts as a transcriptional activator for the alternative sigma factor RpoN (81,83), which in turns derepresses *rpoS* (80,82,86–89). RpoS then regulates a battery of genes that allow for the infection of mammalian hosts (7,12,76). This important activity has led RpoS to be referred to as “gatekeeper” that controls the mammalian-specific host adaptive response (7,12,77,78).

The alternative sigma factor RpoS has a complex regulation and is the key virulence regulator in *B. burgdorferi*. The *rpoS* transcript is expressed *in vitro* by

increases in temperature, CO_2, and a decrease in pH, conditions that mimic tick feeding on a blood meal and when *B. burgdorferi* is being transmitted to mammals (67,69,72,73,77,78). In host-adapted *B. burgdorferi,* produced by implanting dialysis membrane chambers (DMC) containing the spirochetes into the peritoneal cavity of rats, a large number of genes are induced and many are regulated by RpoS (67,78), highlighting the importance of RpoS during active infection.

Transcription of *rpoS* requires Rrp2 and the *Borrelia* oxidative stress regulator (BosR) (7,12,90). In addition, the transcript *rpoS* is repressed during *in vitro* conditions that mimic the unfed tick by BadR (91,92). The regulatory Rrp2-RpoN-RpoS cascade promotes the expression of genes required for the mammalian host and represses the genes necessary for the tick vector (12,39,78,87,93,94). RpoS controls the expression of virulence-associated surface expressed lipoproteins such as OspC (Outer surface protein C), as well as the Decorin binding protein A (DbpA), and BBK32 (78,89,95) adhesins. OspC is essential to establish mammalian infection although its virulence-associated function is not known (96,97). DbpA binds to host decorin, found in the extracellular matrix and within connective tissue (23,98,99). BBK32 binds to fibronectin and promotes *B. burgdorferi* attachment to glycosaminoglycans (GAG) (23,100,101). More recently, our laboratory found that BBK32 can also potently inhibit the classical complement pathway (102). DbpA and BBK32 proteins are important for adhesion of host tissues and are necessary for optimal infection in the mammalian host and mutants lacking either *dbpA* or *bbk32* are significantly attenuated for *B. burgdorferi* virulence (39,41,93,103).

The RpoS regulator is required for the activation of *ospC* and, in contrast, represses *ospA* during host adaptation (94). OspA and OspC have been studied extensively in *B. burgdorferi* because of their importance in tick and mammal infection, respectively, and because of their reciprocal expression (89,96,104,105). The *ospA* locus is highly expressed when *B. burgdorferi* is in the tick midgut and is downregulated as the spirochete migrates from the midgut to the salivary glands during a bloodmeal (105,106). OspA is essential for *Ixodes* colonization and survival within the tick midgut (23,105) where it binds to tick receptor, designated TROSPA (107,108). In contrast, OspC is upregulated during tick feeding (106) and is essential to establish early infection (96,97,104). The *ospA*/*ospC* regulatory dichotomy is one example of a genetic switch that *B. burgdorferi* employs when transiting between tick and mammal.

Both larval and nymphal blood meals stimulate the second two component system (TCS) in *B. burgdorferi* consisting of a sensor histidine kinase, Hk1, and the response regulator, Rrp1 (34). Hk1 has two periplasmic sensor domains, D1 and D2, a conserved cytoplasmic histidine kinase core, REC, and a histidine-containing phosphotransfer domain (Hpt) (85,109). Rrp1 contains the REC domain and the conserved GGDEF domain of diguanylate cyclase activity (84,85,110). Rrp1 directs the synthesis of cyclic dimeric GMP (c-di-GMP) (111,112). The diguanylate cyclase activity of Rrp1 depends on its phosphorylation, which is presumably carried out by its predicted cognate sensor kinase Hk1 (84,85,111,112).

Hk1-Rrp1 TCS, is dispensable for mammalian infection, however, the product of Rrp1, c-di-GMP, mediates the tick-adaptive response. RNA-seq of wild-

type *B. burgdorferi* and *rrp1* mutant suggests c-di-GMP signaling has a global effect by modulating the expression of genes involved in the remodelation of the cell envelope, utilization of alternative carbohydrate sources, and chemotactic responses, to promote the survival of *B. burgdorferi* within the feeding tick (113). In addition, deletion of *rrp1* results in the downregulation of the *glp* operon that is required for glycerol uptake and metabolism (112). Glycerol is an essential carbon source for spirochete fitness in ticks (114). Furthermore, deletion of *rrp1* and *hk1* impaired its ability to utilize chitobiose and *N*-acetylglucosamine (115). Chitobiose is an important source of *N*-acetylglucosamine for cell wall synthesis in *B. burgdorferi* (115–117). Hk1-Rrp1 and consequently c-di-GMP, are essential in regulating tick phase genes and for *B. burgdorferi* survival during acquisition and transmission blood meals (85,109,111–113).

B. burgdorferi encodes two phosphodiesterases (PDEs) that control the turnover of c-di-GMP, PdeA and PdeB (118,119). In addition, the c-di-GMP receptor PlzA, positively and negatively regulates the transcription of the glycerol operon (*glp*) (120). Furthermore, PlzA is involved in motility and contributes to infection (121). Recently, a second c-di-GMP receptor, PlzB, was identified that can also bind to c-di-GMP but is not the primary receptor of c-di-GMP (122).

The two TCS of *B. burgdorferi*, Hk2-Rrp2 and Hk1-Rrp1 communicate with each other (84,112,115). Hk2-Rrp2 is responsible for the transcriptional activation of global regulator RpoS, which is essential for the pathogen to accomplish its tick to mouse transmission and to establish mammalian infection (79,80,87,88,123). Hk1-Rrp1 synthesizes c-di-GMP and is required for tick colonization (85,111,112).

Recent studies demonstrated that the c-di-GMP binding protein PlzA, a downstream effector of Rrp1, links the two TCS by positively modulating the expression of *rpoS* in concert with the BosR transcription regulator (115,123). In ticks, expression of *plzA* is induced turing tick feeding (121,124). Therefore, PlzA is important in stimulating the RpoS regulon for the induction of genes necessary for the transmission from tick to mammal.

Gene expression in the flat tick

B. burgdorferi must adapt and survive extreme nutrient deprivation as the larvae molts into nymphs. In this state, tick phase genes are active and the Rrp2-RpoN-RpoS pathway is inactive, leading to the repression of mammalian phase genes (7,12,76). *B. burgdorferi* adapts to the nutritional limitations presented in the unfed tick by modulating the stringent response. In *B. burgdorferi,* the Rel_{Bbu} protein contains domains homologous to RelA and SpoT in *E. coli* and is responsible for the production of the alarmones guanosine pentaphosphate and guanosine tetraphosphate (p)ppGpp (125–127). These alarmones modulate transcription in response to nutrient stress to promote the persistence of *B. burgdorferi* in the tick (128).

Post-transcriptional regulation in *B. burgdorferi* by RNA binding proteins and RNA helicases

The majority of gene regulation in bacteria occurs at the transcriptional level, however, bacteria also regulate gene expression at the post-transcriptional and

post-translational levels. In *B. burgdorferi,* transcriptional regulation has been an area of extensive investigation (7,12,76). Nevertheless, post-transcriptional regulation has shed light in the spirochete genetic regulatory networks recently. For example, the BBD18 protein, encoded on linear plasmid 17 (lp17), has an apparent post-transcriptional effect on RpoS (129–131). BBD18 represses transcription of RpoS-dependent genes through its indirect regulatory effect to RpoS (129–131). Although unresolved, the effect of BBD18 is seen in the form of protein stability or degradation of RpoS (129–131).

CsrA is a homolog of the carbon-storage regulatory protein encoded by many bacteria, including *E. coli* (64). CsrA post-transcriptionally regulates gene expression by binding to the 5'UTR of specific transcripts, thus altering their translation and/or stability (132). The borrelial CsrA protein only binds to the *flaB* transcript and inhibits its translation; *flaB* encodes the major flagellar subunit in *B. burgdorferi*, (63). Conflicting results of CsrA have been reported in regards of its role in pathogenesis (133–135). Interestingly, CsrA in *E. coli* interacts with two small RNAs, designated CsrB and CsrC, which antagonize CsrA by sequestering the protein (136). No CsrB- or CsrC-like regulatory RNAs have been identified in *B. burgdorferi.*

The Bpur regulatory protein is a homodimer of 122 amino acids, which fold into a 'PUR' domain (137,138). This is a conserved domain for proteins that exhibit high affinity for purine-rich stretches of nucleic acids (138). In *B. burgdorferi,* Bpur binds to its own transcript and inhibits its translation. Bpur is also linked to regulating the translation of the *sodA* transcript, which encodes the sole superoxide dismutase

in *B. burgdorferi* (137,139). Similar to Bpur, the SpoVG protein binds to its own mRNA, as well as the transcript specific to the glycerol operon *glpFKD* (140). SpoVG appears to autoregulate in a post-transcriptional manner (140).

In addition to RNA binding proteins involved in post-transcriptional regulation, RNA helicases have also shown to play a role in gene regulation. RNA helicases are conserved enzymes that use ATP to bind RNA or ribonucleoprotein and are central players in RNA metabolism (141,142). RNA helicases are involved in RNA unwinding, RNA decay, ribosome biogenesis, RNA processing, and translation initiation (142,143). *B. burgdorferi* encodes a single putative RNA helicase, designated HrpA (34). HrpA is a DEAH-box RNA helicase involved in RNA processing (34,144,145). Importantly, *B. burgdorferi* HrpA is associated with infectivity (144). The genetic inactivation of *hrpA*, leads to the loss of *B. burgdorferi* infectivity in mice and has a global impact by modulating the expression of 187 proteins (144). In addition, the absence of *hrpA* resulted in the RNA processing of five *B. burgdorferi* transcripts *in vitro*: *p66, oms28, glpK, glpA,* and *bb0242* (145). This suggests that HrpA stabilizes these transcripts for their increase translation by an unknown mechanism (145).

Small regulatory RNAs are post-transcriptional regulators in bacteria

Post-transcriptional regulation via small regulatory RNAs (sRNAs) is an RNA based gene regulatory scheme found to affect gene expression by altering the stability and/or the translation efficiency of targeted transcripts under conditions including, but not limited to, stress response, quorum sensing, and virulence in

bacteria (146–148). The sRNAs are usually ~50 to 500 nucleotides in size and the regulatory effect of the sRNAs is achieved by base pairing to one or more mRNAs (148–150). It was suggested that sRNA regulation is an advantageous adaptive response as it occurs quickly, is metabolically inexpensive to synthesize, and provides an additional layer of regulation in response to environmental signals (149,151). Documented bacterial sRNA origins include duplication events, horizontal gene transfers (HGT), and de *novo* emergence (151,152).

The roles of sRNAs are diverse in gene regulation due to their ability to upregulate and downregulate the translation of the transcripts they recognize. The mechanisms of downregulation include binding to the ribosomal binding site (RBS) of the mRNAs and inhibiting translation (148,149) (Fig. 2). Also, the sRNA binding to the mRNA can result in the transcript destabilization, and consequently, degradation by RNases (148,149) (Fig. 2). sRNAs can also upregulate gene expression by binding to inhibitory secondary structures present in the mRNA that occlude the RBS. Alternatively, the sRNA binding results in exposure of the RBS and enhanced translation (148,149) (Fig. 2).

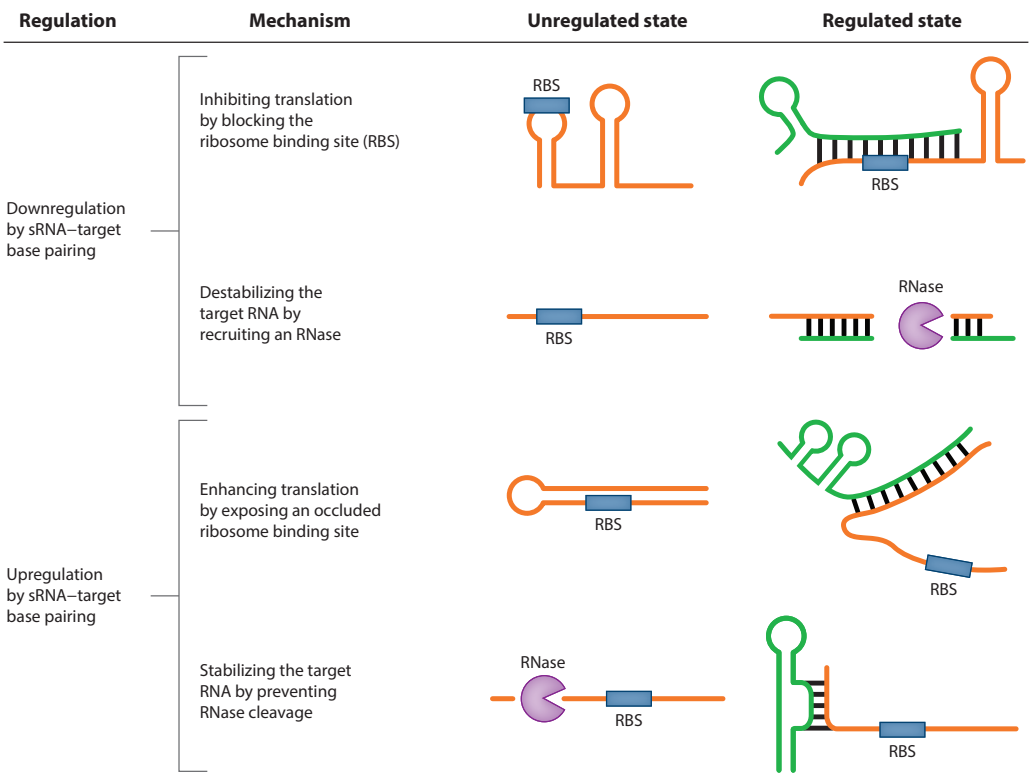

Figure 2. Mechanisms of post-transcriptional regulation by bacterial sRNAs from Nitzan M, *et al*., 2017. sRNAs can downregulate gene expression by binding to the target transcript at the ribosomal binding site (RBS) and blocking translation. In addition, the sRNA binding can destabilize the transcript and recruit RNases for RNA degradation. sRNAs can upregulate gene expression by binding to mRNAs and alleviating inhibitory secondary structures present in the transcript, exposing the RBS and enhancing translation. Furthermore, the sRNA binding can stabilize the transcript and prevent RNase degradation by masking RNase cleavage sites. Reprinted with permission from Annual Review of Biophysics. Copyright date of August 13, 2019.

In addition, sRNAs can bind to mRNAs and stabilize the transcripts by occluding RNase cleavage sites, thus preventing RNA degradation (148,149) (Fig. 2).

General features of sRNAs include a stable secondary structure, promoter responsive to environmental signals, a unstructured region for mRNA base pairing termed the seed region, and a Rho-independent terminator (151,152). The base pairing seed region requires a minimum of 6 to 8 contiguous base pairs (150,153). Some sRNAs have one seed region that pairs to one mRNA while others have multiple seed regions that each base pair with different mRNA targets (154,155).

The most extensively studied sRNAs class are *trans*-acting sRNAs. These are synthesized between two annotated genes (intergenic) regions of the genome and base pair to mRNAs encoded at a genomic location distinct from the sRNA gene (150,156). The *trans*-acting sRNAs have limited complementarity with their mRNA targets. Thus, single sRNAs can target multiple mRNAs and mRNAs can be regulated by multiple sRNAs (152,156). The resulting RNA-RNA duplex formed by the sRNA-mRNA interaction, leads to the modulation of gene expression by affecting mRNA stability and/or translation (148,150,156).

Some *trans*-acting sRNAs are dependent of the RNA chaperone Hfq, which facilitates the interaction between sRNAs and mRNAs (157,158). Hfq is a member of the Sm/Lsm family of RNA binding proteins, forms a homohexameric ring and has been found in both Gram-negative and Gram-positive bacteria (157,158).

A second class of sRNAs are *cis*-acting or antisense sRNAs (159,160). These sRNAs are encoded in the opposite strand of an annotated gene with extended complementarity to the corresponding transcript and influence translation

and/or stability of the transcript (160). Another class of sRNAs are designated as intragenic and, as their name implies, are transcribed from within a protein coding region, often in the same orientation as the coding sequence they are coded within. To date, relatively little is known about their function (161,162).

The 5' untranslated regions (UTR) of transcripts can also be a source of post-transcriptional regulation. One example of this is a riboswitch. Riboswitches can directly sense cellular metabolites to modulate transcription or translation of its downstream genes (163,164). Another example are RNA thermometers. RNA thermometers are structural elements located within the 5'UTR of protein-coding mRNAs that control the mRNA translation by changing its secondary structure in response to temperature fluctuation (165,166). Generally, at low temperatures (<30°C), RNA thermometers mask the RBS by forming a stable secondary structure and blocking translation of the downstream gene (165,166). Upon an increase in temperature, such as host body temperature of 37°C, the RNA thermometer unmask the RBS and allows translation initiation (165,166).

Identification of sRNAs

The identification of sRNAs in bacteria has relied heavily on bioinformatics prediction and experimental validation. Given their heterogeneity in sequence length (50 to 500 nucleotides), different genomic locations, and distinct secondary structures (167,168), validation of sRNAs has been challenging. The use of computer programs often search exclusively in intergenic regions and define sRNAs based on sequence conservation, orphan promoters, and Rho-independent

terminators (150,151,167). Although some sRNAs have been identified in this manner, sRNAs that are transcribed within or antisense to ORFs can be missed. Experimental searches that use Hfq or RNase binding as a prerequisite will miss Hfq- and RNase-independent sRNAs.

For *trans*-acting sRNAs, their imperfect base pairing to mRNAs results in difficulty in predicting the mRNAs they target using bioinformatic approaches, which render experimental validation essential after the computational prediction (147,167). Recently, RNA-seq has become a powerful technique to identify previously undetected transcripts (147,150). Although deep sequencing has been fruitful for finding sRNAs, processing and comparing these large data sets are difficult. Discrepancy in these studies include different cDNA preparation, sequencing platforms, and different thresholds and stringencies for annotating transcripts (147,150). Northern Blot analysis typically is the standard method for validating potential sRNA candidates that stem from RNA-seq data (161,168).

sRNAs in *B. burgdorferi*

The important virulence-associated regulator, RpoS, is also regulated post-transcriptionally by a sRNA denoted $DsrA_{Bb}$ (169). To date, this is the only characterized sRNA in *B. burgdorferi.* The $dsrA_{Bb}$ mutant fails to upregulate RpoS and OspC in response to an increase in temperature, but does regulate RpoS and OspC in response to changes in pH and cell density (169).

Two distinct 5' ends of *rpoS* transcripts have been identified and are differentially regulated by cell density (169). The longer transcript is 171 nucleotides

upstream of the start codon (-171), which is enriched at low cell density and contains the complementary sequence to the sRNA. The high cell density transcript is 50 nucleotides upstream of the start codon (-50) and does not contain the sRNA binding portion (169). It was suggested that the long transcript is transcribed by the housekeeping sigma factor RpoD, rather than RpoN (77,86,169). At low cell density, in a temperature shift to 37°C, $DsrA_{Bb}$ binds to the *rpoS* transcript leading to an increase of the translation of the RpoS protein (169). It is hypothesized that $DsrA_{Bb}$ regulation of *rpoS* is relevant for tick to mammal transmission of *B. burgdorferi* (169).

Furthermore, a Hfq-like RNA chaperone has been identified in *B. burgdorferi* (170). *B. burgdorferi hfq* mutants are non-infectious in mice and Hfq was found to bind to the sRNA $DsrA_{Bb}$ and the *rpoS* transcript, suggesting that it functions as the RNA chaperone for this specific sRNA-mRNA interaction (170). Because of the strong phenotype in *hfq* mutants, it is hypothesized that Hfq regulates additional sRNAs important for virulence-associate gene expression in *B. burgdorferi.*

Bacteria sRNAs can work as negative regulators of gene expression by destabilizing mRNAs, resulting in transcript degradation by RNases (171,172). In some instances, sRNAs function as positive regulators, by stabilizing mRNAs, which will in turn increase the translation of the gene and/or protect them from mRNA degradation by masking RNase specific cleavage sites (148,149,173). RNA degradation by RNases is an important mechanism for controlling the gene expression of an organism where it provides an additional layer of regulation, specifically those that affect post-transcriptional targets (173,174). In *B. burgdorferi,* homologs of RNase III, RNase M5, RNase Y, RNase J1 and RNase Z, have been

identified (34,175). The best characterized RNases in spirochetes include RNase P, which is responsible for the maturation of tRNAs (176), and RNase III, which was recently found to process the 23S rRNA gene (177). Interestingly, it appears that the mechanism for mRNA degradation in *B. burgdorferi* is far more similar to *B. subtilis* than *E. coli* (175). Notably, *B. burgdorferi* lacks a homologue of RNase E, the primary endoribonuclease involved in transcript decay in *E. coli,* but instead encodes a homolog of RNase Y, the major regulator of RNA metabolism in *B. subtilis* (175). RNase Y is associated with sRNA-mediated post-transcriptional regulation in *C. perfringens* (171). This suggests that the borrelial RNase Y could serve a similar function in the post-transcriptional regulation of borrelial sRNAs.

Recently a plethora of sRNAs were by RNA-seq identified in *B. burgdorferi* (161,178). Of the 1,005 sRNAs identified, 43% were shown to be temperature dependent at either 23°C or 37°C, conditions *in vitro* that mimic the tick vector and mammalian host environments, respectively (161). This subscription to differentially regulated sRNAs suggests that *B. burgdorferi* utilizes sRNAs regulation as an adaptive cue during the enzootic cycle. Among the sRNAs upregulated at 37°C was a *trans*-acting sRNA, denoted SR0736 (161), located in the intergenic (IG) region in between genes *bbd18* and *bbd21* of lp17. In addition, previous studies found attenuated phenotypes in *B. burgdorferi* harboring truncations of the linear plasmid 17 (131,179) that would have eliminated the SR0736 sequence. However, based on the large deletions made in these studies, it was unclear if SR0736 was a key component in the borrelial infectivity defect observed. Since the sRNA is upregulated when *B. burgdorferi* is grown at conditions of 37°C (161), we

hypothesized that SR0736 regulates genes important in the infectious process. In the work presented herein, we describe the role that SR0736 plays in *B. burgdorferi* infectivity and begin to define the mRNAs it targets. SR0736 is required for optimal infection and dissemination in mice. Furthermore, the loss of SR0736 lead to differential expression of genes, suggesting SR0736 may affect mRNA stability and/or degradation. Moreover, the loss of SR0736 lead to a significant decrease of two proteins, suggesting SR0736 stabilizes the transcripts encoding these proteins, to promote their ability to be translated.

Summary

Lyme disease is an emerging infectious disease with approximately 329,000 cases diagnosed each year (9,10). The causative agent of Lyme disease, *Borrelia burgdorferi*, is maintained in nature in an enzootic cycle involving an arthropod vector and mammalian hosts (7). For *B. burgdorferi* to survive in these vastly different milieus, the spirochete must sense environmental cues and regulate its gene expression accordingly to survive within these disparate hosts (7,12,76). Post-transcriptional regulation by sRNAs in *B. burgdorferi* affects RpoS levels (169) and some additional sRNAs have been identified that are temperature regulated under conditions that mimic the tick vector and mammalian host (161). This suggests that sRNAs play a role in regulating genes needed in the enzootic cycle. In this work we have characterized two *trans*-acting sRNAs. One is encoded between the gene *bbd04* and the pseudogene *bbd05a* on lp17, designated SR0725, and is dispensable for mammalian infection. The second *trans*-acting sRNA is encoded

between the genes *bbd18* and *bbd21* of lp17, and is denoted SR0736 (161). We found here that SR0736 is required for optimal infection in mice. The loss of SR0736 led to the dysregulation of 19 genes and the reduction in the abundance of two proteins. This result suggests that SR0736 may exert its regulatory effect by affecting the stability of several borrelial transcripts and/or altering their translation efficiency. Taken together, these results indicate that SR0736 regulates multiple targets and is important for the optimal infection and dissemination of *B. burgdorferi* in the experimental model of Lyme borreliosis.

CHAPTER II

ANALYSIS OF TRANSPOSON MUTANTS IN SMALL REGULATORY RNAs OF *Borrelia burgdorferi* AND THEIR ROLE IN THE MAMMALIAN HOST INFECTION

Introduction

Lyme disease is a tick-transmitted bacterial infection caused by the spirochete *Borrelia burgdorferi* (7,12). The bacterium is transmitted to a variety of small mammals and birds via the bite of ticks from the *Ixodes* genus (7). Initial infection of Lyme disease in humans is characterized by a flu-like illness, accompanied by a painless skin rash denoted as Erythema Migrans (24,32). If untreated, the infection can progress to a multi-stage disorder as the spirochete disseminates throughout the host to colonize distal tissues and organs, resulting in cardiac, neurological, and arthritic manifestations (19,32,56). Lyme disease is the most common vector-borne disease in the United States with approximately 30,000 cases confirmed to the Centers for Disease Control and Prevention (CDC) each year, but it is estimated that the actual number of diagnosed cases is as high as 329,000 (9,10). Thus, Lyme borreliosis is a significant, re-emerging infectious disease.

B. burgdorferi is a slow-growing, fastidious organism (6,12), that is only found associated with its arthropod vector or mammalian hosts (7,12). The spirochete can only be grown *in vitro* in a rich, complex and poorly defined media (42). *B.*

burgdorferi has a segmented genome consisting of a linear chromosome and up to 21 circular and linear plasmids (34,35). Several of these plasmids encode genes required for the enzootic cycle (7,12,76,181–183).

Approximately fifteen years after the discovery of *B. burgdorferi* (2), the development of genetic tools started to become available to assess the role of individual genes in borrelial physiology and pathogenesis (6,184–187). Genetic manipulation in *B. burgdorferi* includes site-directed mutagenesis, gene disruption by allelic exchange, addition of inducible promoters, development of shuttle vectors, and transposon mutagenesis (6,12,13). *B. burgdorferi* is typically transformed by electroporation (188), but this is challenging due to low frequency transformation rate, 6-8 hours of doubling time, and spontaneous plasmid loss (12,189). Certain plasmids that are essential for borrelial infection, but are dispensable for *in vitro* growth, can be lost by *in vitro* passaging and electroporation (181–183). Thus, it is important to score for the plasmid content of *B. burgdorferi* isogenic mutant strains, prior to examination in the mammalian host.

Site-directed mutagenesis of a particular gene in *B. burgdorferi* may require 3-6 months of transformation process including outgrowth of transformants, screening for an appropiate insertion or deletion event, and assessment of plasmid content (6,190). However, the advancement of genetic tools in *B. burgdorferi* have identified genes required for the enzootic cycle and virulence factors in the bacterium (6,7,12). For example, molecular analyses determined that the outer surface protein A (OspA) was essential for tick colonization in the midgut (12,105,107) and that outer surface protein C (OspC) was essential for establishing

mammalian infection (12,96). Nonetheless, the challenges of targeted mutagenesis in the spirochete has resulted in fewer than 100 genes of the 1739 ORFs in infectious *B. burgdorferi* to be subjected to genetic analyses (6,7,190).

Transposons are DNA elements with the ability to move or transpose from one location to another in the genome (191–193). Transposable elements are widely spread in prokaryotic and eukaryotic organisms (191–193). Transposons of the *mariner* family are elements in between 1 and 5 kb in length, that encode the *mariner* (*Himar1*) transposase (191,194). For the “cut and paste” mechanism of *mariner*-specific elements, the *Himar1* transposase is required to excise the transposon from one location in the genome, and reintegrate it at another place of the genome, utilizing the TA dinucleotide as the preferred insertion site (191,194).

As genetic tools, transposons can be used to randomly introduce a piece of foreign DNA into coding and non-coding sequences in genomes (191–193). The *mariner*-transposable element *Himar1*, originally isolated from the horn fly *Haematobia irritans* (194), has been employed for the generation of transposon mutant libraries in a broad range of prokaryotes (191,192), including *B. burgdorferi* (189,195–197). Recently, a research group assembled a sequence-defined, signature-tagged mutagenesis (STM) library of 4,479 transposon (Tn) mutants of *B. burgdorferi* (189). Of the 4,479 Tn mutants, 3,865 are unique Tn insertion sites (189).

Massive parallel sequencing was combined with transposon mutagenesis (Tn-seq) to determine the frequency of a particular insertion within a population (190,198). Tn-seq is a powerful tool with the capacity to examine thousands of Tn

clones simultaneously (192,199). After the growth of the Tn library under a test condition, or the use of a Tn library in mice infections, the frequency of the insertion mutants are determined by sequencing the transposons flanking regions *en masse* to obtain the output (190,199). In addition, the frequency of the mutants in the initial inoculum are sequenced to obtain the input, and the change in frequency can be calculated as a ratio of the output over input (190,199). The change in frequency is presumed to be the effect of the insertion on fitness (190,199). Tn-seq studies in *B. burgdorferi* have been useful in examining genes involved in metabolism (200), identifying novel genes required for resistance against reactive oxygen and nitrogen species (201), and identifying novel genes required for tick survival (202).

The *B. burgdorferi* transposon library has Tn insertions in genes and at intergenic regions of the genome (in between genes) (189). Intergenic regions in bacteria have been found to contain small regulatory RNAs (sRNAs) with ability to post-transcriptionally regulate genes in different cell processes, including, but not limited to, chemotaxis, metabolism, and virulence (149,150,153,203). The bacterial sRNAs work by binding to transcripts, leading to an increase or decrease of the translation of the genes (150,152,153). In *B. burgdorferi*, only one sRNA has been characterized, $DsrA_{Bb}$ (169). $DsrA_{Bb}$ binds to the transcript of the RpoS alternative sigma factor and increases its translation at 37°C (169). RpoS is important for the expression of genes required for the mammalian host and controls the expression of virulence-associated surface expressed lipoproteins (12,77,78). Recently, 1,005 sRNAs were identified in *B. burgdorferi* by RNA-seq (161). Of the sRNAs identified, 43% were temperature dependent, a known environmental cue for *B. burgdorferi*

transiting between the tick and mammal (12,76). This observation suggests that *B. burgdorferi* sRNAs may regulate gene expression during transmission within the enzootic cycle.

Here, we hypothesize that *B. burgdorferi* encodes novel sRNAs associated with virulence. To test this hypothesis, we used Tn-seq data to identify transposon mutants that inactivated sRNAs within intergenic domains (161), and examined their individual infectivity using the mouse model of Lyme borreliosis. Specifically, we evaluated seven *B. burgdorferi* transposon mutants (189) in putative sRNAs (161). Of the seven transposon mutants tested, three displayed an attenuated phenotype in single strain mouse infections. The transposon inactivating the SR0725 sRNA (161) from the 17 kilobase linear plasmid (lp17) was investigated further. To independently confirm the Tn infection results for the SR0725 sRNA, we genetically inactivated this sRNA and tracked its ability to disseminate *in vivo* using bioluminescent imaging. Despite its initial purported link to an infectivity phenotype, here we report that the SR0725 sRNA is dispensable for mammalian infection.

Results

Infectivity potential of putative sRNA Tn mutants

A subset of seven transposons (189) interrupting putative intergenic sRNAs (161) were found to have an attenuated phenotype in a previous Tn-seq screen (Table 1 and L. Hu *et al*., unpublished data), and were selected for single Tn strain mice infections (Table 2). The Tn-seq screen was performed by using the entire *B. burgdorferi* Tn library (189) grown *in vitro* in BSK-II media supplemented with

appropriate antibiotics. Groups of six C3H/HeJ mice were inoculated with $5x10^5$ organisms in the right flank by needle inoculation. Following 14 days of infection, the tibiotarsal joint was collected and cultured in BSK-II media for borrelial expansion. DNA was extracted, pooled from twenty-four mice and sequenced to determine the frequency of the Tn mutants. Frequency of the Tn mutants present in the joint tissue (output), over the frequency of the Tn mutants present in the initial inoculum (input), was used to determine fitness of the clones (output/input) (Table 1 and L. T. Hu *et al*., unpublished data).

For the single Tn infections, C3H/HeN mice were inoculated with seven transposon mutant strains (Table 3) at 10^4 dose for 21 days via the intradermal route. After 21 days, tissues were collected and cultured in BSK-II media to score for the presence or absence of spirochetes. Of the seven Tn mutants tested, three held the attenuated phenotype (Table 3). The attenuated transposons of sRNAs were located intergenic (IG) of genes *bbb13-bbb14* in circular plasmid 26 (cp26), IG *bbd04-bbd05a* in linear plasmid 17 (lp17), and IG *bbd18-bbd21* in lp17 (161). The three sRNAs identified as potentially associated with virulence, were selected for genetic inactivation to independently confirmed these results. The genetic inactivation of sRNA IG *bbb13-bbb14* was unsuccessful. The sRNA IG *bbd18-bbd21* will be discussed in Chapter III. For Chapter II, the sRNA IG *bbd04-bbd05a* will be discussed.

Table 1. Reduction of candidate sRNA mutants of intergenic (IG) regions based on Tn-seq[a].

Location of Tn insert	Tn Clone[b]	sRNA ID[c]	Input 1[d]	Input 2[d]	Input 3[d]	Output 1[e]	Output 2[e]	Output 3[e]	Avg.Output /Avg.Input	Comments
cp26; *guaA* (*bbb18*)		N/A	1.2032	0.7411	0.7736	0.0009	0.0018	0.0009	0.0013	Control; attenuated
lp54; *dbpA* (*bba24*)		N/A	0.0041	0.0073	0.0084	ND[f]	ND[f]	ND[f]	0[g]	Control; attenuated
lp25; *pncA* (*bbe22*)		N/A	0.0089	0.0045	0.0027	ND[f]	ND[f]	0.0003	0.0185	Control; attenuated
lp28-2; *bbg22*		N/A	0.0672	0.0991	0.0927	0.1688	0.2016	0.0267	1.53	Unchanged
chrom.; *glpK* (*bb0241*)		N/A	0.0245	0.1221	0.0882	3.5503	0.0933	0.0697	15.8	Unchanged[h]
lp36; *bbk52*		N/A	0.00057	0.00028	0.00038	0.00126	0.00070	0.00051	2.01	Unchanged
cp26; *bbb28*		N/A	1.5432	1.0517	1.1083	1.3479	3.5336	4.1401	2.44	Unchanged
lp54; IG *bba34-bba36*	T05TC355	SR0897	0.0201	0.0210	0.0085	ND[f]	ND[f]	ND[f]	0[g]	$6.5x10^5$ reads[i]
lp54; IG *bba66-bba68*	T10TC061	SR0912	0.1001	0.1327	0.2092	0.00005	ND[f]	0.00006	0.00025	$6x10^5$ reads[i]
cp26; IG *bbb03-bbb04*	T11TC387	SR0948	0.2269	0.1362	0.0982	0.0001	ND[f]	0.0006	0.0015	$1.8x10^4$ reads[i]
cp26; IG *bbb13-bbb14*	T10TC351	SR0962	0.0258	0.0107	0.0062	ND[f]	ND[f]	ND[f]	0[g]	$3x10^6$ reads[i]
lp17; IG *bbd04-bbd05a*	T04TC273	SR0725	0.0378	0.0323	0.0145	ND[f]	0.00006	ND[f]	0.00071	$2x10^6$ reads[i]
lp17; IG *bbd18-bbd21*	T06TC412	SR0736	0.0244	0.0549	0.0454	0.0001	ND[f]	0.00006	0.0013	$1x10^5$ reads[i]
lp28-3; IG *bbh36a-bbh36b*	T08TC464	SR0795	0.1628	0.2209	0.1344	0.00005	ND[f]	0.00006	0.00021	$1x10^5$ reads[i]
lp38; IG *bbj37-bbj41*	T09TC160	SR0869	0.0384	0.0456	0.0337	ND[f]	ND[f]	0.00006	0.00051	$2.5 x10^3$ reads[i]

[a] Data following a two week infection with all Tn mutants; [b] Transposon clones from the *B. burgdorferi* Tn library (Lin *et al*., 2012); [c] sRNAs from the *B. burgdorferi* sRNA library (Popitsch *et al*., 2017); [d] % of Tn-seq reads from the libraries made from the inoculum used for mouse infection; [e] % of Tn-seq reads from the libraries made from bacteria recovered from infected mice; Output is pooled data from 24 mice; [f] ND = not detected; [g] indicates that no sequences were observed following Tn-seq; [h] one high Output set skewed ratio; [i] represents rounded number of reads from sRNA-specific libraries (Popitsch *et al*., 2017).

Table 2. Subset of *B. burgdorferi* transposon (Tn) mutants in sRNAs used in single Tn mice infection.

Name of Tn[a]	sRNA ID[b]	Replicon	Location	Insertion site	Tn orientation
T05TC355	SR0897	Plasmid lp54	IG *bba34-bba36*	23489	Reverse
T10TC061	SR0912	Plasmid lp54	IG *bba66-bba68*	46175	Forward
T11TC387	SR0948	Plasmid cp26	IG *bbb03-bbb04*	2348	Forward
T10TC351	SR0962	Plasmid cp26	IG *bbb13-bbb14*	10841	Forward
T04TC273	SR0725	Plasmid lp17	IG *bbd04-bbd05a*	2886	Reverse
T06TC412	SR0736	Plasmid lp17	IG *bbd18-bbd21*	11784	Reverse
T08TC464	SR0795	Plasmid lp28-3	IG *bbh36a-bbh36b*	24530	Forward

[a] Transposon mutants from the *B. burgdorferi* Tn library (Lin *et al.,* 2012); [b] sRNAs from the *B. burgdorferi* sRNA library (Popitsch *et al*., 2017).

Table 3. Infectivity of *B. burgdorferi* intergenic (IG) sRNA transposon mutants relative to its genetic parent[a].

Strain[b]	sRNA ID[c]	Genomic location	Ear	Skin[d]	Lymph node	Heart	Bladder	Joint	Total sites	% Positive Tissues
5A18NP1 (parent)			4/4	4/4	4/4	4/4	4/4	4/4	24/24	100%
T05TC355	SR0897	lp54; IG *bba34-bba36*	3/4	3/4	3/4	3/4	3/4	3/4	18/24	75%
T10TC061	SR0912	lp54; IG *bba66-bba68*	4/4	4/4	4/4	4/4	4/4	4/4	24/24	100%
T11TC387	SR0948	cp26; IG *bbb03-bbb04*	4/4	4/4	4/4	4/4	4/4	4/4	24/24	100%
T10TC351	**SR0962**	**cp26; IG *bbb13-bbb14***	**2/4**	**1/4**	**2/4**	**2/4**	**2/4**	**2/4**	**11/24**	**46%**
T04TC273	**SR0725**	**lp17; IG *bbd04-bbd05a***	**2/4**	**2/4**	**2/4**	**2/4**	**2/4**	**2/4**	**12/24**	**50%**
T06TC412	**SR0736**	**lp17; IG *bbd18-bbd21***	**0/4**	**1/4**	**3/4**	**0/4**	**2/4**	**0/4**	**6/24**	**25%**
T08TC464	SR0795	lp28-3; IG *bbh36a-bbh36b*	4/4	4/4	4/4	4/4	4/4	4/4	24/24	100%

[a] Dose of 10^4 per strain of *B. burgdorferi* tested; [b] Transposons from Tn library of *B. burgdorferi* (Lin, T., *et al.*, 2012); [c] sRNAs from *B. burgdorferi* sRNA library (Popitsch *et al*., 2017); [d] skin from abdominal area (inoculation site).

The Tn strain T04TC273 (also referred to as Tn273), contains a Tn insertion between genes *bbd04-bbd05a* and exhibited an infectivity of 50% in the mouse tissues surveyed relative to its parent strain (Table 3), suggesting that this sRNA might be required for optimal infection. This sRNA has been recently designated SR0725 (161).

Characterization of the intergenic Tn mutant strains by PCR

Some of the isolates provided from the Tn library have additional transposons in their genome. To determine if strain Tn273 has the transposon in the correct insertion site, we designed primers that flank the Tn (Table 4 and Table 8) and assessed this by PCR (190). Oligonucleotide primers that flanked the Tn273 insertion amplified a 534 bp band corresponding to the parent strain and an approximate 2 kb amplicon in the Tn273 strain, consistent with the presence of the transposable element (Fig. 3). These results indicate that strain Tn273 has a transposon insertion between *bbd04* and the pseudogene *bbd05a,* as expected. For the remaining six transposons tested (Table 4), strain T11TC387 contained a Tn insertion at the predicted location (Table 4; data not shown). Strains T06TC412 and T05TC355 appeared as mixed populations. Specifically, each isolate amplified both a parent sized amplicon and a fragment that contains a transposable element at the correct locale based on the oligonucleotide primers used for PCR (Table 4; data not shown). Finally, strains T10TC061, T10TC351, and T08TC464 did not contain the Tn in the known insertion site (Table 4; data not shown) but grew in the presence of

Table 4. PCR analysis of the Tn mutants used in the mice infection determine that only a subset of the strains carried the transposable element in the correct locale.

Name of Tn[a]	Replicon	Location	Single Tn amplification [b]
T04TC273	Plasmid lp17	IG *bbd04-bbd05a*	Yes
T11TC387	Plasmid cp26	IG *bbb03-bbb04*	Yes
T06TC412	Plasmid lp17	IG *bbd18-bbd21*	Mix population
T05TC355	Plasmid lp54	IG *bba34-bba36*	Mix population
T10TC061	Plasmid lp54	IG *bba66-bba68*	No Tn in insertion site
T10TC351	Plasmid cp26	IG *bbb13-bbb14*	No Tn in insertion site
T08TC464	Plasmid lp28-3	IG *bbh36a-bbh36b*	No Tn in insertion site

[a] Transposon mutants from the *B. burgdorferi* Tn library (Lin *et al.,* 2012); [b] primers that flank the Tn insertion were used to determine if single Tn present in insertion site by PCR.

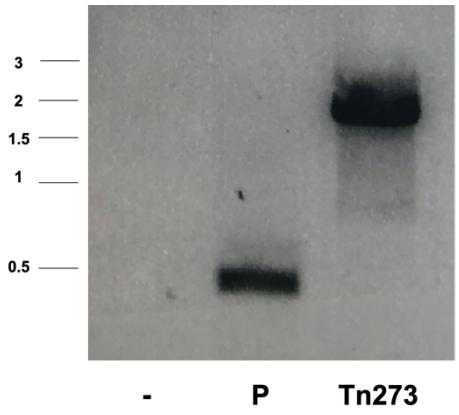

Figure 3. Transposon strain Tn273 contains Tn at insertion site. The parent strain 5A18NP1 (P), and the transposon strain Tn273, were subjected to PCR analysis using primers that flank the transposon insertion from Table 8. The insertion site is located in between gene *bbd04* and pseudogene *bbd05a* of lp17. The no template control is denoted '-'. The DNA ladder is shown at the left and the corresponding kilobase pair values are indicated.

antibiotic selection, suggesting that the transposon is present at another location within the genome.

Genetic inactivation of the sRNA located between the gene bbd04 and the pseudogene bbd05a

To independently evaluate the loss of the SR0725 sRNA of lp17 (161) that lies between *bbd04* and the pseudogene *bbd05a*, we genetically inactivated the SR0725 sRNA in the parent strain ML23 (Fig. 4A) (39–41,181,204,205). The ML23 genetic background is engineered for *in vivo* luminescence and has been used by our group to characterize the loss of numerous borrelial genes (39–41,204,205). The sRNA coordinates in lp17 are nucleotides 2,883-2,934 (161). The genetic inactivation of SR0725 replaced nucleotides 2,888-2,920 from lp17 with a streptomycin resistance cassette (P_{flgB}-*aadA*) (206).

Following transformation and selection, candidate mutants were screen to assess whether the desired mutant was obtained using the oligonucleotide primers illustrated in Fig. 4 and listed in Table 8. For the SR0725 sRNA mutant strain, a 2.4 kb band was observed using P1 and P3 as primers while no fragment was observed in the parent strain due to the absence of the antibiotic cassette (Fig. 4B). Primer pair P2 and P4 (Table 8) resulted in the amplification of 2.7 kb fragment in the SR0725 sRNA mutant and, again, no amplification in the parent, as expected (Fig. 4B).

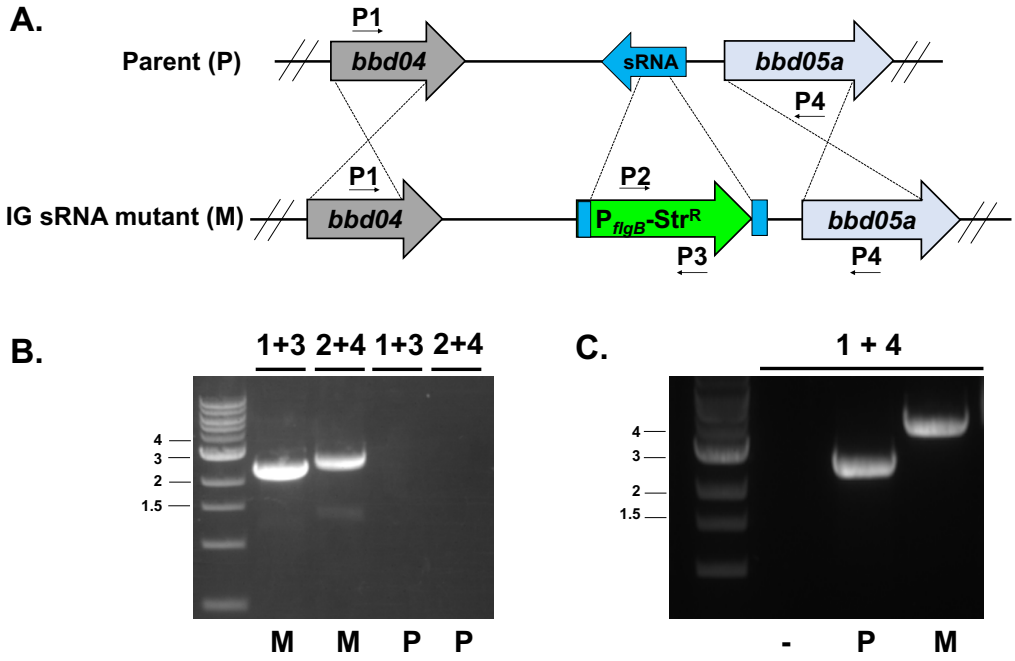

Figure 4. (**A**) Schematic representation of the insertional inactivation strategy of the IG sRNA SR0725. The region of lp17 from the *B. burgdorferi* parent strain, ML23 (P for parent), is shown on the top. The middle portion of the sRNA was replaced by a P_{flgB}-Str^R cassette by a double crossover homologous recombination event and the SR0725 sRNA mutant strain was designated as (M for mutant). (**B** and **C**) Primer pairs P1/P3, P2/P4 and P1/P4 (Table 8), were used to confirm the presence of the P_{flgB}-Str^R in the mutant (M), relative to its parent (P) by PCR. No template control is denoted as '−.' The DNA ladder is shown at the left and the corresponding kilobase pair values are indicated.

Finally, PCR with the primer pair P1 and P4 resulted in a 3 kb and 3.7 kb products in the parent strain and SR0725 sRNA mutant, respectively. This difference in size reflects the presence of the antibiotic resistance cassette (Fig. 4B). The resulting SR0725 sRNA mutant candidates were screened for total borrelial plasmid content and were found to contain all plasmids carried by the parent strain ML23 (181). The resulting SR0725 sRNA strain was designated DM102.

Loss of the SR0725 sRNA does not exhibit a polar effect on flanking pseudogene

The SR0725 sRNA is located between gene *bbd04* and the pseudogene *bbd05a* of lp17 (161). SR0725 lies 82 bases upstream of pseudogene *bbd05a* and 1.1 kb downstream of *bbd04.* Testing for the expression of *bbd04* was deemed unnecessary because of the over 1 kb in distance between the sequences and, thus, the unlikely event of a polar effect. Since some pseudogenes can be transcribed to RNA (207,208), we tested if the pseudogene *bbd05a* is expressed in *B. burgdorferi.* To test for the expression of *bbd05a* in the parent ML23 and the SR0725 sRNA mutant strain DM102, total RNA was prepared, converted to cDNA with reverse transcriptase (RT), and tested with primers specific to the *bbd05a* sequence to determine if a product was detected. A 508 bp fragment was detected in both the parent and SR0725 mutant strain but only when RT was used (Fig. 5). This indicates that the *bbd05a* pseudogene is expressed in both parent and mutant strain and, importantly, that this RNA species is not adversely affected by the inactivation of the SR0725 sRNA.

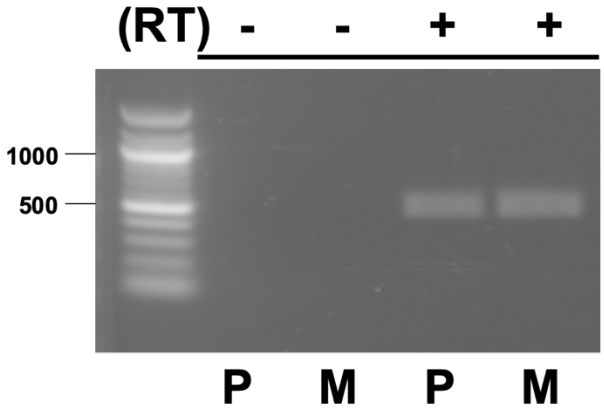

Figure 5. The expression of the pseudogene *bbd05a* is not affected in the SR0725 sRNA mutant strain. The parent (P) and the sRNA mutant (M) strains were grown *in vitro* at conventional microaerophilic conditions of 32°C, 1% CO_2, pH 7.6 and total RNA was purified from each. Oligonucleotide primers specific for *bbd05a* were used without (-) and with (+) added reverse transcriptase (RT). The DNA ladder is shown at the left and the corresponding base pair values are indicated.

The loss of the intergenic SR0725 sRNA is dispensable for B. burgdorferi infectivity

We tested whether the loss of the SR0725 sRNA affected the *in vitro* growth of *B. burgdorferi* and observed no differences relative to the parent strain (Fig. 6). We then evaluated whether the loss of SR0725 sRNA was needed for experimental murine infection. First, borrelial codon-optimized firefly luciferase strains were tested for their luminescence emission and production of firefly luciferase protein *in vitro* and no differences were observed between the strains, as expected (Fig. 7).

To spatially and temporally track the infection of live mice, we infected C3H/HeN mice with the parent strain (ML23/pBBE22*luc*) and the SR0725 sRNA mutant strain (DM102/pBBE22*luc*), both containing borrelial codon-optimized firefly luciferase (Fig. 8; 52), at doses of 10^3 and 10^5, and quantified light emission (Fig. 8). For each imaging experiment, a single infected mouse was not given the luciferase substrate D-luciferin to serve as a background control for luminescence (leftmost mouse in each panel, Fig. 8). Independent of dose, both the parent and the SR0725 mutant displayed similar light emission (Fig. 8). This observation was also confirmed by quantification of the *in vivo* luminescence where no significant differences in light emission were observed in any of the time points (Fig. 9). Following 21 days of infection, the mice were sacrificed, and tissues were cultured in BSK-II media to qualitatively score for infection. As shown in Table 5, at the dose of 10^5, all mice tissues were infected comparable to the parent strain. For the dose of 10^3 organisms, one mouse was uninfected for both strains (Table 5).

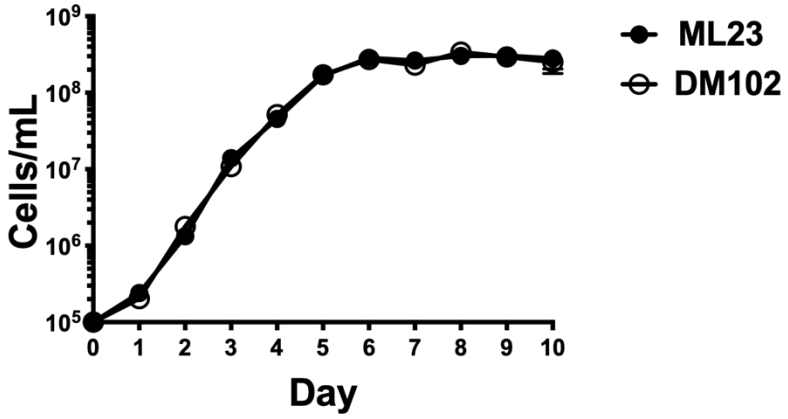

Figure 6. *In vitro* growth of the *B. burgdorferi* strains used in this study. The *B. burgdorferi* parent strain ML23 and the SR0725 sRNA mutant DM102, were grown in conventional microaerophilic conditions of 32°C, 1% CO_2, pH 7.6, in triplicate in BSK-II media and enumerated by dark field microscopy daily out to day 10. No significant differences in growth were observed. Data points shown reflect average value with standard error.

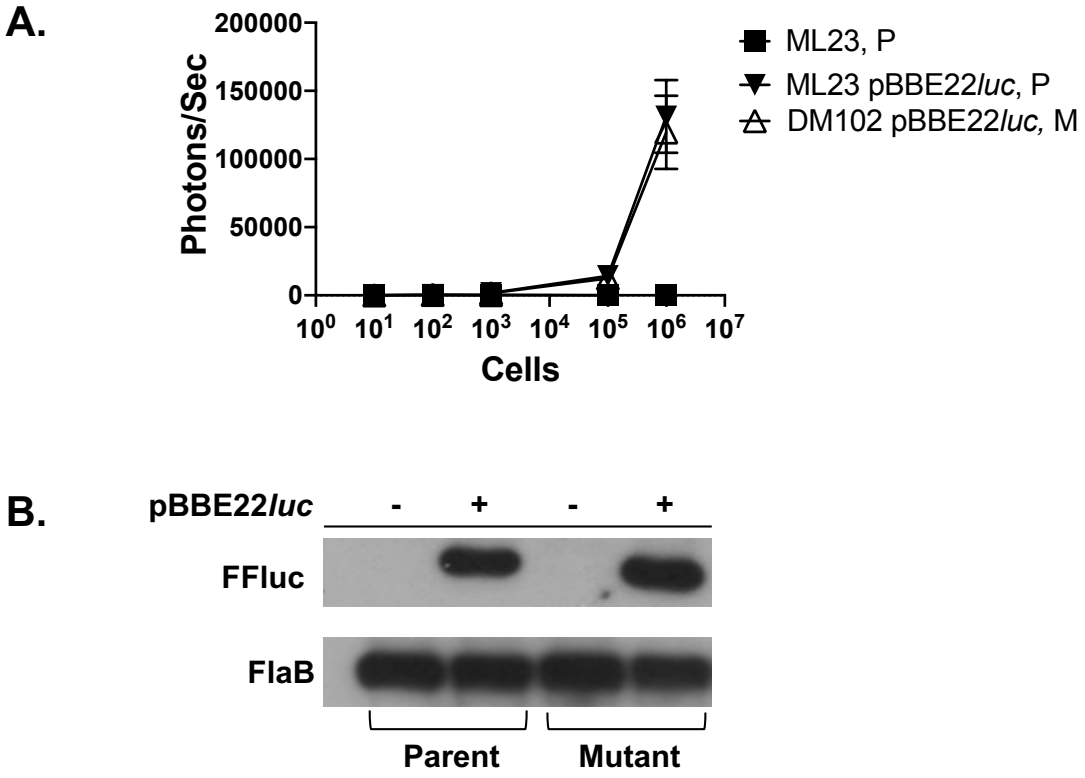

Figure 7. Bioluminescent *B. burgdorferi* strains display similar light emission and production of firefly luciferase protein. (**A**) Equivalent light is produced in the strains tested. Borrelial parent strains, ML23 and ML23/pBBE22*luc* (P), as well as the SR0725 sRNA mutant DM102/pBBE22*luc* (M), were grown to mid-log phase and serially diluted from 10^6 to 10 cells and incubated with D-luciferin. Parent strain ML23, without the plasmid encoding for firefly luciferase (pBBE22*luc*), was used as a negative control. Luminescence was measured for each sample after subtracting the background levels observed in complete BSK-II media. Cultures for all strains were grown in triplicate and the resulting luminescent values were averaged. There was no statistical significance in the amount of light emitted between the strains. (**B**) Similar amounts of luciferase protein are produced in the strains tested. Protein lysates from *B. burgdorferi* strains with and without the plasmid pBBE22*luc* were tested for the production of firefly luciferase (FFluc). Samples were immunoblotted and probed with antisera to antigen indicated on the left. Constitutively produced borrelial FlaB was used as a control for cell equivalents between samples.

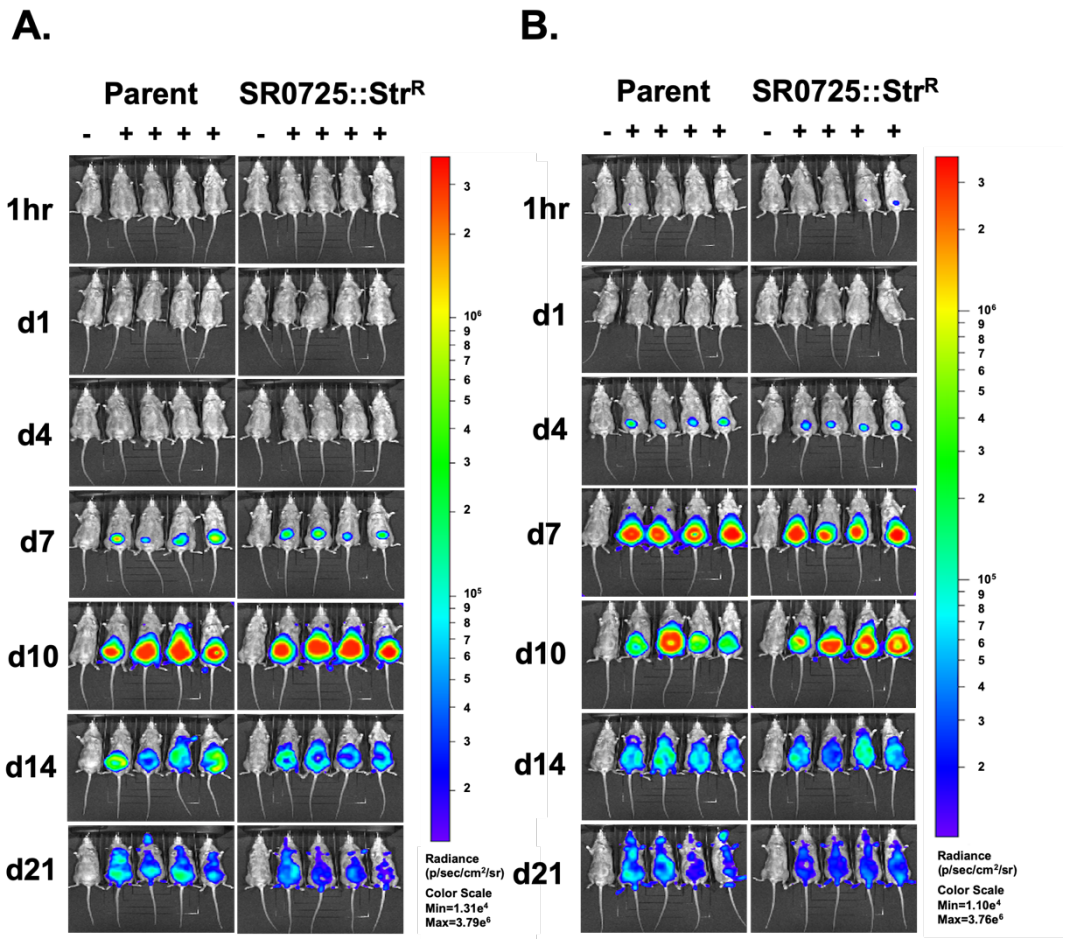

Figure 8. Temporal and spatial tracking of *B. burgdorferi* strains following infection with 10^3 and 10^5 spirochetes. C3H mice were infected with either the parent strain (ML23/pBBE22*luc*) or the SR0725 sRNA mutant (DM102/pBBE22*luc*) at a dose at 10^3 (**A**) and 10^5 (**B**). Mice were infected for 21 days and imaged on the time or day (d) listed on the left. For each image shown, the mouse on the far left (denoted with a '−') was infected with *B. burgdorferi* but did not receive D-luciferin to serve as a background control. Mice denoted with a '+' were infected with the strain indicated and treated with D-luciferin to promote light emission. All images were normalized to the same scale (shown on the right).

A.

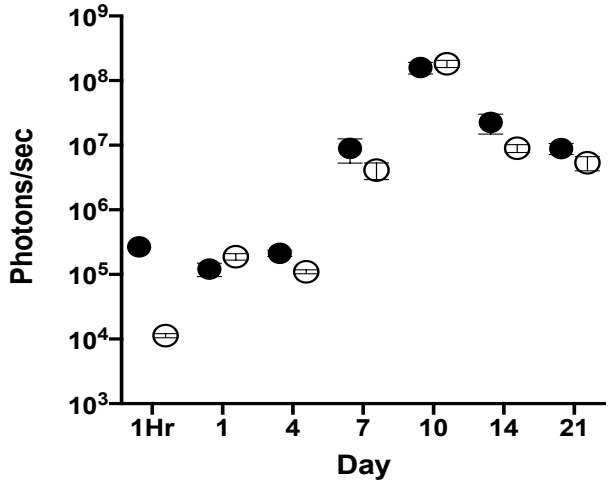

B.

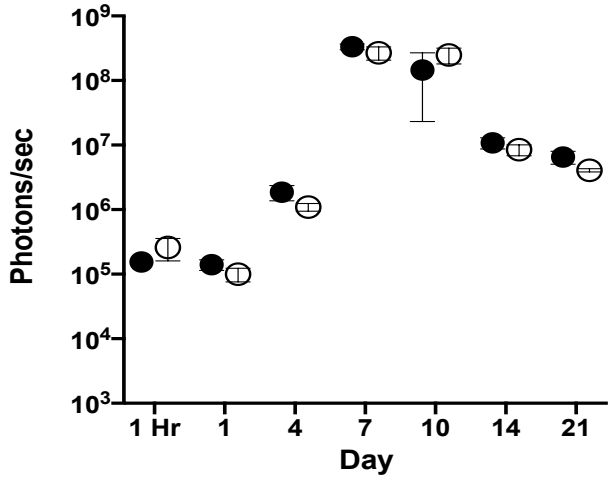

Figure 9. Quantification of *in vivo B. burgdorferi* luminescence. Mice were infected with parent strain, ML23/pBBE22*luc,* depicted as black circles and the SR0725 sRNA mutant, DM102/pBBE22*luc,* as open circles with 10^3 (**A**) and 10^5 dose (**B**). Mice were treated with D-luciferin at 1 hour and at 1, 4, 7, 10, 14 and 21 days post-infection and 1 minute exposure images were obtained for quantification photons/sec of the entire mouse body. Luminescence measurements were normalized by subtracting background values obtained from an infected mouse not treated with D-luciferin. Each time point represents the average value and the standard error. Two-way analysis of variance (ANOVA) was employed to the strains and no differences in luminescence were observed.

Table 5. Infectivity of the sRNA mutant strain DM102 relative to its parent[a].

Strain	Dose	Pinna[b]	Skin[c]	Lymph node	Heart	Bladder	Joint	Total sites
ML23 pBBE22*luc* (Parent)	10^3	4/5	4/5	4/5	4/5	4/5	4/5	24/30
ML23 pBBE22*luc* (Parent)	10^5	5/5	5/5	5/5	5/5	5/5	5/5	30/30
DM102 pBBE22*luc* (Mutant)	10^3	4/5	4/5	4/5	4/5	4/5	4/5	24/30
DM102 pBBE22*luc* (Mutant)	10^5	5/5	5/5	5/5	5/5	5/5	5/5	30/30

[a] C3H mice were used for the infection; [b] represents cultivation from the ear pinna; [c] represents the site of inoculation, i.e., skin from abdomen.

These results indicate that the SR0725 sRNA is not required for experimental infection by *B. burgdorferi*.

Isolation of B. burgdorferi individual colonies by semisolid plating

To identify additional sRNAs associated with virulence, four Tn mutants that mapped to sRNAs were tested by PCR using primers flanking the insertion site to determine if they were mixed populations or if the Tn was present at the correct insertion site (Table 6 and Table 8). The mutant strains T04TC388, T09TC160, and T04TC171 were found to contain the Tn at the insertion site and no additional PCR products were detected in the specific locale (Table 6; data not shown). However, the Tn insertion strain T05TC355 (Tn355) amplified two PCR products, suggesting it was a mixed population (Fig. 10A). The parent strain amplified an 894 bp fragment consistent with a non-mutagenized sequence while the Tn mutant strain Tn355 demonstrated a 2.3 kb fragment due to the presence of the transposable element (Fig. 10A). To isolate an isolate from the mixed population of Tn355 with only Tn at the correct insertion site, the culture was plated in semi-solid agarose to obtain individual colonies (186). Single colonies were selected, expanded in BSK-II media, and DNA extraction was performed for subsequent PCR analysis using the primers that flanked the Tn insertion (Table 8). As observed in Fig. 10B, a representative isolate amplified an appropriate sized PCR product. The four Tn isolates can now be tested to determine infectivity potential in the murine model of Lyme borreliosis.

Table 6. PCR analysis of additional intergenic Tn mutants of sRNAs[a] for future animal experiments to determine infectivity potential.

Name of Tn[b]	Replicon	Location	Insertion site	Isolate[c]	Single colony isolation[d]
T05TC355	Plasmid lp54	IG *bba34-bba36*	23489	Mixed population	Yes
T04TC388	Plasmid lp54	IG *bba16-bba18*	11280	Tn present	N/A
T09TC160	Plasmid lp38	IG *bbj37-bbj41*	29534	Tn present	N/A
T04TC171	Chromosome	IG *bb0645-bb0646*	684984	Tn present	N/A

[a] sRNAs from *B. burgdorferi* sRNA library (Popitsch *et al*., 2017); [b] transposon mutants from the *B. burgdorferi* Tn library (Lin *et al.,* 2012); [c] primers that flank the Tn insertion were used to determine if Tn is present in the correct locale; [d] mixed populations of transposon mutants were made clonal by semi solid BSK-II plating, isolation of single colony and confirmation by PCR.

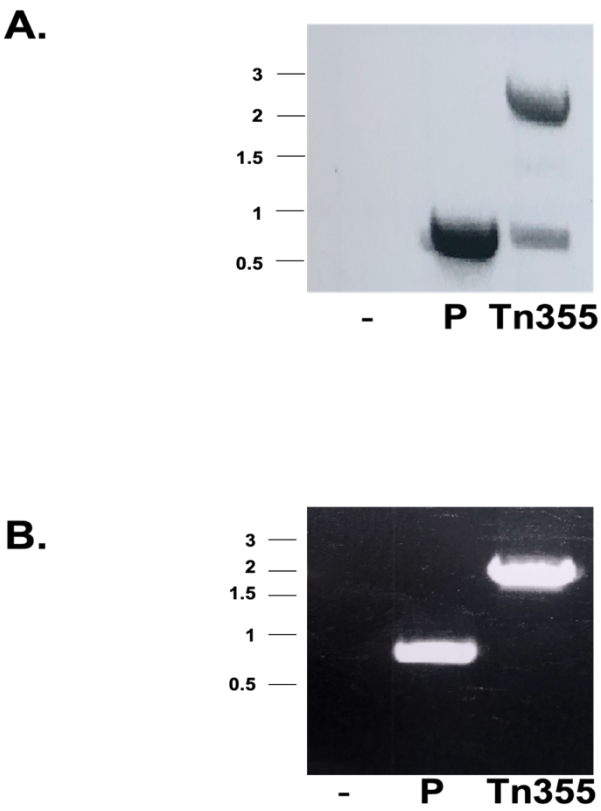

Figure 10. Isolation of transposon mutant T05TC355 (Tn355) with Tn in correct locale. (**A**) Primers that flank the T05TC355 transposon mutant were used to determine if the stock was a mixed population. (**B**) Individual colonies of strain T05TC355 were isolated by semisolid agarose BSK-II plating, selected for outgrowth, and checked by PCR for a single amplified species due to the desired Tn insertion site. DNA ladder on the left of the image is shown in kilobases.

Discussion

In this study, we utilized the *B. burgdorferi* Tn mutant library (189), coupled with Tn-seq (Table 1, L. Hu *et al*., unpublished data), to identify putative sRNAs (161) involved in *B. burgdorferi* infectivity. Bacteria sRNAs have been found to regulate virulence genes in a post-transcriptional manner by binding to transcripts and increasing and/or decreasing translation of genes (149,150,152). We hypothesized that *B. burgdorferi* use sRNAs to promote their pathogenic potential. To confirm the phenotype previously seen in the Tn-seq screen of the *B. burgdorferi* Tn library (Table 1, L. Hu *et al*., unpublished data), we performed single infections of a subset of seven transposons of sRNAs (Table 3). Of the seven Tn strains tested, three displayed an attenuated phenotype (Table 3).

The inconsistency observed when the attenuated phenotypes of the Tn-seq, assessed in the single infection analysis, highlights the importance of confirming candidates that stem from a Tn-seq screen. Tn mutants lost in a Tn-seq screen can be fitness-independent by population constrictions due to experimental bottlenecks where Tn mutants are lost due to chance instead of their inability to cause infection (190,192,198). In *B. burgdorferi*, a bottleneck effect can occur at the site of inoculation, where the innate immune response limits bacterial loads (198). However, experimental bottlenecks can be reduced by combining results from multiple animals experimentally infected with the same inoculum (190). In addition, Tn-seq lacks plasmid content information of the transposon mutants; that is, the loss of a particular Tn mutant in a Tn-seq screen can be related to plasmid loss in the strain and independent of the Tn insertion event (190).

Strain Tn273 contains a Tn insertion in the SR0725 sRNA (161). Specifically, the SR0725 sRNA sits between *bbd04* and pseudogene *bbd05a* that maps to the 17 kilobase linear plasmid (lp17) of *B. burgdorferi* strain B31 (161). Mice infected with Tn273 displayed an attenuated phenotype (Table 3). To independently confirm this phenotype, we created a strain with the genetic inactivation of the SR0725 sRNA (Fig. 4) in our parent strain ML23 (40,41,181,204,205). *In vitro* growth of parent and mutant strains showed no differences (Fig. 6). Subsequent *in vivo* imaging of the infectious process showed no differences in light emission when the parent and mutant SR0725 sRNA strains were compared (Fig. 8). Most tissues were infected in the SR0725 sRNA mutant in both doses and the infectivity observed was identical to the parent (Table 5). This indicates that the SR0725 sRNA is dispensable for experimental murine infection of *B. burgdorferi*. The possibility of SR0725 playing a role in tick colonization, acquisition or transmission of *B. burgdorferi* remains to be tested.

It was unexpected that two different strategies to inactivate a target sRNA exhibited contrasting results in mice, notably, the transposon mutant phenotype as compared to the genetic insertion mutant. Both genetic backgrounds used for the mutant strains are derivatives from *B. burgdorferi* sensu stricto strain B31 (181,209). The transposon mutant background strain is 5A18NP1 (209), while the parent strain used for the genetic inactivation is strain ML23/pBBE22*luc* (40,41,181,204,205). The genetic parent of the transposon mutant (5A18NP1), lacks linear plasmids lp28-4 and lp56, but retains infectivity in mice (209). ML23 lacks lp25 (181). The absence of lp25 in ML23 renders it non-infectious in the mammalian host (181,183).

However, when the lp25 *bbe22* gene, encoding a nicotinamidase (PncA), is added back in *trans*, infectivity in this background is restored (39–41,183,204). Taken together, both parental strains are infectious in the mammalian host.

The inoculum dose for the mice infected with the Tn insertion strain between *bbd04* and *bbd05a* (Tn273) was 10^4 organisms (Table 3). This infection yielded 12/24 culture positive tissues with 2 out of 4 mice infected (Table 3). The genetic inactivation of the SR0725 sRNA (i.e., strain DM102) was completely infectious in all tissues tested at doses of 10^3 and 10^5 organisms with the lone exception of one mouse infected at the 10^3 dose that was not infected for either strain (Table 5). Both the Tn mutant (Tn273) and the SR0725 sRNA mutant (strain DM102), used C3H/HeN mice for the infectious model and were infected via the intradermal route for a 21 day duration. It is unlikely that the differences in infectivity observed are due to the different doses administered because, for both genetic backgrounds, the doses utilized were higher than the ID_{50} of each strain tested. For example, the ID_{50} of the Tn parent 5A18NP1 is estimated at 83 organisms (209) whereas the ID_{50} of the parent strain ML23/pBBE22*luc* is approximately 150 organisms (39).

One possibility for the difference in infectivity observed between the strains is that the Tn insertion has a polar effect on the *bbd05a* pseudogene. The SR0725 sRNA sits between gene *bbd04* and the *bbd05a* pseudogene. The SR0725 sRNA is physically closer to the *bbd05a* pseudogene, i.e., approximately 80 nucleotides upstream, whereas the gene on the other flank, *bbd04,* is greater than 1.1 kb away. In strain Tn273, the Tn insertion is 130 nucleotides upstream of *bbd05a*; however, since *bbd05a* expression has not been tested in the Tn strain, it is not known if the

strain generates a *bbd05a* RNA species. The parent strain ML23 and the SR0725 sRNA mutant strain DM102, both express the pseudogene *bbd05a* (Fig. 5). Analysis of the *bbd05a* sequence identified multiple premature stop codons. The first one produces a 30 amino acid long protein, instead of its full length 196 amino acid protein (data not shown). This suggests that *bbd05a* is transcribed (Fig. 5), but the protein it translates is truncated (data not shown). Furthermore, *bbd05a* pseudogene is downregulated when *B. burgdorferi* is cultivated *in vitro* at 37°C, as well as with the addition of blood, suggesting that *bbd05a* is poorly expressed during mammalian infection (75).

It is plausible that the plasmids missing in the transposon mutant, which are present in the ML23 and DM102 background, have hypothetical genes and/or regulatory sequences, such as sRNAs, that optimize the pathogenic potential of *B. burgdorferi*. The Tn273 strain is missing plasmids lp38, lp28-4, and lp56 (data not shown). The absence of lp56 correlates with lower number of spirochetes in ticks after feeding on mice (210), but its absence does not influence mouse infectivity. *B. burgdorferi* lacking lp38 are fully infectious in mice and can be acquired by ticks (211). Previously in our lab, the loss of lp28-4 in the *B. burgdorferi* B31 clonal derivative MSK7 exhibited a 1-log-unit increase in ID_{50} relative to B31 derivative containing all plasmids, MSK5 (181). One hypothesis posits that sequences in lp28-4 may contribute to the increased infectivity of ML23 and DM102 over Tn273. No known virulence determinants map to lp28-4 but several surface proteins of unknown function are encoded on this plasmid. It is possible that one or more of

these genes and the proteins they encode contribute to the differences observed. Further experimentation is needed to address this possibility.

Recently, the *en masse* deletion of the borrelial genes *bbd01* to *bbd05* (*bbd05a*) from lp17 did not alter the infectivity of this strain following experimental infection in mice (212). This region encompass the SR0725 sRNA (161). These results support our findings that the SR0725 sRNA is dispensable in experimental mouse infections (Fig. 8 and Table 5). This leads us to speculate that the Tn273 strain must have additional mutations that affect its fitness in mice. The strain might have incorporated additional Tn insertions in other parts of the genome that may be contributing to its reduced fitness independent of the Tn in the SR0725 sRNA.

Experimental Procedures

Bacteria strains and culture conditions

Escherichia coli strains were grown aerobically at 37°C in Luria Broth (LB) media. Concentration of antibiotics used for selective pressure in *E. coli* are as follows: kanamycin, 50 μg/ml and spectinomycin, 50 μg/ml. *B burgdorferi* strains were grown in BSK-II media supplemented with 6% normal rabbit serum (Pel-Freez Biologicals, Rogers, AR) under conventional microaerobic conditions at 32°C, pH 7.6, under 1% CO_2 atmosphere. *Borrelia burgdorferi* B31 ML23 (181) and derivative strains were grown under antibiotic selective pressure, dependent on genetic composition, with kanamycin at 300 μg/ml or streptomycin at 50 μg/ml. *B. burgdorferi* 5A18NP1 (209) was grown in the presence of kanamycin at 300 μg/ml

and the *B. burgdorferi* transposon mutants (189) were grown in the presence of both gentamicin at 50 μg/ml and kanamycin at 300 μg/ml.

Table 7. Strains and plasmids used in this study.

***E. coli* strains**	**Genotype**	**References**
Mach-1^{TM} -T1^{R}	F^{-} φ80(*lacZ*)ΔM15 Δ*lacX74 hsdR*(r_K^- m_K^+) Δ*recA1398 endA1 tonA*	Invitrogen
***B. burgdorferi* strains**		
ML23	*B. burgdorferi* B31 clonal isolate missing lp25; parent strain.	(181)
ML23 pBBE22*luc*	Clonal isolate of strain B31 lacking lp25; shuttle vector encodes *bbe22* and *B. burgdorferi* codon optimized *luc* gene under the control of a strong borrelial promoter (P_{flaB}-luc); Kan^{R}.	(41)
DM102	ML23, IG sRNA SR0725::Str^{R}.	This study
DM102 pBBE22*luc*	ML23, IG sRNA SR0725::Str^{R} ;contains shuttle vector (P_{flaB}-luc); Kan^{R}.	This study
5A18NP1	*Borrelia burgdorferi* B31 clone missing lp28-4 and lp56 with disruption of *bbe02*::Kan^{R}.	(209)
T04TC273	5A18NP1 background, Kan^{R} and Gen^{R}, Tn IG *bbd04-bbd05a*	(189)
T06TC412	5A18NP1 background, Kan^{R} and Gen^{R}, Tn IG *bbd18-bbd21*	(189)
T10TC061	5A18NP1 background, Kan^{R} and Gen^{R}, Tn IG *bba66-bba68*	(189)
T04TC388	5A18NP1 background, Kan^{R} and Gen^{R}, Tn IG *bba16-bba18*	(189)

Table 7. Continued.

***B. burgdorferi* strains**	**Genotype**	**References**
T05TC355	5A18NP1 background, Kan^R and Gen^R, Tn IG *bba34-bba36*	(189)
T09TC160	5A18NP1 background, Kan^R and Gen^R, Tn IG *bbj37-bbj41*	(189)
T04TC171	5A18NP1 background, Kan^R and Gen^R, Tn IG *bb0645-bb0646*	(189)
T11TC387	5A18NP1 background, Kan^R and Gen^R, Tn IG *bbb03-bbb04*	(189)
T10TC351	5A18NP1 background, Kan^R and Gen^R, Tn IG *bbb13-bbb14*	(189)
T08TC464	5A18NP1 background, Kan^R and Gen^R, Tn IG *bbh36a-bbh36b*	(189)
Plasmids		
pCR®-Blunt	pCR®-Blunt vector, Kan^R, $Zeocin^R$.	Invitrogen
pKFSS1	*B. burgdorferi* shuttle vector containing P_{flgB}-Str^R cassette; $Spec^R$ in *E. coli,* Str^R in *B. burgdorferi.*	(206)
pBBE22*luc*	Borrelial shuttle vector containing *bbe22* and *B. burgdorferi* codon-optimized *luc* gene under the control of a strong borrelial promoter (P_{flaB}-*luc*); Kan^R.	(41)
pDM102	*B. burgdorferi* IG SR0725 sRNA mutant construct. Contains sequences 1213 bp upstream of the sRNA, the P_{flgB}-Str^R cassette from pKFSS1 inserted into the sRNA sequence, and sequences 1478 bp downstream of the sRNA; pCR®-Blunt vector backbone; Str^R and Kan^R.	This study

Tn-seq

The Tn-seq screen consisted of a single pool containing the entire Tn library of 4,479 clones grown *in vitro* in BSK-II media. The Tn library was grown for 48 hours in the presence of kanamycin and gentamicin. Cell density was determined by dark-field microscopy. Groups of six 9-14 week old C3H/HeJ mice (Jackson laboratories) were injected in the right flank with $5x10^5$ *B. burgdorferi* by needle inoculation. As a control to prevent *in vitro* growth defects from affecting the results of the *in vivo* screen, $5x10^5$ organisms from the inoculum used to inject the mice were cultured in 12 ml BSK-II media supplemented with kanamycin and gentamicin. The *in vitro* control cultures were grown for 3 days to parallel time in culture for the tissue cultures. The bacteria in the culture were collected using centrifugation for 20 minutes at 3,000 rcf and the pellet frozen at -80ºC.

The mice infected with the transposon library were sacrificed two weeks post-infection. The tibiotarsal joint closer to the inoculation site was removed under aseptic conditions. The tibiotarsal joints from each group of injected mice were cultured together in 12 ml of BSK-II media supplemented with kanamycin and gentamicin. The cultures were checked daily for growth. When the density of the cultures reached late exponential phase, the bacteria were centrifuged and the pellet frozen as described above. Genomic DNA was obtained from the frozen bacteria pellets using a DNeasy Blood and Tissue Kit (Qiagen, Valencia, CA) as per the manufacturer's instructions. The preparation of the libraries for sequencing was performed as described previously (200).

Genetic inactivation of the B. burgdorferi intergenic SR0725 sRNA

The intergenic (IG) small regulatory RNA (sRNA) SR0725 located between gene *bbd04* and pseudogene *bbd05a* in lp17 was inactivated by the elimination of 32 bases (nucleotides 2,888-2,920) and the insertion of P_{flgB}-*aadA* (streptomycin resistant; Str^R) antibiotic cassette (206) via homologous recombination. The DNA sequences that flanked the sRNA locus were amplified using PCR with PrimeSTAR GXL polymerase (Takara, Mountain View, CA). For the upstream fragment, a 1.2 kb fragment was amplified using primers d04US-F and US-SpecR (Table 8). A separate 1.2 kb fragment containing the P_{flgB}-Str^R cassette was PCR amplified from pKFSS1 (206) using the oligonucleotide primers pair US-SpecF and SpecDS-R (Table 8). An additional 1.5 kb PCR product, which amplified sequences downstream from the SR0725 sRNA, was engineered with primers SpecDS-F and DS-R (Table 8). All three fragments had 20 base pair overlap sequences and were assembled by overlap PCR (213,214) as previously described (40,204). All inserts were cloned into pCR®-Blunt (Invitrogen, Carlsbad, CA) and verified by Sanger sequencing prior to transformation into Mach-1™ competent cells (Invitrogen, Carlsbad, CA).

Transformation of B. burgdorferi

Plasmids were linearized with *Xho*I prior to transforming into *B. burgdorferi* strain B31 derivative ML23 made competent as previously described (39,40,188,204). Borrelial plasmid content was confirmed by PCR (181) to determine the plasmid content of SR0725 sRNA mutant.

Table 8. Oligonucleotides used in this study.

Oligonucleotides	5'-3'	Use
P1	CTGGGGCACTATTTGG	Primers used to confirm the sRNA mutant.
P2	AATTAATTAGGAAGCATTATCTGATTTTTAAACTTTTTCA	Primers used to confirm the sRNA mutant.
P3	TGAAAGCTTTAGAGGCCTTTCAATTGGCGTGGAAGATTTC	Primers used to confirm the sRNA mutant.
P4	CTAATAATTGAGTATTAAATATTCTCC	Primers used to confirm the sRNA mutant.
Tn273F Tn273R	GCGATAAGGGCTTTAAGTAAC CTCCAATTGTACACTAC	Primer pair that flanks Tn in strain T04TC273. PCR product is 534 bp in the parent strain and ~1.5 kb larger in Tn mutant.
Tn412F Tn412R	GCTTCATATTGAGAATTTCC GCCTCTACCGATATC	Primer pair that flanks Tn in strain T06TC412. PCR product is 409 bp in the parent strain and ~1.5 kb larger in Tn mutant.
Tn355F Tn355R	GAGATTACAGTAGCAATGC GAAATATTGTCAAAAGAGC	Primer pair that flanks Tn in strain T05TC355. PCR product is 894 bp in the parent strain and ~1.5 kb larger in Tn mutant.
Tn061F Tn061R	GGGTACGGTTGTAACGGCTTGAATAG ATACTTTAAAACCTGCCTTTTAC	Primer pair that flanks Tn in strain T10TC061. PCR product is 998 bp in the parent strain and ~1.5 kb larger in Tn mutant.
Tn388F Tn388R	CAGGTAAATGGGAAGACAG CAAGAGTTGGGCTTGGGTGAAGG	Primer pair that flanks Tn in strain T04TC388. PCR product is 467 bp in the parent strain and ~1.5 kb larger in Tn mutant.
Tn171F Tn171R	GCCACTAAGGTTATTATTGGGC CGCAATTATTGCAATGATGGGCC	Primer pair that flanks Tn in strain T04TC171. PCR product is 546 bp in the parent strain and ~1.5 kb larger in Tn mutant.
Tn160F Tn160R	GCACCTAAAGTGTGCTTGGATG GGAAAGGTCGATCCAAAACCCG	Primer pair that flanks Tn in strain T09TC160. PCR product is 565 bp in the parent strain and ~1.5 kb larger in Tn mutant.
Tn387F Tn387R	GTACTAGGATGCATAATAAACC CCACTTCCTCATATTTTAGCGGG	Primer pair that flanks Tn in strain T11TC387 PCR product is 651 bp in the parent strain and ~1.5 kb larger in Tn mutant.

Table 8. continued.

Oligonucleotides	5'-3'	Use
D04US-F USspecR	CTGGGGCACTATTTGG GAAATCTTCCACGCCAATTGAAAGGCCTCTAAAGCTTTCA	Primer pair used to amplify 1213 bp of the flanking region upstream of the sRNA SR0725 in lp17. Amplicon has 20 bp at the 3' end with homology to the 5' end of P_{flgB}-$Spec^R$ of pKFSS1 (206).
USspecF SpecDSR	TGAAAGCTTTAGAGGCCTTTCAATTGGCGTGGAAGATTTC AATTAATTAGGAAGCATTATCTGATTTTTAAACTTTTTCA	Primer pair used to amplify 1226 bp region of P_{flgB}-$Spec^R$ (206). The 5' end has 20 bp with homology to the 3' end of the upstream flanking region. The 3' end of the amplicon has 20 bp with homology to the 5' end of the downstream flanking region.
SpecDSF D05DS-R	TGAAAAAGTTTAAAAATCAGATAATGCTTCCTAATTAATT CTAATAATTGAGTATTAAATATTCTCC	Primer pair used to amplify the downstream flanking region of 1478 bp. The amplicon has 20 bp at the 5' end with homology to the 3' end of P_{flgB}-$Spec^R$ (206).
*bbd05a*F *bbd05a*R	CAATGAAAATCTATAAAAAACGGGC CAATACAAGATTTAGTAAAGCG	Primer pair used to amplify 508 bp of pseudogene *bbd05a* for RT-PCR.
Tn464F Tn464R	GGCGGTAGTATGTGTTGAT GCTATGGTAAAGCTCATTTG	Primer pair that flanks Tn in strain T08TC464 PCR product is 619 bp in the parent strain and ~1.5 kb larger in Tn mutant.
Tn351F T351R	GAATAATAAGTTGGCTACCAC CCTTTATTGCTGCTGGATGGAAC	Primer pair that flanks Tn in strain T10TC351 PCR product is 411 bp in the parent strain and ~1.5 kb larger in Tn mutant.

RNA Isolation for conventional RT-PCR

Cultures of *B. burgdorferi* strains ML23 (181) and the SR0725 sRNA mutant strain DM102, were grown to mid-log phase (i.e., 5 x10^7 cells per ml) under conventional microaerophilic conditions of 32°C, pH 7.6, and 1% CO_2. The cultures were centrifuged at 4500 x *g* for 20 minutes at 4°C, washed with 1 ml PBS, and centrifuged at 14,000 rpm for 15 minutes. The pellet was resuspended in 100 μl of sterile water and 300 μl of TRIzol (Invitrogen, Carlsbad, CA) was added prior to employing the Direct-zol RNA Miniprep system (Zymo Research, Irvine, Ca, USA)

for total RNA isolation. The resulting RNA was treated with DNAse I (Roche, Indianapolis, IN) and RNAsin (Promega, San Luis Obispo, CA) to eliminate contaminating DNA and inhibit RNAse activity, respectively. For the conventional RT-PCR of the *bbd05a* pseudogene, 200 ng of total RNA from conventionally grown *B. burgdorferi* cells were used for reverse transcription into cDNA using primer *bbd05a*R with SuperScript III (Thermo Fisher Scientific, Waltham, MA). The primer pair *bbd05a*F and *bbd05a*R from Table 8 were used to detect *bbd05a* expression in the strains.

In vitro bioluminescence assay

Bioluminescence of strains following *in vitro* growth was quantified as done previously (41). Briefly, parent strains ML23 and ML23/pBBE22*luc*, as well as the SR0725 sRNA mutant DM102/pBBE22*luc,* were grown to mid-log phase and concentrated to 10^8 cells/ml. Cells were serially diluted from 10^7 to 100 cells/ml and 100 µl of the appropriate dilutions were transferred to a white flat-bottom microtiter 96 well plate. Luminescence was measured using the 2104 EnVision Multilabel Plate Reader (Perkin Elmer, Inc., Waltham, MA). All samples were treated with final concentration of 667 µM D-luciferin in PBS (GoldBio, St Louis MO). Each cell concentration for all the strains was measured for luminescence in triplicate, values were averaged, and the standard error was calculated.

Infectivity studies and bioluminescent imaging

Infectivity studies were performed as previously described (39,41). Briefly, 8-week-old C3H/HeN female mice were inoculated intradermally with 10^4 spirochetes with the different transposon mutants. For the infection of bioluminescent *Borrelia* strains, the mice were infected with either 10^3 or 10^5 of the *B. burgdorferi* parent strain ML23/pBBE22*luc* or the SR0725 sRNA mutant strain, DM102/pBBE22*luc*. Imaging of infected mice to detect bioluminescent *B. burgdorferi* strains was done as described previously (40,41,204). After 21 days, the mice were sacrificed and ear skin, abdominal skin, inguinal lymph node, heart, bladder, and tibiotarsal joint tissues were collected from each mouse aseptically and subjected to *in vitro* cultivation in complete BSK-II media.

SDS PAGE and immunoblotting

B. burgdorferi protein lysates were resolved by SDS-PAGE, and transferred to a PVDF membrane, and blocked using non-fat powdered milk as done previously (39,204). Primary antibodies were used at the following dilutions: goat polyclonal anti-Firefly luciferase (AbCam Inc., Cambridge, UK) at 1:1000 and mouse anti-FlaB (Affinity Bioreagents, Golden, CO) at 1:5,000. Secondary antibodies with horseradish peroxidase (HRP) conjugates were used to detect immunocomplexes, specifically, anti-mouse Ig-HRP (Invitrogen, Carlsbad, CA, USA) or anti-goat Ig-HRP (Thermo Fisher Scientific, Waltham, MA) both diluted to 1:5,000. Following incubation with both primary and secondary antibodies, the membranes were washed extensively in PBS, 0.2% Tween-20 and developed using the Western

Lightning Chemiluminescent Reagent plus system (Perkin Elmer, Waltham, MA, USA).

Semisolid plating for B. burgdorferi cells

To isolate individual colonies, the Tn strain T05TC355 (Tn355) was grown to mid-log phase and plated in semisolid BSK-II agarose overlays (186). Briefly, BSK-II agarose underlay with antibiotics kanamycin at 300 μg/ml and gentamicin at 50 μg/ml, was poured in sterile petri dishes and allowed to solidify. Next, dilutions were made for the strain T05TC355 for colony forming units (CFU) of 100, 50 and 25 cells in 1 ml of BSK-II media. The cells were mixed with BSK-II agarose and the overlay was poured on top of the already solidified underlay. Plates were placed in incubator under conventional microaerophilic conditions of 32°C, pH 7.6, 1% CO_2. *B. burgdorferi* colonies appeared approximately 10 days after plating and colonies were selected, placed in liquid BSK-II media for expansion with appropriate antibiotics, and tested for the Tn presence by PCR using primers from Table 8 and PrimeSTAR GXL polymerase (Takara, Mountain View, CA).

Statistical analysis

For the analysis of the *in vivo* luminescence of mice, two-way analyses of variance (ANOVA) was performed. Statistical significance was accepted when the *P* values were less than 0.05 for all statistical analyses employed.

CHAPTER III

THE INTERGENIC SMALL NON-CODING RNA SR0736 IS REQUIRED FOR OPTIMAL INFECTIVITY AND TISSUE TROPISM IN *Borrelia burgdorferi*

Introduction

In the previous Chapter, we utilized *Borrelia burgdorferi* transposon mutants (189) that map to putative intergenic sRNAs (161) to determine if these sRNA mutants resulted in attenuated phenotypes in the murine experimental model. From the initial screen, the intergenic sRNA SR0736, located in between genes *bbd18* and *bbd21* of linear plasmid 17, was significantly attenuated in the mammalian host. The characterization of SR0736 in the mammalian host serves as the basis for this Chapter of the dissertation.

Bacterial gene expression is predominantly regulated at the transcriptional level. In *B. burgdorferi,* several transcriptional regulators have been identified and characterized, as well as a growing list of DNA interacting proteins, which serve to alter borrelial gene expression either directly or indirectly (12,64,76,83,88–91,128,129,134,205,215–217). Many of these regulators govern, in part, the production of surface proteins involved in borrelial virulence (77,87,89,218). In addition to these regulators, recent results indicate that *B. burgdorferi* produces a battery of small, non-coding RNA molecules, designated sRNAs (161,178,219). The

influence of how these sRNAs affect transcripts in *B. burgdorferi,* or their impact on borrelial pathogenesis, is not well understood.

Post-transcriptional regulation via sRNAs is an RNA-based gene regulation found to globally modulate gene expression in bacteria, including those that can affect pathogenesis (150,220,221). sRNAs can be intergenic, localized between annotated genes. Intergenic sRNAs are often *trans*-acting and genetically unlinked to the transcripts they influence (146,148,150,153,203). In general, *trans*-acting intergenic sRNAs have partial complementarity to the transcripts that they target. In addition, *trans*-acting sRNAs can target multiple transcripts (167,222). The resulting sRNA-mRNA duplex that forms can alter gene expression by affecting mRNA stability and/or translation (150,152,223,224).

Recently, the sRNA transcriptome of *B. burgdorferi* was reported and over 1,000 sRNA species were observed, many of which are upregulated at 37˚C, a condition that models the mammalian host temperature *in vitro* (161). Independently, a Luminex-based procedure for the detection of Signature-tagged mutagenesis (STM) clones of the transposon (Tn) library of *B. burgdorferi* strain B31 (189), identified several candidate sRNAs that, when genetically inactivated, exhibited infectivity deficits (189). Here, we further characterize one of these sRNAs, designated SR0736, that maps between *bbd18* and *bbd21* on the 17 kb linear plasmid (lp17). The results presented herein demonstrate that SR0736 is required for optimal infectivity of *B. burgdorferi* strain B31. Furthermore, the loss of the SR0736 led to the dysregulation of 19 transcripts suggesting its involvement in the regulation of multiple unlinked genes. Taken together, our data suggests that

SR0736 targets several unlinked genetic targets and affects their production in a manner that is required for optimal infection and dissemination throughout the host.

Results

Genetic inactivation of the SR0736 sRNA in B. burgdorferi

In Chapter II, seven transposon (Tn) mutants with a phenotype in mice were identified from a Tn-seq screen (Chapter II, Table 1; Linden Hu, *et al*., unpublished data). The individual transposons interrupting intergenic sRNAs (161), were individually tested in C3H/HeN mice at a 10^4 dose (Chapter II, Table 3). From the seven transposons, three maintained an attenuated phenotype (Chapter II, Table 3). One of the attenuated transposon mutants mapped to the sRNA SR0736 (161). The Tn mutant for SR0736 strain T06TC412, exhibited tissue tropism and severe infectivity defects with only 25% of the mice tissues colonized (Chapter II, Table 3). To independently test the role of the SR0736 sRNA in borrelial pathogenesis, we genetically inactivated SR0736 that maps between *bbd18* and *bbd21* on the 17 kilobase (kb) linear plasmid (lp17) of *B. burgdorferi* (Fig. 11A). The parent strain used is the strain B31 derivative ML23 that lacks the 25 kb linear plasmid (lp25)(41,181,204,225). Due to the absence of lp25, this strain is non-infectious but becomes infectious in the murine model of experimental infection when a region of lp25, containing the *bbe22* gene, is provided *in trans* (41,183). The shuttle vector pBBE22*luc* contains *bbe22* and the firefly luciferase reporter that facilitates bioluminescent imaging as we have done previously (40,41,204).

ML23 was transformed with pDM103 to insertionally inactivate the SR0736 sRNA (Fig. 11A). Transformants were selected in the presence of streptomycin. To test whether the SR0736 mutant candidates contained the P_{flgB}-Str^R cassette, PCR was employed to distinguish the parent from potential mutants (Fig. 11B). Oligonucleotide primers P1 and P4 (Table 11) amplify a fragment of 1 kb bp and 2.3 kb from the parent strain and mutant, respectively, due to the insertion of the P_{flgB}-Str^R cassette in the latter (Fig. 11B). Primers specific (Table 11) to the P_{flgB}-Str^R cassette amplifed a 1.2 kb fragment in the mutant but, as predicted, failed to amplify a product in the parent. Similarly, the primer pair P1 and P3 (Table 11) were only able to amplify a 1.5 kb fragment in the mutant strain (Fig. 11B). The resulting SR0736 mutant strain was designated DM103.

To genetically restore the SR0736 sRNA in a *cis* complement manner, the pDM113 construct was transformed into DM103 and selected for resistance to gentamicin and then tested for sensitivity to streptomycin. Candidates predicted to encode SR0736 were screened by PCR (Fig. 11C). Here, oligonucleotide primers (Table 11) pair P5 and P6 amplified a 324 bp PCR product in the complement but failed to amplify a product in the mutant. Primer P1 and P6 (Table 11) produce a 1.3 kb amplicon in the complement with no amplification within the mutant. Finally, primers P5 and P4 amplify a 1 kb amplicon in the complement with no product observed in the mutant. Following the aforementioned confirmation of the mutant SR0736 strain DM103 and the complement (strain DM113), both were transformed with pBBE22*luc* so they could be tested in the murine experimental model of infection.

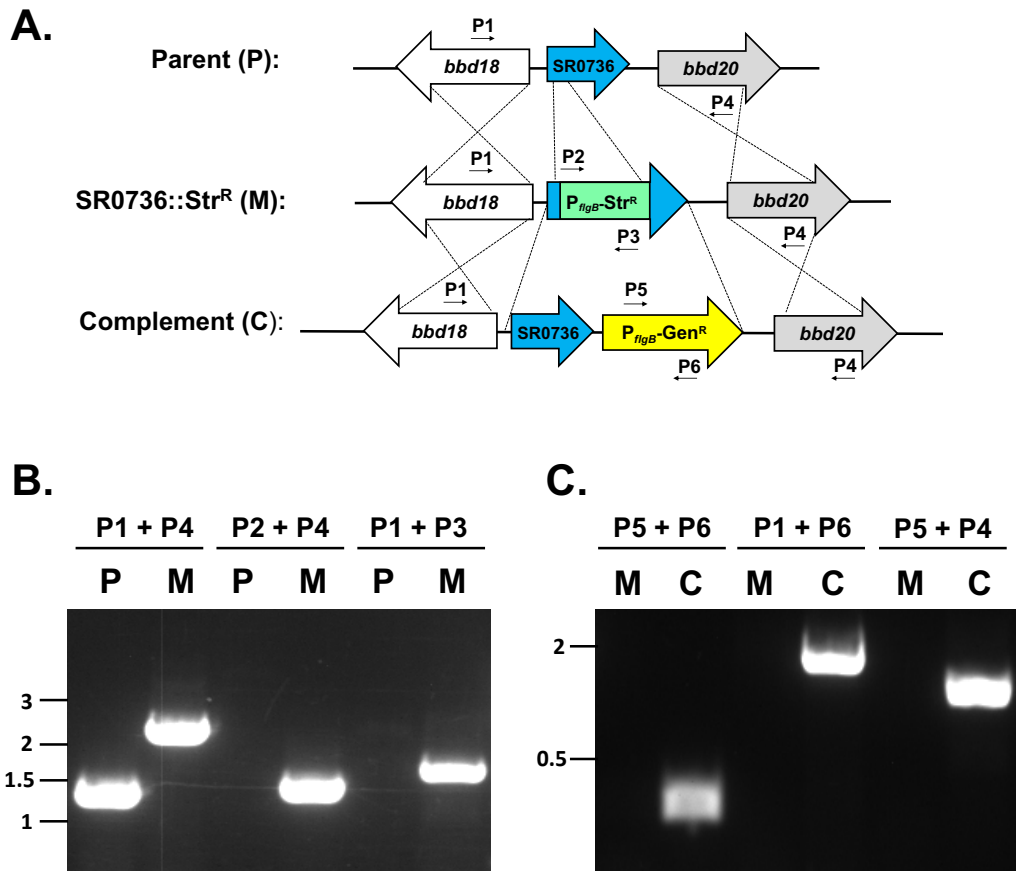

Figure 11. Strategy and confirmation of the insertional inactivation of the SR0736 sRNA. (**A**) Schematic representation of the SR0736 insertional inactivation strategy. The region of Ip17 from the parent strain (P) is shown on the top. A P_{flgB}-Str^R cassette was inserted into the 3' end of the SR0736 sRNA and the mutant, designated M, obtained following homologous recombination. Following isolation of the mutant strain, a strategy to reintroduce the SR0736 sRNA is shown below and is indicated as C for complement. (**B**) Primer pairs P1/P4, P2/P4 and P1/P3 were used to confirm the presence of the P_{flgB}-Str^R in the mutant (M), relative to its parent strain (P) by PCR. (**C**) For the *cis* complementation of the SR0736 sRNA mutant strain (M), the P_{flgB}-Str^R cassette and the flanking region were replaced by the SR0736 sRNA sequence linked to a P_{flgB}-$Gent^R$ cassette by a double crossover homologous recombination event. The resulting complement strain (C) was evaluated by PCR using primer pairs P5/P6, P1/P6 and P5/P4. Note that the distances between genetic loci are not shown to scale.

To confirm that the SR0736 mutant and complement strains lacked and restored the SR0736 sRNA, respectively, both Northern blot and Reverse Transcriptase PCR (RT-PCR) were performed (Fig. 12). Notably, the SR0736 sRNA is detected in the parent strain (P) and the complement strain (C), but not in the mutant strain (M), in both the Northern blot (Fig. 12A) and the RT-PCR analysis (Fig. 12B). Despite having a 3' insertion to inactivate the sRNA, we were unable to detect any SR0736 sequence (Fig. 12).

Considering the nature of intergenic sRNAs (e.g., between two annotated genes), one concern in deleting the SR0736 sRNA is the potential polar effect this alteration might have on expression of flanking genes. When RT-PCR was employed, no qualitative difference effect was seen for the expression of either *bbd18* or *bbd21*, the only intact encoding genes in the region (Fig. 13). Note that both *bbd19* or *bbd20* are no longer annotated as intact ORFs and, consistent with this, no transcript was detected for *bbd20* by RT-PCR for any of the strains (data not shown). Taken together, this data suggests no polar effects occur due to the inactivation of the SR0736 sRNA. The parent, the SR0736 mutant, and the *cis* complement strains all grew similarly *in vitro*, indicating that the loss of this sRNA did not impair replication of these borrelial strains under these growth conditions (Fig. 14).

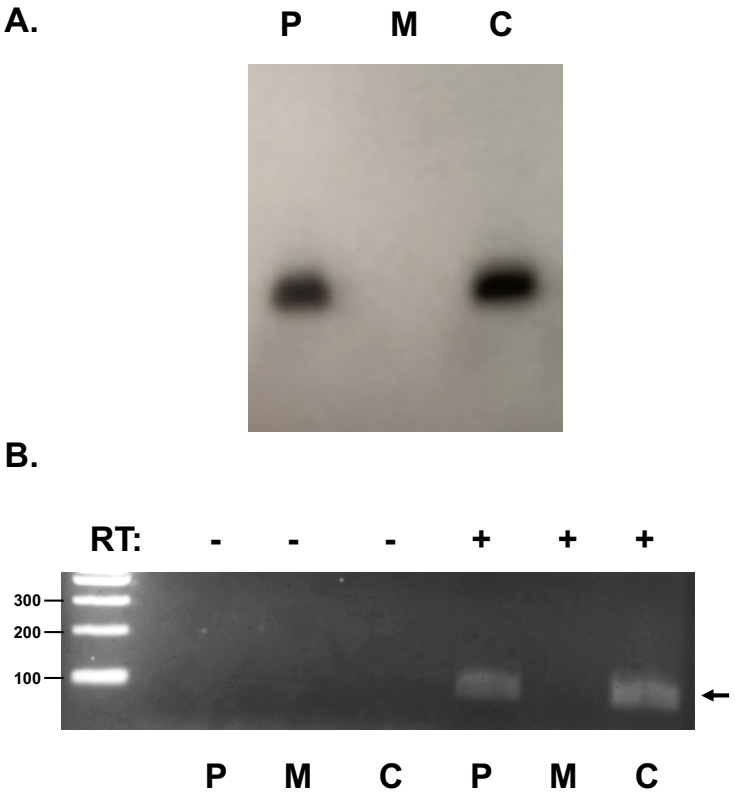

Figure 12. Confirmation that the SR0736 is not made in the mutant strain and is restored in the genetic complement. (**A**) Northern blot of total RNA isolated from the parent strain ML23 (denoted P), the SR0736 mutant strain DM103 (denoted M), and the SR0736 *cis* complemented strain DM113 (denoted C). (**B**) RT-PCR using purified total RNA from the *B. burgdorferi* parent (P), mutant (M), and genetic complement (C) strains. The first three lanes did not have reverse transcriptase (RT) added to the reactions (indicated with a "–") whereas the next three lanes included reverse transcriptase (designated with a "+"). The DNA ladder is shown to the left and base pair values are indicated. The arrow on the right indicates the presence of the sRNA species observed in the parent and complement strains.

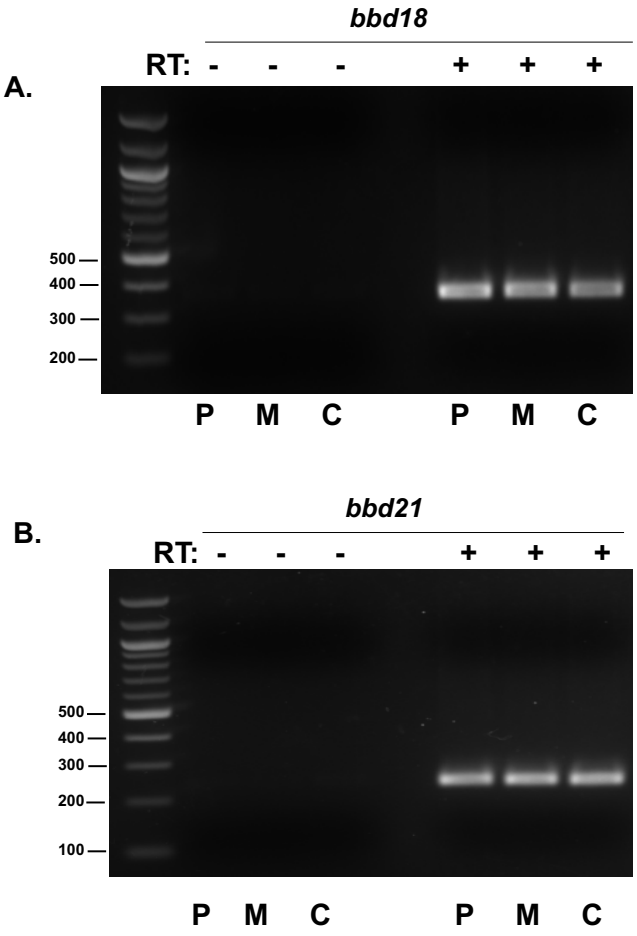

Figure 13. The expression of genes *bbd18* and *bbd21* are not affected in the sRNA mutant strain. The parent (P), sRNA mutant (M) and complement (C) strains were grown *in vitro* and total RNA was purified from each. Oligonucleotide primers specific for *bbd18* (**A**) and *bbd21* (**B**) were used without (-) and with (+) added reverse transcriptase (RT). The DNA ladder is shown at the left and the corresponding base pair values are indicated.

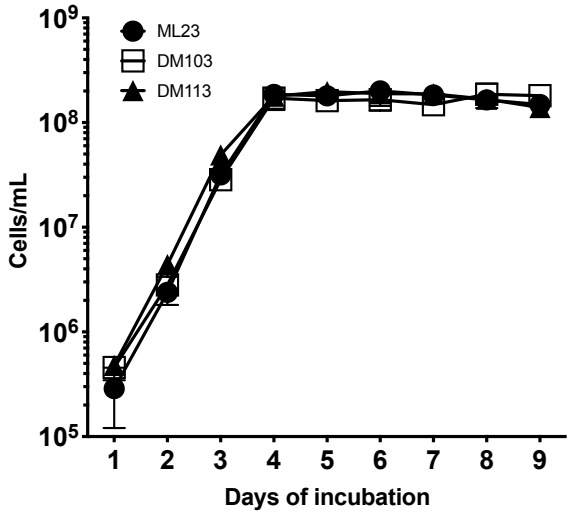

Figure 14. *In vitro* growth of the *B. burgdorferi* parent, sRNA mutant and complement strains. The *B. burgdorferi* parent strain (ML23), the sRNA mutant (DM103) and the sRNA complement (DM113) were grown in conditions of 32°C, 1% CO_2, pH 7.6 in triplicate in BSK-II media and enumerated by dark field microscopy daily out to day 9. No significant differences in growth were observed. Similar growth kinetics were observed between these three strains when the cells were grown at conditions of 37°C, 5% CO_2 and pH 6.8 (data not shown). Data points shown reflect average value with standard error.

The loss of the SR0736 attenuates B. burgdorferi infectivity

We then evaluated how the loss of the SR0736 sRNA affected murine infectivity. To spatially and temporally track infection, C3H/HeN mice were inoculated at a 10^3 dose with the parent *B. burgdorferi* strain, the SR0736 mutant, and the complement, and light emission was quantified (Fig. 15). As a background control for luminescence, a single infected mouse was not given the luciferase substrate D-luciferin (leftmost mouse in each panel, Fig. 15A). At the dose tested (10^3 *B. burgdorferi*), no signal is detected for any of the strains prior to day 4. At day 4, a clear signal is observed in mice infected with all three strains except for one mouse infected with the sRNA mutant strain (Fig. 15A). Subsequently, the signal increased with a peak at day 7 and then decreased concomitant with the development of the adaptive immune response (226)(Fig. 15A). All strains displayed similar light emission until day 10 when the sRNA mutant strain exhibited a reduction in signal and remained low through 21 days, e.g., the duration of the infectivity analysis (Fig. 15A). The quantification of *in vivo* luminescence of mice revealed significantly lower light emission by the sRNA mutant compared to the parent on days 10 and on day 14 of infection (Fig. 15B). The complement strain emitted more light than the sRNA mutant on days 7, 14 and 21 (Fig. 15B). These results demonstrate that the parent and complement display similar light emission and exhibit similar bacterial load relative to the signal observed for the sRNA mutant (Fig. 15).

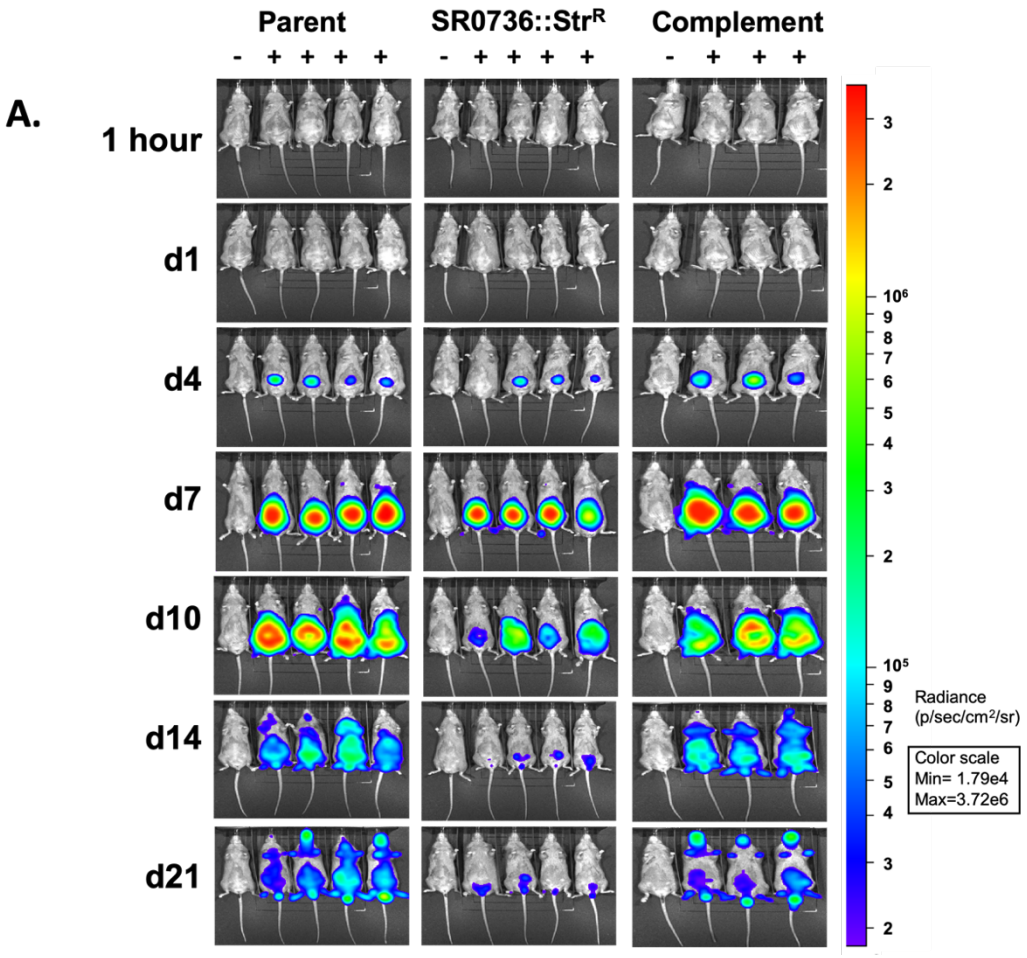

Figure 15. Spatial and temporal infectivity analysis of the SR0736 mutant. (**A**) The fate of bioluminescent *B. burgdorferi* strains were tracked following the infection of C3H mice with 10^3 of each *B. burgdorferi* isolate. Mice were infected for 21 days total with the parent, SR0736 sRNA mutant, and the SR0736 genetic complement and imaged on the time or day (d) listed on the left. For each image shown, the mouse on the far left (denoted with a '−') was infected with *B. burgdorferi* but did not receive D-luciferin to serve as a background control. Mice denoted with a '+' were infected with the strain indicated and treated with D-luciferin to promote light emission. All images were normalized to the same scale (shown on the right). (**B**) Quantification of *in vivo* luminescence images of mice infected at a dose of 10^3 of *B. burgdorferi.* Parent strain ML23/pBBE22*luc* is depicted as black circles, the SR0736 sRNA mutant DM103/pBBE22*luc* as red squares, and the genetic complement strain DM113/pBBE22*luc* as blue triangles. Each time point represents the average value and the standard error from the four mice given D-luciferin substrate for the parent and sRNA mutant strains and three mice for the complement strain. *$P < 0.05$; **$P < 0.01$.

B.

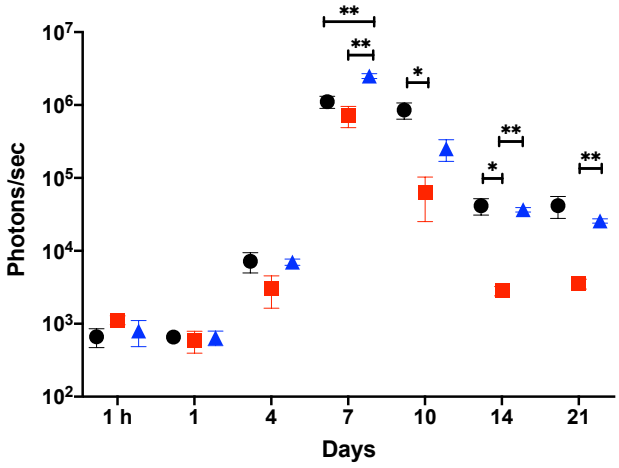

Figure 15 continued.

Following 21 days, the mice were sacrificed, and tissues cultured to qualitatively score for infection. As shown in Table 9, the sRNA mutant that was inoculated on the ventral side (abdomen) is unable to colonize peripheral skin (ear) and it is attenuated in its ability to disseminate and colonize heart tissue with overall infectivity reduced by 40%.

In addition to this qualitative assessment of infection, we also scored for spirochete load using quantitative PCR (qPCR) analysis to enumerate borrelial genome copies relative to murine β-actin copies. As observed in Fig. 16, the SR0736 mutant strain had significantly lower bacterial burden in all tissues analyzed relative to its parent and complement strains, with the notable exception of the lymph node, consistent with the reduced signal observed in the imaging results (Fig. 15). The complement strain exhibited bacterial burden comparable to the parent strain, thus demonstrating full complementation during infection. Taken together, this data suggests that SR0736 is required for optimal tissue tropism and/or dissemination during experimental infection by *B. burgdorferi.*

Table 9. Infectivity of the sRNA mutant strain DM103 relative to its parent and genetic complement[a].

Strain	Ear	Inoculation site (skin)	Lymph node	Heart	Bladder	Joint	Total sites	% Positive Tissues
ML23 pBBE22*luc*	10/12	11/12	12/12	11/12	12/12	12/12	68/72	94%
DM103 pBBE22*luc*	1/13	12/13	13/13	1/13	9/13	11/13	47/78	60%
DM113 pBBE22*luc*	12/12	10/12	12/12	12/12	12/12	12/12	70/72	97%

[a] Dose of 10^3 per strain of *B. burgdorferi* tested.

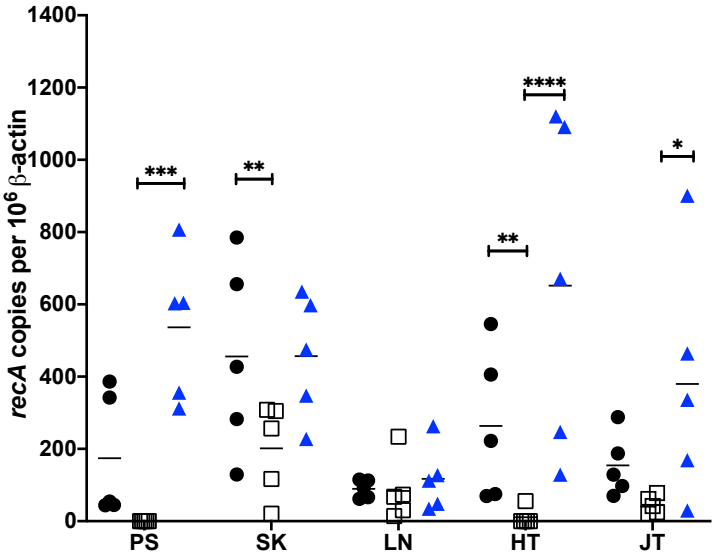

Figure 16. Quantitative assessment of *B. burgdorferi* load from infected mice tissues. Quantitative PCR (qPCR) of tissues from mice infected with the parental strain (black circles), the sRNA mutant (open boxes), and the genetic complement (blue triangles) was used to enumerate borrelial genomic equivalents relative to the murine samples. Mice were infected with 10^3 dose of *B. burgdorferi* strains for 21 days. Tissues tested are shown at the bottom: PS for peripheral ear skin; SK for skin at the site of infection; LN for Lymph node; HT for heart; and JT for the tibiotarsal joint. The results are represented as the number of borrelial *recA* genomic copies per 10^6 mouse β-actin copies. The horizontal line in each data set depicts the mean value. Each data point shown represents an independent sample from a single mouse tissue assayed in triplicate and averaged. ** $P < 0.05$; ** $P < 0.01$; *** $P < 0.001$; **** $P < 0.0001$.*

Transcriptional profile of the SR0736 mutant

Given the infectivity defect observed, we were then interested in determining how SR0736 affects the transcriptional profile of *B. burgdorferi.* To assess this, we performed RNA-seq to compare the global transcriptional profile of the parent and the sRNA mutant under conditions that mimic mammalian-like conditions in an unbiased manner. It is important to note that the cultures used for this analysis were also utilized for the subsequent proteomic analysis described below.

For our transcriptional comparison, we found that the sRNA mutant exhibited differential expression of transcripts in 19 genes when compared to the infectious parent (Fig. 17). From the 19, 13 transcripts were upregulated in the sRNA mutant strain, including transcripts predicted to be involved in pathogenesis (*vraA* [*bbi16*] (227) and a locus required for effective transmission from the tick vector to mice and expressed during mammalian infection, *bba66* (228,229). In addition, there were 6 transcripts downregulated in the sRNA mutant strain, which included *ospD* (*bbj09*), *ospA* (*bba15*), and *oms28* (*bba74*) (Fig. 17). Overall, these results suggest that the SR0736 sRNA affects either the stability of the transcripts observed or indirectly alters the expression of these transcripts using an unknown regulatory mechanism.

qRT-PCR confirms differential expression of transcripts in the sRNA mutant

We next utilized quantitative RT-PCR (qRT-PCR) to assess the expression of the candidate genes identified to corroborate our RNA-seq analysis (Fig. 18) using the parent, mutant, and complement strains under mammalian-like conditions. A constitutively expressed gene, *flaB*, which was not affected by any of strains

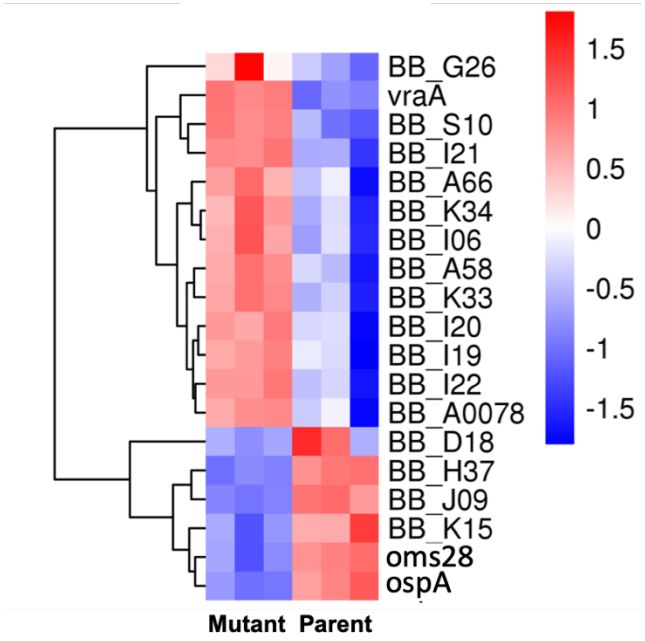

Figure 17. RNA-seq of the *B. burgdorferi* SR0736 mutant strain relative to its parent reveals differences in transcript populations. Nineteen transcripts with differential expression in comparison to the parent were determined via RNA-seq analysis. The SR0736 mutant (left side) and the parent strain (right side) were grown in biological triplicates *in vitro* using conditions that mimic mammalian infection, RNA was purified, and the samples subjected to RNA-seq. Subsequent bioinformatics indicated that 19 transcripts were dysregulated with 13 upregulated and 6 downregulated in the sRNA mutant relative to the parent strain. The *B. burgdorferi* genes affected are listed on the right side. The heat map depicts those that were upregulated (red) and those that were down-regulated (blue).

tested in this study, was used for normalization as previously described (73,74). As a control, we tested *ospC* and found that this transcript was not affected by the loss of SR0736 sRNA, as predicted. Five genes were tested, *bba66*, *vraA*, *oms28* (*bba74*), *ospD*, and *ospA* (Fig. 18). The qRT-PCR confirmed the upregulation or downregulation observed in the RNA-seq experiment for each gene (Fig. 17 and 18). Unexpectedly, only *bba66* was restored to wild type levels in the complemented strain (Fig. 18). This discrepancy in transcript level is surprising given that the complement restores infectivity back to the parent strain level *in vivo* (Fig. 15) and that both the Northern blot and qualitative RT-PCR data indicates a product specific to the sRNA in the parent and complement but missing from the mutant (Fig. 12).

SR0736 alters the borrelial proteome

We hypothesized that the loss of SR0736 might result in the decrease or enhancement of borrelial proteins due to the predicted post-transcriptional regulation inherent to sRNAs (148–150). To address this, we used a global proteomic screen to identify and quantify the entire borrelial proteome of both the parent and SR0736 mutant under conditions that mimic mammalian-like conditions (Fig. 19). The samples used here were identical to those used for RNA-seq analysis shown in Fig. 17. From this assessment we found two proteins, OspD and Oms28, that were significantly downregulated in the SR0736 sRNA mutant (Fig. 19).

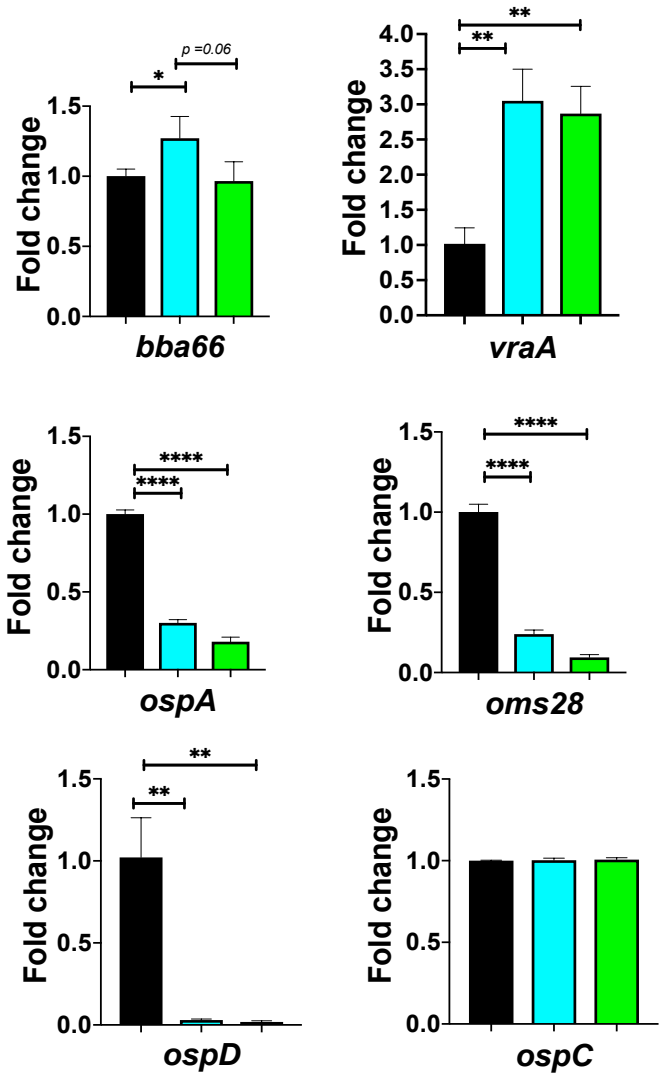

Figure 18. Quantification of transcripts by qRT-PCR. Quantitative RT-PCR (qRT-PCR) of the parent (black bars), SR0736 mutant (blue bars), and complement strain (green bars) were performed for a subset of transcripts indicated at the bottom of each panel. The error bars indicate standard error. The data for all samples was normalized to the endogenous control, *flaB*, whose transcription was not affected by the conditions used in this experiment. Significance is denotated as * *P < 0.05, ** P < 0.01, *** P < 0.001. **** P < 0.0001.*

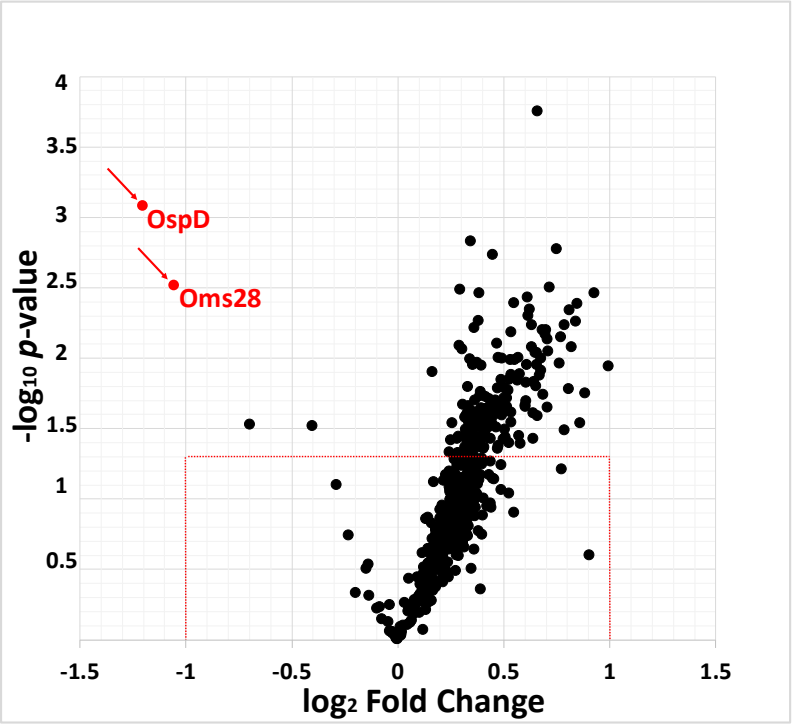

Figure 19. Proteomic evaluation of the parent relative to the sRNA mutant. Tandem Mass tags (TMT) was used to determine the total protein composition of the parent and SR0736 mutant. Volcano plot showing the protein abundance fold change (Log_2) plotted against the *P*-value ($– Log_{10}$) from parent and sRNA mutant strain. Strains were grown *in vitro* in biological triplicates in mammalian-like conditions and subjected to TMT (see Methods for details). OspD and Oms28 were found to be significantly lower in abundance in the mutant relative to the parent strain.

Since both *ospD* and *oms28* transcripts were identified in our RNA-seq data and were decreased in amount (Fig. 17), we hypothesize that the targeted sRNA stabilizes these transcripts and thus, allows for the increased translation of OspD and Oms28. In the absence of the SR0736 sRNA, the transcript of *ospD* and *oms28* are destabilized, resulting in reduced levels of OspD and Oms28 proteins. A predictive algorithm, IntaRNA (Freiburg RNA tools) indicated potential SR0736 binding sites found at the 3' end of the *ospD* and *oms28* transcripts that may prevent RNase-dependent turnover (Fig. 20). Whether this sRNA-mRNA interaction occurs and stabilizes the *ospD* and *oms28* transcript directly, or if this effect is due to other SR0736-regulated targets that indirectly affect this process, remains to be determined.

To provide additional validation for the effect seen for OspD and Oms28 in the SR0736 sRNA mutant background, we performed Western blot analysis of proteins lysates from parent, SR0736 mutant, and complement grown *in vitro* under mammalian-like conditions. We observed lower levels of OspD and Oms28 in the sRNA mutant then the parent, consistent with the proteomic analysis (Fig. 21). Of note, the complement did not produce OspD to levels similar to that observed in the parent strain, consistent with the expression of *ospD* not being restored in the qRT-PCR analysis (Fig. 17). For Oms28, the complement produced proteins levels comparable to the parent. These results demonstrate partial complementation of the SR0736 mutant relative to the parent strain using both qRT-PCR and Western immunoblot metrics of assessment.

A.

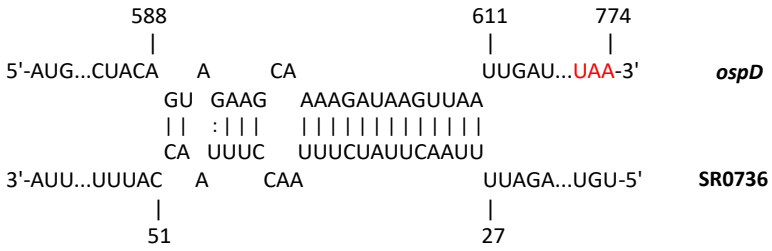

B.

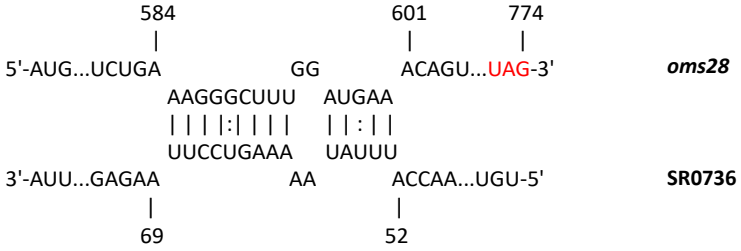

Figure 20. IntaRNA (Freiburg RNA Tools) predictions of interactions of the SR0736 sRNA with the *ospD* and *oms28* transcripts. A. Potential interaction of the SR0736 sRNA with within the coding region of *ospD* (upper). B. Potential interaction of the SR0736 sRNA within the coding sequence of *oms28* (lower).

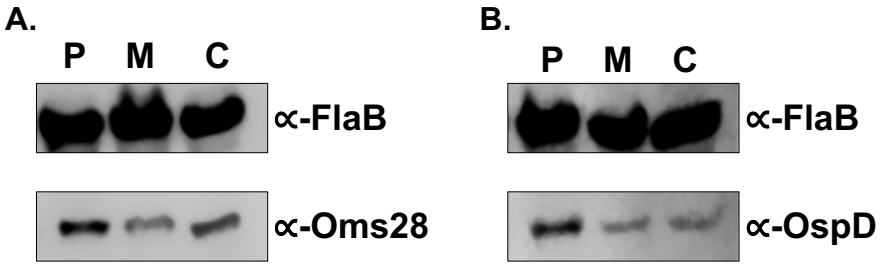

Figure 21. Evaluation of OspD and Oms28 in *B. burgdorferi* lacking SR0736. Protein lysates were derived from parent (P), SR0736 sRNA mutant (M), and SR0736 complement (C) strains grown under mammalian-like conditions *in vitro* and probed against anti-OspD (**A**) and anti-Oms28 (**B**). FlaB was used as a loading control for both immunoblots shown.

Discussion

Bacterial sRNAs are important in regulating gene expression by modulating the translation efficiency of its target transcripts (146,147). However, the loss of a single sRNA species often has a limited effect on measurable phenotypes. This is likely due to the subtle effect of the sRNA-mRNA interaction and the lack of an absolute effect seen by this event; that is, the target transcript is not entirely inhibited or activated, depending on the relative abundance of these RNA molecules and the fine-tuning that is associated with their transient binding (147,230). Modest phenotypes may also be due to redundancy, as a given mRNA can be regulated by multiple sRNAs; therefore, the elimination of a single sRNA may not drastically alter mRNA turnover or translation (147,150,230). Nevertheless, sRNAs encoded by pathogenic bacteria are recognized as important players in adaptive responses with some identified as important effectors in regulatory pathways (149,150,231).

Due to the enzootic nature of *B. burgdorferi* and its ability to quickly adapt to environmental factors encountered during their lifecycle, we hypothesized that *B. burgdorferi* use sRNAs to affect post-transcriptional regulatory processes that calibrate these responses. Recently, 1,005 putatives sRNAs were identified in *B. burgdorferi*, suggesting that these spirochetes exploit this type of genetic regulation (161). However, how *B. burgdorferi* utilizes these sRNA candidates remains largely unknown. Understanding the role these sRNAs play in post-transcriptional gene regulation in *B. burgdorferi* should provide significant insight into how the Lyme disease spirochete refines its molecular pattern to survive and persist within the disparate environments that they reside, e.g., arthropods versus mammals. In this

study, we inactivated a *trans*-acting, intergenic (IG) sRNA, designated SR0736, and demonstrate that this sRNA is required for optimal murine infection, as well as dissemination to distal tissues, and show that transcript and protein production are affected when SR0736 is missing from *B. burgdorferi*. To our knowledge, no other sRNA from *B. burgdorferi* has been vetted to this extent.

As a first step to link a *B. burgdorferi trans*-acting intergenic sRNA to an infectivity phenotype, mice were infected with the transposon library of *B. burgdorferi* strain B31 (189) and decreased infectivity was scored using Tn-seq (190,198). These data were compared against the recently described *B. burgdorferi* sRNA-specific library (161) to identify intergenic sRNA species that mapped to existing Tn mutants. We tested each identified intergenic sRNA Tn mutant individually using the experimental murine infection model. One sRNA mutant, designated SR0736, exhibited the most severe infectivity defect. Subsequent *in vivo* imaging of an independently derived mutant strain relative to its parent and complement (Fig. 15) confirmed the attenuated phenotype observed for the qualitative infectivity assessment (Table 9). The inactivation of the SR0736 affected tissue tropism of *B. burgdorferi* where spirochetes were cultured out of peripheral ear skin and heart in less than 8% of the samples tested (Table 9). Even though the qualitative assessment of infection showed some degree of colonization in all tissues except the lymph nodes, the total bacterial load of *B. burgdorferi* was significantly lower for the mutant relative to the parent and complement strains (Fig. 16). These data indicate that SR0736 is needed for optimal borrelial colonization and/or dissemination.

To globally assess the role of the SR0736 sRNA we used transcriptomic and proteomic approaches to identify transcripts and proteins that are altered in the absence of SR0736, respectively. Two proteins, OspD and Oms28 (BBA74), were produced at lower levels in the SR0736 mutant consistent with their respective transcripts being reduced in the mutant background (Figure 17 and 19). This concordance of the data suggests that the SR0736 sRNA binds to the *ospD* and *oms28* transcripts, prevents their degradation, and consequently enhances OspD and Oms28 translation.

Of the nineteen transcripts identified as being altered due to the loss of the SR0736 sRNA, only six have been characterized to varying degrees: *ospA*, *ospD*, *oms28*, *bbd18*, *vraA*, and *bba66*. From these three, *bba66*, *vraA* and *bbd18*, have been associated with some aspect of mammalian-based virulence; four of these genes, including *ospA*, *ospD*, *oms28*, and *bba66*, are expressed in the arthropod vector and some have significant phenotypes in this stage of the *B. burgdorferi* life cycle, particularly *ospA* and *bba66* . OspA is a well characterized surface lipoprotein that functions as an adhesin in the midgut of *Ixodes* ticks; as such, OspA is required for this aspect of the borrelial lifecycle (12,94,105,107). BBA66 is a lp54 encoded surfaced expressed lipoprotein that is upregulated during nymph blood meal and is highly expressed in the mammal for more than three months post infection, suggesting a role in persistent infection (229). Needle inoculation of mice with genetically inactivated *bba66* in *B. burgdorferi* results in lower bacteria burden of joint tissue and significantly lower joint swelling relative to the parent strain, suggesting that BBA66 contributes to borrelial-mediated inflammation (228).

Mutants in *bba66* are acquired by larvae and persist through molting, but were significantly impaired in its ability for infecting mice when introduced by tick bite compared to that of mice fed upon by wild type ticks, suggesting a role for BBA66 in transmission (228).

Recently, an additional function of BBA66 was found, whereby BBA66 binds to neuroglial and macrophage protein Daam1 (237). Daam1 is in the formin family of proteins involved in regulating cytoskeletal reorganization in mammalian cells (238). A prior study showed that Daam1 co-localized to pseudopods on macrophages that were processing *B. burgdorferi* by coiling phagocytosis (239). A more recent report showed that BBA66 mediated the attachment of *B. burgdorferi* to these cells via the Daam1 protein (237). Interestingly, the *bba66* mutant exhibited reduced levels of internalized *B. burgdorferi* while borrelial cells that produced greater amounts of BBA66 were phagocytosed more efficiently (237). In the RNA-seq data (Fig. 17), higher expression of *bba66* was observed in the sRNA mutant compared to the parent. From this it is tempting to speculate that the increase of *bba66* expression in the sRNA mutant may lead to increased phagocytosis and local clearance of *B. burgdorferi* by macrophages as a result of BBA66-mediated binding of Daam1. This could help explain the lower bacteria burden in the majority of the mice tissues examined in the sRNA mutant, where BBA66 levels are predicted to be greater (Fig. 15). Taken together, the dysregulation of *bba66* expression may be an important factor in the phenotype observed for the SR0736 sRNA mutant (Fig. 15 and 16).

One significant and confounding issue stemmed from the incomplete complementation observed for the SR0736 sRNA. While the *cis*-acting complement restored infectivity to wild type levels as assessed by *in vivo* metrics (e.g., *in vivo* imaging as well as both qualitative and quantitative measure of infected tissues), *in vitro* indicators did not. Surprisingly, several of the transcripts and proteins affected by the absence of SR0736 were not restored to wild type levels in the complement. Of the five targets tested for transcript levels, only *bba66* was restored to wild type levels in the SR0736 complemented strain. At the protein level, we were limited by available reagents, and of the three candidates tested, OspD, VraA, and Oms28, only Oms28 appeared restored to the levels observed in the parent strain when assessed by Western immunoblotting. The reasons for the discrepancy between the *in vivo* and *in vitro* readouts remains unresolved but may be due to a heretofore unknown host specific factor that is lacking during the *in vitro* growth of *B. burgdorferi* but needed for a proper integrated regulatory response by SR0736. Further studies will be needed to address this experimental conundrum.

Another limitation of this study in the absence of data that directly links the SR0736 sRNA to interaction with targeted transcripts. Although the RNA interactive algorithm IntaRNA predicts binding by SR0736 to the *ospD* and *oms28* transcripts (Fig. 20), we have yet to accumulate direct evidence that SR0736 does anneal to these and other target transcripts. Recently, several methods have been developed to identify endogenous RNA-RNA complexes in eukaryotes and have been adapted for the identification of sRNA-mRNA complexes in bacteria. These methods identify the RNA-RNA interactions through *in vivo* crosslinking, ligation and detection of the

chimaeric RNAs by sequencing (240–242). Such approaches could be used to confirm the borrelial mRNA species identified in the data presented herein by SR0736 as well as other novel transcripts.

In conclusion, sRNA-mediated regulation has been proven to be complex but important in fine-tuning gene expression in many bacteria species (159,243). Our findings suggest that the SR0736 regulates different gene targets expressed at different stages of *B. burgdorferi* life cycle; that is, during infection or during blood meal of the tick (66,218,228,229,234,235). One possibility posits that this sRNA may help in a quick adaptive response that is needed to transmit from the tick vector and/or colonize the mammalian host. In wild type *B. burgdorferi*, the SR0736 sRNA coordinates the proper expression of different targets due to post-transcriptional processing. When SR0736 is lost, the dysregulation of its targets has a synergistic effect that results in an attenuated phenotype. Here, there is an additional layer of complexity, seen in the form of tissue tropism, such that colonization at remote skin and cardiac tissue sites is impaired. As such, this work suggests that sRNA-based regulation is important in maintaining appropriate levels of gene expression in its affected target transcripts to promote *B. burgdorferi* colonization and dissemination during experimental infection.

Experimental Procedures

Bacteria strains and culture conditions

Bacterial strains and plasmids used in this study are described in Table 10. *Escherichia coli* strains were grown aerobically at 37°C in Luria Broth (LB).

Concentration of antibiotics used in *E. coli* are as follows: kanamycin, 50 μg/ml; spectinomycin, 50 μg/ml; and gentamicin, 5 μg/ml. *B burgdorferi* strains were grown in BSK-II media supplemented with 6% normal rabbit serum (Pel-Freez Biologicals, Rogers, AR) under conventional microaerobic conditions at 32°C, pH 7.6, under 1% CO_2 atmosphere, or conditions that mimic the mammalian-like environment, namely, 37°C, pH 6.8, under 5% CO_2 atmosphere. *Borrelia burgdorferi* B31 ML23 (181) and derivative strains were grown under antibiotic selective pressure, dependent on genetic composition, with either kanamycin at 300 μg/ml, streptomycin at 50 μg/ml, or gentamicin at 50 μg/ml. *B. burgdorferi* 5A18NP1 (209) was grown in the presence of kanamycin at 300 μg/ml and the *B. burgdorferi* transposon mutants (189) were grown in the presence of both gentamicin at 50 μg/ml and kanamycin at 300 μg/ml.

Genetic inactivation of the B. burgdorferi SR0736 intergenic sRNA

The intergenic (IG) small regulatory RNA (sRNA) located between genes *bbd18* and *bbd21* in lp17 was insertionally inactivated via homologous recombination by replacing the 3' end of the sRNA (nucleotides 11,820-11,850) with the P_{flgB}-*aadA* (streptomycin resistant; Str^R) antibiotic cassette (206). DNA sequences that flanked the SR0736 sRNA locus were amplified using PCR with PrimeSTAR GXL polymerase (Takara, Mountain View, CA).

Table 10. Strains used in the SR0736 study.

***E. coli* strains**		
Mach-1^{TM}-T1^{R}	F^{-} ϕ80(*lacZ*)ΔM15 Δ*lacX74 hsdR*($r_K^- m_K^+$) Δ*recA1398 endA1 tonA*	Invitrogen
***B. burgdorferi* strains**		
ML23	*B. burgdorferi* B31 clonal isolate missing lp25; parent strain.	(181)
ML23 pBBE22*luc*	Clonal isolate of strain B31 lacking lp25; shuttle vector encodes *bbe22* and *B. burgdorferi* codon optimized *luc* gene under the control of a strong borrelial promoter (P_{flaB}-luc).	(41)
DM103	ML23 IG sRNA SR0736::Str^{R}.	This study
DM103 pBBE22*luc*	DM103 background carrying shuttle vector pBBE22*luc*; Str^{R} and Kan^{R}	
DM113	ML23 containing intact sRNA SR0736::Gen^{R} complemented in *cis* in same genetic location of lp17 (between genes *bbd18* and *bbd21*) using native promoter.	This study
DM113 pBBE22*luc*	DM113 background carrying shuttle vector pBBE22*luc*; Gen^{R} and Kan^{R}	
5A18NP1	*Borrelia burgdorferi* B31 clone missing lp28-4 and lp56 with disruption of *bbe02*::Kan^{R}.	(209)
Plasmids		
pCR®-Blunt	pCR®-Blunt vector, Kan^{R}, Zeocin^{R}.	Invitrogen
pKFSS1	*B. burgdorferi* shuttle vector containing P_{flgB}-Str^{R} cassette; Spec^{R} in *E. coli,* Str^{R} in *B. burgdorferi.*	(206)
pBSV2G	*B. burgdorferi* shuttle vector containing P_{flgB}-Gen^{R} cassette.	(244)
pBBE22*luc*	Borrelial shuttle vector containing *bbe22* and *B. burgdorferi* codon-optimized *luc* gene under the control of a strong borrelial promoter (P_{flaB}-*luc*).	(41)
pCR2.1Bactin	Murine β-actin gene cloned into pCR2.1 vector; Kan^{R}.	(41)
pCR2.1*recA*	*B. burgdorferi recA* gene cloned into pCR2.1 vector; Kan^{R}.	(41)
pDM103	*B. burgdorferi* IG sRNA SR0736 mutant construct. Contains sequences 1280 bp upstream of the sRNA, the P_{flgB}-Str^{R} cassette from pKFSS1 inserted into the sRNA sequence, and sequences 1233 bp downstream of the sRNA; pCR®-Blunt vector backbone; Str^{R} and Kan^{R}.	This study
pDM113	Complement construct of the sRNA SR0736 located in between genes *bbd18* and *bbd21*. Contains sequences 1359 bp upstream of sRNA, a gentamicin cassette from pBSV2G, and 1171 sequences downstream of the sRNA; pCR®-Blunt vector backbone; Gen^{R} and Kan^{R}.	This study

For the upstream fragment, 1280 bp were amplified using primers US-F and US-SpecR (see Table 11). The 1266 bp fragment containing P_{flgB}-Str^R was PCR amplified from pKFSS1 (206) using the oligonucleotide primers pair US-SpecF and SpecDS-R (Table 11). An additional 1,233 bp PCR product, which amplified sequences downstream from the SR0736 sRNA, was engineered with primers SpecDS-F and DS-R (Table 11). All three fragments had 20 base pair overlap sequences and were assembled by overlap PCR (40,204,213).

For the creation of the sRNA *cis* complement strain, the P_{flgB}-Str^R cassette of the sRNA mutant was replaced on lp17 using the native SR0736 containing sequence with a linked P_{flgB}-$Gent^R$ marker downstream of the sRNA (244). The US-F and compUS-gentR primers were used to PCR amplify the 1359 bp portion containing SR0736 (Table 11). The 983 bp gentamicin cassette from pBSV2G (244) was produced using primers compUS-gentF and compgentDS-R (Table 11). A 1171 bp region downstream from SR0736 was amplified using the primers compgent-DSF and compDS-R (Table 11). As before, all three fragments had 20 base pair overlap sequences and were assembled by NEBuilder HiFi DNA Assembly Master Mix (New England Biolabs, Ipswich, MA). All constructs were verified by Sanger sequencing prior to transformation into the *B. burgdorferi* strain B31 derivative ML23 (181).

Table 11. Oligonucleotides used in the SR0736 study.

Oligonucleotides	5'-3'	Use
US-F US-SpecR	GCTGCCTTAAGTAAGGC GAAATCTTCCACGCCAATTGTCTTAAGGACTTTTTATAAA	Primer pair used to amplify 1280 bp of the flanking region upstream of the sRNA in lp17. Amplicon has 20 bp at the 3' end with homology to the 5' end of P_{flgB}-$Spec^R$ of pKFSS1 (206).
US-SpecF Spec-DSR	TTTATAAAAAGTCCTTAAGACAATTGGCGTGGAAGATTTC ATTCTTCATTATTCTTTATT CTGATTTTTAAACTTTTTCA	Primer pair used to amplify 1266 bp region of P_{flgB}-$Spec^R$ (206). The 5' end has 20 bp with homology to the 3' end of the upstream flanking region. The 3' end of the amplicon has 20 bp with homology to the 5' end of the downstream flanking region.
Spec-DSF DS-R	TGAAAAAGTTTAAAAATCAGAATAAAGAATAATGAAGAAT CTATATTCACGGCTTTTGTCTC	Primer pair used to amplify the downstream flanking region 1233 bp amplicon. The amplicon has 20 bp at the 5' end with homology to the 3' end of P_{flgB}-$Spec^R$ (206).
US-F compUS-gentR	GCTGCCTTAAGTAAGGC CCTTGAAGCTCGGGTATTACCCAAATTTATTTTGAAATT	Primer pair used to amplify 1359 bp of upstream amplicon with 20 bp homology sequence at the 3' end to the 5' end of P_{flgB}-Gen^R from pBSV2G (244).
compUS-gentF compgent-DSR	AATTTCAAAATAAATTTGGGTAATACCCGAGCTTCAAGG CTATTTTACAAACCTACCCTTAGGTGGCGGTACTTGGGT	Primer pair used to amplify 983 bp amplicon of the P_{flgB}-Gen^R (244) with 20 bp on the 5' end with homology to the 3' end of the upstream flanking region and 20 bp on the 3' end with homology to the 5' end of the downstream flanking region.
compgent-DSF compDS-R	ACCCAAGTACCGCCACCTAAGGGTAGGTTTGTAAAATAG ACGGCTTTTGTCTCATTCTACG	Primer pair used to amplify 1171 bp of downstream flanking region with 20 bp on the 5' end with homology to the 3' end of P_{flgB}-Gen^R (244).
nTM17FrecA nTM17RrecA	GTGGATCTATTGTATTAGATGAGGCT GCCAAAGTTCTGCAACATTAACACCT	Primer pair used to enumerate copies of *B. burgdorferi recA* by qPCR (5) .
b-actin-F b-actin-R	ACGCAGAGGGAAATCGTGCGTGAC ACGCGGGAGGAAGAGGATGCGGCAGTG	Primer pair used to enumerate copies of mouse β-actin by qPCR (40,246).
P1	GTCATAATCGTAATTTTCACCGGTTTGC	Primers used to confirm sRNA mutant and complement strains.
P2	CGACCTTTTGGAAACTTCGGC	Primers used to confirm sRNA mutant and complement strains.
P3	GGACCTACCAAGGCAACGCTATGTTCTC	Primers used to confirm sRNA mutant and complement strains.
P4	GAAATCCTTGTGTTCTATCCCTC	Primers used to confirm sRNA mutant and complement strains.
P5	GCAGTCGCCCTAAAACAAAGTTAGGTGG	Primers used to confirm sRNA complement strain.
P6	GCCTCCGGTGCTCGCCGGAGACTG	Primers used to confirm sRNA complement strain.
*bbd18*F *bbd18*R	CCCATGATTTCCTTTTAATTTTTTAG CGATTATGACACATTTATTACC	Primers used to amplify 367 bp amplicon via Reverse-transcriptase PCR (RT-PCR) of *bbd18*.
*bbd21*F *bbd21*R	GGTGGTGTTGGGAAAACTACC CTAAAAGTTCCACTCGGCACACATGGC	Primers used to amplify 242 bp amplicon via Reverse-transcriptase PCR (RT-PCR) of *bbd21*.
sRNA-F sRNA-R	GTCCTTAAGAGAGAAATTTC GGGCAATTCTTCATTATTC	Primers used to amplify 65 bp amplicon via Reverse-transcriptase PCR (RT-PCR) of the sRNA SR0736.

Table 12. Oligonucleotides used for qRT-PCR.

Oligonucleotide	Sequence 5'-3'	Reference
*oms28*F	GCTGTTTCTGTTGCTGGTGAAG	(247)
*oms28*R	AACTTTTTGAGCCTCTTGAACTG	(75)
*ospD*F	GGCAAATAAAGTTGTAGAAGCG	(75)
*ospD*R	TTTCAGCAGAATCAGAATAGTCAG	(75)
*bba66*F	GCAAGAGCTGCATCACTAACAAA	(229)
*bba66*R	TGTTGGCAGCCCGCTATT	(229)
*ospA*F	GGCGTAAAAGCTGACAAAAGTAAAGTA	(74)
*ospA*R	TAGTGTTTTGCCATCTTCTTTGAAAA	(74)
*ospC*F	CGGATTCTAATGCGGTTTTACTTG	(74)
*ospC*R	CAATAGCTTTAGCAGCAATTTCATCT	(74)
*vraA*F	AAGCAAATAGAATCGGCCTACAA	(74)
*vraA*R	CCCAATTCAATCCCCTAAAAGAC	(74)
*flaB*F	CAGCTAATGTTGCAAATCTTTTCTCT	(74)
*flaB*R	TTCCTGTTGAACACCCTCTTGA	(74)

Transformation of B. burgdorferi

B. burgdorferi were made competent for DNA transformation as previously described (39,40,188,204). Prior to transformation via electroporation, all plasmid constructs were linearized with *Xho*I. Following antibiotic selection for the desired strain, putative transformants were tested for the presence of the genetic constructs using a PCR-based screen. Subsequent mutant or complemented strains were tested for *B. burgdorferi* strain B31 plasmid content by PCR (181).

Infectivity studies and bioluminescent imaging

Infectivity studies were performed as previously described. Briefly, 8-week-old C3H/HeN female mice were inoculated with 10^3 organisms of the *B. burgdorferi* parent strain ML23/pBBE22*luc,* the sRNA SR0736 genetic inactivation strain DM103/pBBE22*luc,* or the genetic complement strain DM113/pBBE22*luc,* by intradermal injection in the abdominal area. For the parent and complement strains, twelve mice were infected, for the sRNA inactivation strain, thirteen mice were infected.

The bioluminescent imaging was performed as done previously (40,41,204). Described briefly, five mice were imaged for the parent and mutant strains and four mice were imaged for the complement strain. The mice were injected intraperitoneally with 5 mg of D-luciferin dissolved in 100 µL of PBS 10 minutes prior to imaging with an IVIS Spectrum live animal imaging system (Caliper Life Sciences, Hopkinton, MA), with the exception of one mouse that was infected with *B. burgdorferi* but did not receive D-luciferin to serve as a negative control for

background luminescence (41). Imaging of the mice was performed 1 hour and at 1, 4, 7, 10 14 and 21 days post-infection (41). After 21 days, the mice were sacrificed and the ear, abdominal skin, inguinal lymph node, heart, bladder, and tibiotarsal joint tissues were collected from each mouse aseptically for *in vitro* cultivation. Samples from ear, abdominal skin, inguinal lymph node, heart and tibiotarsal joint tissues were also collected from these mice for qPCR analysis of *B. burgdorferi* burden as described previously (39,41).

RNA Isolation for conventional RT-PCR and qRT-PCR

Three independent cultures of *B. burgdorferi* strains ML23 (181), the sRNA inactivation strain DM103, and the genetic complement strain DM113, were grown to mid-log phase of 5 x10^7 cells per ml at either mammalian-like conditions, defined as: 37°C, pH 6.8, under 5% CO_2 or at conventional microaerophilic conditions of 32°C, pH 7.6, under 1% CO_2. The cultures were centrifuged at 4500 x *g* for 20 minutes at 4°C, washed with 1 ml PBS, and centrifuged at 14,000 rpm for 15 minutes. The pellet was resuspended in 100 μl of sterile water and 300 μl of TRIzol (Invitrogen, Carlsbad, CA) was added prior to employing Direct-zol RNA Miniprep (Zymo Research, Irvine, Ca, USA) for total RNA isolation. The resulting RNA was treated with DNAse I (Roche, Indianapolis, IN) and RNAsin (Promega, San Luis Obispo, CA) to eliminate contaminating DNA and inhibit RNAse activity, respectively. For conventional RT-PCR, 200 ng of total RNA was used to reverse transcribe into cDNA using SuperScript III (Thermo Fisher Scientific, Waltham, MA) using appropriate primers listed in Table 11.

For qRT-PCR analysis, 1 μg of total RNA was used for reverse transcription into cDNA using random primers (Thermo Fisher Scientific, Waltham, MA) and SuperScript III (Thermo Fisher Scientific, Waltham, MA). Oligonucleotide primers from Table 12 were used to amplify specific *B. burgdorferi* strain B31 targets. The expression of each gene was normalized to *flaB* as done previously using the ΔΔCt method (73,74).

Northern blot Analysis

Northern blotting of SR0736 was conducted using the same probe described previously (161,248).

DNA extraction of B. burgdorferi from infected tissues and qPCR analysis

Total DNA was isolated from ear, abdominal skin, inguinal lymph node, heart, and tibiotarsal joint using Roche High Pure PCR template preparation kit (Roche, Indianapolis, IN) as previously described (39,40,204). Total DNA of 100 ng was used for each qPCR reaction. Quantitative real-time PCR analysis was conducted using the Applied Biosystems StepOnePlus Real-Time PCR system. *B. burgdorferi* genome copies and mammalian cell equivalents were determined using either the oligonucleotide primers nTM17FrecA and nTM17RrecA (39,245) along with the primer set β -actin-F and β -actin-R (246), respectively (Table 11).

RNA Sequencing (RNA-seq)

Three independent cultures of *B. burgdorferi* cells were grown to mid-log phase of 5 x 10^7 cells per ml at 37°C, pH 6.8 and 5% CO_2, e.g., *in vitro* conditions that mimic mammalian-like infection (7,12). Cells were centrifuged at 4,500 x *g* for 30 minutes at 4°C. Approximately 1 x 10^9 cells were lysed in 1ml of TRIzol (Invitrogen, Carlsbad, CA) and RNA extracted following manufacturer's instructions. RNA was checked for quality using the Agilent TapeStation 2200 standard RNA screen tape and quantified using the Qubit 2.0 Broad Range RNA assay. Total RNA was normalized between all samples for sequencing library preparation using the TruSeq Stranded Total RNA library preparation kit with ribosomal depletion. Each sample was uniquely barcoded, then the libraries were pooled at equal concentrations. Library pools were sequenced using NextSeq 500 System on a 2 x 75 bp paired-end sequencing run generating ~15 million reads/sample by the Texas A&M Institute for Genome Sciences and Society (TIGSS).

Tandem Mass Tags (TMT)

Three independent cultures of *B. burgdorferi* cells were grown to mid-log phase of 5 x 10^7 cells per ml at 37°C, pH 6.8 and 5% CO_2 (note: the cells used here were the same as those used for RNA-seq). Cells were centrifuged at 4,500 x *g* for 30 minutes at 4°C and washed twice with 10ml of cold PBS. Cells were resuspended in 50 mM triethylammonium bicarbonate (TEAB) and 5% SDS. Samples were quantified using Pierce BCA protein assay kit (Thermo Fisher Scientific, Waltham, MA) and approximately 1.2 mg of protein was used for Tandem Mass tags (TMT)

experiment. For this approach, protein extracts were isolated from the cells, reduced, alkylated, and proteolytically digested overnight. Samples were labeled with the TMT reagents in a 6-plex experiment and combined before sample fractionation and clean up. Labeled samples were analyzed by high-resolution Orbitrap LC-MS/MS. Identification and quantification of proteins was performed using Proteome Discoverer 2.2 software. The University of Texas Southwestern proteomics core performed the TMT analysis.

SDS PAGE and immunoblotting

Borrelia burgdorferi protein lysates were resolved on a 12.5% polyacrylamide gel, transferred to a PVDF membrane, and blocked using non-fat powdered milk as done previously (39,249). Primary antibodies were used at the following dilutions: anti-Oms28 at 1:1000; anti-OspD at 1:5,000 and anti-FlaB at 1:5,000. Secondary antibodies with horseradish peroxidase (HRP) conjugates were used to detect immunocomplexes, specifically, anti-mouse Ig-HRP (Invitrogen, Carlsbad, CA, USA) or anti-rabbit Ig-HRP (GE Healthcare, Chicago, IL, USA) both diluted to 1:5,000. The membranes were washed extensively in PBS, 0.2% Tween-20, and developed using the Western Lightning Chemiluminescent Reagent plus system (Perkin Elmer, Waltham, MA, USA).

RNA prediction modeling

The coding sequence and 100 bp upstream of the start codon of the candidate genes *ospD* and *oms28* were subjected to RNA binding predictions using IntaRNA (Freiburg RNA Tools; (250) against the SR0736 sequence.

Statistical analysis

For real-time qPCR and quantitative reverse transcription PCR (qRT-PCR) analysis, multiple one unpaired *t*-test were performed to analyze the strains. For the analysis of *in vivo* luminescence of mice, two-way analyses of variance (ANOVA) was performed. For the RNA sequencing (RNA-seq) of the strains, differential expression analysis was performed using the *DESeq2* Bioconductor package. For the volcano plot, multiple one unpaired *t*-test in both strains for each protein identified was performed to obtain the *P* values that were used to calculate the y-axis ($-\log_{10}$ of the *P*-value). Statistical significance was accepted when the *P* values were less than 0.05 for all statistical analyses employed.

CHAPTER IV

CONCLUSIONS AND DISCUSSION

The Lyme disease causing spirochete, *Borrelia burgdorferi*, is maintained in nature in an enzootic cycle involving *Ixodes* spp. ticks and a variety of mammalian hosts (7,12). The spirochete is an auxotroph for nucleic acids, amino acids, and fatty acids, scavenging its nutrients from its hosts (7,12). The tick and mammal are vastly different environments. *B. burgdorferi* dramatically changes its gene expression and its outer surface expressed proteins, when transiting between the tick vector and the mammalian host (7,12,23). The modulation of gene expression is caused by the bacterium sensing and responding to environmental cues, such as temperature, pH, dissolved gases, and unidentified mammalian host factors (7,12,23).

Bacteria must adapt to rapid changes in the environment to survive. Small regulatory RNAs (sRNAs) are particularly adept at mobilizing rapid adaptative responses (148,149). Bacteria sRNAs are important regulators of gene expression in metabolism, quorum sensing, virulence, and other cell processes (146,148,150). Specifically, sRNAs post-transcriptionally regulate mRNAs by binding to them and altering their stability or their ability be translated into protein (149,150).

Trans-acting sRNAs have limited complementarity with their mRNA targets and thus bind imperfectly to transcripts (149,150). Due to the nature of *trans*-acting sRNAs, each sRNA may bind to multiple mRNAs (148,149). In addition, mRNAs can

be regulated by multiple sRNAs in this manner, establishing sRNA networks for the fine-tuning of gene expression (148,149).

B. burgdorferi produces 1,005 putatives sRNAs *in vitro* under conditions that mimic the tick and mammalian host at temperatures of 23°C and 37°C, respectively (161). From the total amount of sRNAs identified, 43% were found to be temperature dependent (161), which represents an important environmental cue for the modulation of gene expression in *B. burgdorferi* as they move between arthropod and mammalian hosts (7,12). This finding suggests a potential role for sRNAs in the enzootic cycle of the spirochete. However, not much is known about the role of sRNAs in post-transcriptional regulation of *B. burgdorferi.* In this work, we have initiated the characterization of a novel *trans*-acting sRNA termed SR0736 that was recently assigned as a part of the identification of all the detectable sRNAs in *B. burgdorferi* (161). Herein, we performed studies to identify the mRNAs that SR0736 targets to carry out its regulatory function. In addition, we mutated SR0736 and found that it is required for the optimal infection and dissemination of *B. burgdorferi* during experimental infection.

The work presented herein is relevant and timely inasmuch as only one sRNA has been characterized in *B. burgdorferi* (169). sRNAs serve as additional layers of regulation and are considered an advantageous strategy for bacteria to utilize given that a single sRNA can modulate the expression of multiple transcripts in a positive or negative manner simultaneously (149,150). In addition, sRNAs play key roles in bacteria regulatory networks, which can result in indirect regulatory effects, further complicating defining how they coordinate a distinct regulatory response (148,149).

With the identification of over a thousand sRNAs in *B. burgdorferi* (161), more borrelial sRNAs will be examined for their regulatory effects on gene regulation in diverse cell processes of the spirochete. The future identification of sRNAs in borrelial regulatory networks will further the understanding of strategies that *B. burgdorferi* utilizes for gene regulation in regard to specific responses they encounter.

SR0736 is a novel trans-acting sRNA

Gene expression is regulated by proteins and sRNAs in bacteria (148,156). RNA-based regulation by sRNAs is widely used to reshape transcriptomes (146,156). In Chapter III, we described the characterization of the novel *trans*-acting sRNA designated SR0736. The SR0736 sRNA is upregulated at 37°C *in vitro*, a temperature that mimics the mammalian host, suggesting a potential role during infection (161). To test this hypothesis, we genetically inactivated the SR0736 sRNA in *B. burgdorferi* (Fig. 11). This resulted in a significant infectivity defect, in comparison to the parent and genetic complement, demonstrating that the attenuation observed was due to the loss of the SR0736 sRNA (Fig. 15 and 16). The SR0736 sRNA inactivation resulted in significantly less bacteria burden in the majority of the tissues examined by qPCR, specifically, ear skin, skin at the site of inoculation, heart, and joint (Fig. 16). In addition, the SR0736 sRNA mutant displayed tissue tropism in distant tissues of ear and heart, as evidenced by the reduction of colonization for the SR0736 mutant with only 8% tissues colonized

(Table 9). These results demonstrated that SR0736 is required for the optimal infection and dissemination of *B. burgdorferi* in experimental murine infection.

Furthermore, we applied RNA-seq and Tandem Mass Tags (TMT) technologies to the parent and the SR0736 mutant strain to identify and quantify global transcriptomic and proteomic differences, respectively. Nineteen transcripts were found dysregulated in the RNA-seq analysis of the SR0736 sRNA mutant when compared to the parent strain (Fig. 17). In addition, as determined by TMT, OspD and Oms28 were found in lower abundance in the SR0736 sRNA mutant relative to the parent strain (Fig. 19).

Of the transcripts identified in the RNA-seq analysis, six have been characterized to a certain extent in *B. burgdorferi* (7,12,23,130,131,227,228) with *bba66* previously found to be virulence-associated (228,232). The *vraA* gene was also identified in the RNA-seq as dysregulated in the SR0736 mutant strain. The *vraA* locus maps to one of the 28 kilobase linear plasmids (lp28-4)(34,227). *B. burgdorferi* cells that are missing this plasmid are 10-fold less infectious than borrelial cells that carry lp28-4 (181), however, whether a single gene like *vraA* or other genes contribute to this effect is not currently known. The other thirteen transcripts are hypothetical genes of unknown function. One caveat from our experimental design is that by inactivating the SR0736 sRNA in *B. burgdorferi* and performing RNA-seq with this strain, the dysregulated transcripts identified might be indirectly affected by the SR0736 sRNA. That is, it is possible that SR0736 regulates transcripts that, in turn, affect other genes. Thus, the RNA-seq analysis could have potentially identified transcripts that are indirectly regulated by the SR0736 sRNA.

Five selected transcripts, *bba66*, *oms28*, *ospD*, *ospA*, and *vraA*, were assessed by qRT-PCR in the parent, the SR0736 mutant, and the *cis*-acting complement derivative. The RNA-seq results observed for the selected transcripts were confirmed by qRT-PCR for the parent and the SR0736 sRNA mutant strain. However, of the five gene targets tested, the complement strain was only able to restore the expression of *bba66* back to the levels seen in the parent strain. Western blot analysis of OspD and Oms28 were also performed for the parent, mutant, and complement strain. The SR0736 sRNA mutant displayed a decrease of these two proteins in the TMT results. Unexpectedly, the complement strain was only able to restore Oms28 protein levels similar to the parent levels, but not for OspD. The genetic complement strain was engineered to restore the SR0736 sRNA *in cis* and was placed in the same location in the linear plasmid 17 (lp17) of *B. burgdorferi*. Moreover, the complement strain expression of SR0736 sRNA is comparable to the parent strain, as confirmed by Northern blot and RT-PCR (Fig. 12). Finally, the complement restored infectivity to the SR0736 mutant, comparable to parent levels *in vivo* (Fig. 15 and 16). The partial complementation of SR0736 based on transcript quantification *in vitro* will require further experimentation to understand what is occurring.

The two proteins found in lower abundance in the proteomic analysis, OspD and Oms28, also exhibited a decrease in their detectable transcripts in the RNA-seq analysis. In Figure 22, *oms28* was used as the example for our working model, but our data suggests that *ospD* is potentially regulated by SR0736 sRNA in a similar fashion. We hypothesize that the SR0736 sRNA binds to *ospD* and *oms28*

mRNAs to stabilize these transcripts, resulting in subsequent enhancement of their translation (Fig. 22). The loss of the SR0736 sRNA results in *ospD* and *oms28* transcripts destabilization, most likely by increased RNA degradation, with subsequent decreased translation (Fig. 22). The IntaRNA program (250) predicts an SR0736 sRNA binding site in the coding region of each transcript toward the 3' end of each of these transcripts. It has been reported for other bacterial organisms that sRNAs can mediate positive regulation (150,251) by protection against RNases, thus, stabilizing transcripts (174,252). As such, it is possible that the SR0736 sRNA carries out this protective function for the *ospD* and *oms28* transcripts (Fig. 22). Further experimentation is required to confirm that the SR0736 sRNA directly binds to *ospD* and *oms28* transcripts and promotes their increased translation.

Detection of direct SR0736 sRNA binding to transcripts

One limitation of the potential SR0736 mRNA targets that we have identified in this study is their identification through indirect approaches, i.e., transcriptomics and proteomics. SR0736 direct binding to its predicted transcripts is required to prove that the SR0736 sRNA can execute a post-transcriptional regulatory effect on its mRNA targets. This could be done by performing EMSAs of *in vitro* synthesized SR0736 and predicted target transcripts, e.g., *ospD* and *oms28,* as it has been done for other bacteria (253). If SR0736 binds to the target transcript, it will form an RNA-RNA duplex that could be visualized as a gel shift by EMSA. Once the direct RNA-RNA binding interactions are confirmed by EMSA, predicted mechanisms of the

sRNA can be tested. For example, if RNA duplexes are detected, subsequent RNase treatment that eliminates single stranded RNA would leave the protected sequences for both the transcript and the sRNA. From this, subsequent sequencing could identify these specific sequences (assuming they retain a linear arrangement) to provide detail needed to define the regions bound by the sRNA and mRNA being analyzed. Another approach that could define the linkage of sRNAs to mRNAs involves crosslinking these molecules in living cells followed by extraction, cleaving of single stranded RNA ends, and covalently connecting the sRNA and mRNA directly (240–242). Given that the two RNA molecules are now contiguous, the known sequence of the sRNA can be used to identify the transcript that it is attached via direct sequencing. With proper controls, e.g., mutants lacking the sRNA of interest, one can then get an unbiased read of the transcripts affected by a specific sRNA.

BBA66 is potentially downregulated by SR0736

BBA66 is a surface expressed lipoprotein encoded by lp54 that is upregulated during transmission from the tick vector to the mammalian host (228,229,232). Mutants of *bba66* in *B. burgdorferi* lead to an attenuated mouse infection by tick bite, suggesting a potential role in transmission (228). In addition, *bba66* was expressed as long as three months post-infection, suggesting a potential role for BBA66 in persistent infection (229). In the RNA-seq of the SR0736 sRNA mutant from Chapter III, *bba66* was upregulated (Fig. 17). This suggests that the SR0736 sRNA potentially binds to the *bba66* message, resulting in the

destabilization of the transcript, increasing mRNA turnover, and consequently decreasing translation (Fig. 22).

Recently, BBA66 was found to interact with phagocytosis protein Daam1 in human neuroglial cells (237). The authors found that the BBA66-Daam1 interaction led to an increase in internalization of *B. burgdorferi* by coiling phagocytosis (237). Interestingly, it has been previously shown that Daam1 is important for the phagocytosis of *B. burgdorferi* in primary macrophages (239). Macrophages are among the first immune cells of the host to come in contact with infecting *B. burgdorferi* (239,254,255). Uptake of the spirochetes by macrophages, following intracellular processing, and elimination is important in preventing dissemination of the bacteria (254,255). As such, the dysregulation of *bba66* in the absence of the SR0736 sRNA, which results in more BBA66 protein made, might put *B. burgdorferi* at risk of enhanced innate immune clearance and may explain the decreased infectivity observed for the SR0736 sRNA mutant.

To test the hypothesis that the SR0736 sRNA leads to dysregulation of *bba66* and that this interaction adversely affects *B. burgdorferi*, direct evidence of the SR0736 sRNA and the *bba66* transcript *in vitro* would be instructive. To start, an EMSA could be performed using *in vitro* synthesized SR0736 sRNA and the *bba66* transcript, to determine if they form an RNA-RNA duplex. Alternatively, other aforementioned direct approaches could be used to vet the SR0736 sRNA::*bba66* mRNA interaction.

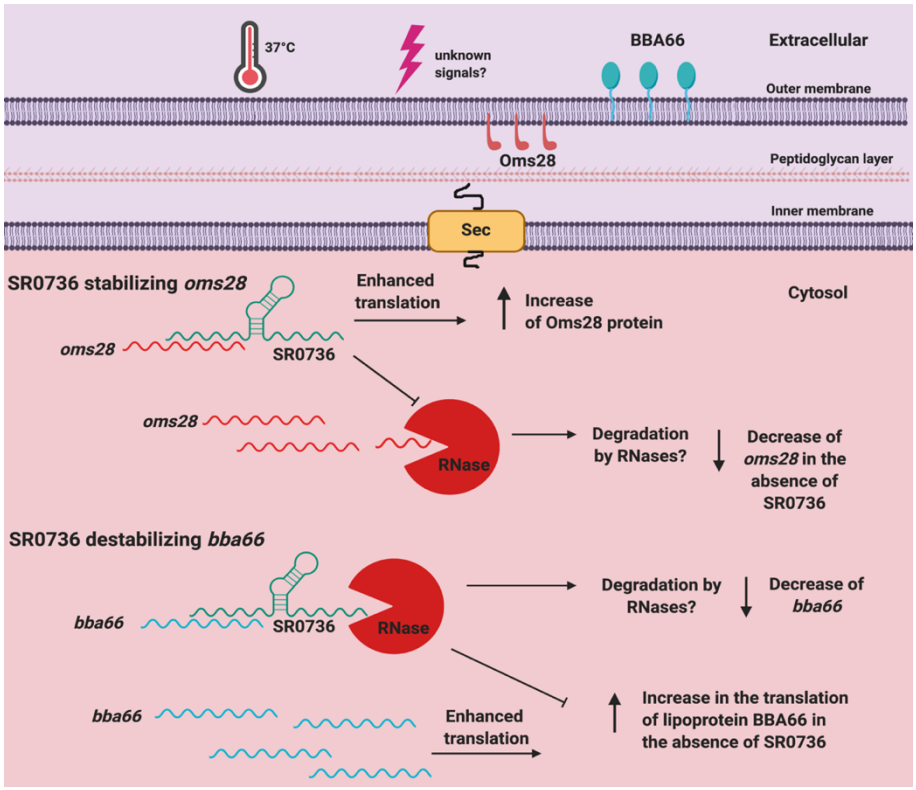

Figure 22. A model for the *trans*-acting sRNA SR0736 post-transcriptional regulatory mechanisms of two selected transcripts. Mammalian-like temperature (37°C) is an environmental cue that upregulates SR0736 expression as identified by RNA-seq in the *B. burgdorferi* sRNA library (161), but other unknown signals may contribute to SR0736 upregulation that have not been identified. When the SR0736 sRNA is expressed at 37°C, it is presumed to bind to the *oms28* transcript thereby stabilizing the transcript and most likely preventing RNA degradation. The net result is an increase in Oms28 translation. In the absence of SR0736, *oms28* is more readily degraded, most likely by RNases, resulting in less Oms28 being made. In contrast, when the SR0736 sRNA presumably binds to the transcript *bba66* and this interaction destabilizes the transcript, resulting in the reduced translation of BBA66. In the absence of the SR0736 sRNA, *bba66* translation is enhanced, resulting in more BBA66 being produced in these cells.

If once such binding was confirmed, phagocytosis assays could be performed with primary human macrophages using a *B. burgdorferi* wild type parent, the SR0736 sRNA mutant, a *bba66* mutant, and a *B. burgdorferi* overexpressing *bba66* strain. Our expectation is that the SR0736 sRNA mutant would yield to an increase in phagocytosis as a result of the upregulation of *bba66*. The increased phagocytosis level observed for the SR0736 sRNA mutant could be compared to the overexpressing *bba66* strain. The *bba66* mutant would be used as a negative control in this assay with the expectation that this strain would also be subject to some phagocytosis in a BBA66 independent process. Given its link to pathogenesis, as well as its interaction with a relevant host structure, the identification of *bba66* likely explains, in part, the phenotype observed when the sRNA is inactivated. Although we do not know much about several of the other transcripts affected, since most are in hypothetical genes, it is possible that their aberrant regulation contributes collectively to the significant decrease in infectivity observed for the SR0736 sRNA mutant as well. Further studies are needed to assess this possibility.

Concluding Statement

In conclusion, we have demonstrated that a single sRNA, specifically SR0736, affects the transcriptome and proteome of *B. burgdorferi*. Moreover, we have shown how the inactivation of the SR0736 sRNA yields a severely attenuated phenotype following experimental infection in mice. Our data suggests that the SR0736 sRNA binds to multiple transcripts, resulting in the modulation of mRNA stability and/or translation efficiency. We hypothesize that the SR0736 sRNA

regulates multiple genes to provide appropriate expression levels, resulting in optimal infectivity by *B. burgdorferi*. When the SR0736 sRNA is lost, the fitness of *B. burgdorferi* is reduced in the murine infection model. This is possibly due to a synergistic effect caused by the dysregulation of the SR0736 sRNA target mRNAs. In this work, we have furthered the understanding of post-transcriptional regulation in *B. burgdorferi* by examining the role of the SR0736 sRNA in borrelial infection. Our data contend that *trans*-acting sRNAs like SR0736 represent an important RNA-based tool that can fine-tune gene expression and transcript translation in *B. burgdorferi*. The characterization of additional sRNAs identified in these studies, specifically those that are currently undefined in their abilities to affect borrelial pathogenesis, may shed additional light on this regulatory phenomenon in the context of *B. burgdorferi* infectivity and pathogenic outcomes.

REFERENCES

1. Steere AC, Malawista SE, Snydman DR, Shope RE, Andiman WA, Ross MR, et al. An epidemic of oligoarticular arthritis in children and adults in three connecticut communities. Arthritis & Rheumatism. 1977;20(1):7–17.

2. Burgdorfer W, Barbour AG, Hayes SF, Benach JL, Grunwaldt E, Davis JP. Lyme disease-a tick-borne spirochetosis? Science. 1982 Jun 18;216(4552):1317–9.

3. Steere AC, Grodzicki RL, Kornblatt AN, Craft JE, Barbour AG, Burgdorfer W, et al. The Spirochetal Etiology of Lyme Disease. New England Journal of Medicine. 1983 Mar 31;308(13):733–40.

4. Benach JL, Bosler EM, Hanrahan JP, Coleman JL, Habicht GS, Bast TF, et al. Spirochetes Isolated from the Blood of Two Patients with Lyme Disease. New England Journal of Medicine. 1983 Mar 31;308(13):740–2.

5. Hyde FW, Johnson RC. Genetic relationship of lyme disease spirochetes to Borrelia, Treponema, and Leptospira spp. Journal of Clinical Microbiology. 1984 Aug 1;20(2):151–4.

6. Rosa PA, Tilly K, Stewart PE. The burgeoning molecular genetics of the Lyme disease spirochaete. Nat Rev Micro. 2005 Feb;3(2):129–43.

7. Radolf JD, Caimano MJ, Stevenson B, Hu LT. Of ticks, mice and men: understanding the dual-host lifestyle of Lyme disease spirochaetes. Nature Reviews Microbiology. 2012 Jan 9;10(2):87–99.

8. Kilpatrick AM, Dobson ADM, Levi T, Salkeld DJ, Swei A, Ginsberg HS, et al. Lyme disease ecology in a changing world: consensus, uncertainty and critical gaps for improving control. Philos Trans R Soc B-Biol Sci. 2017 Jun 5;372(1722):20160117.

9. Hinckley AF, Connally NP, Meek JI, Johnson BJ, Kemperman MM, Feldman KA, et al. Lyme Disease Testing by Large Commercial Laboratories in the United States. Clin Infect Dis. 2014 Sep 1;59(5):676–81.

10. Nelson CA, Saha S, Kugeler KJ, Delorey MJ, Shankar MB, Hinckley AF, et al. Incidence of Clinician-Diagnosed Lyme Disease, United States, 2005-2010. Emerging Infectious Diseases. 2015 Sep;21(9):1625–31.

11. Schwartz AM, Hinckley AF, Mead PS, Hook SA, Kugeler KJ. Surveillance for Lyme Disease - United States, 2008-2015. Morbidity And Mortality Weekly

Report Surveillance Summaries (Washington, DC: 2002). 2017 Nov 10;66(22):1–12.

12. Samuels DS. Gene regulation in Borrelia burgdorferi. Annu Rev Microbiol. 2011;65:479–99.

13. Brisson D, Drecktrah D, Eggers CH, Samuels DS. Genetics of Borrelia burgdorferi. Annual Review of Genetics. 2012;46(1):515–36.

14. Radhey S. Gupta, Sharmeen eMahmood, Mobolaji eAdeolu. A Phylogenomic and Molecular Signature Based Approach for Characterization of the Phylum Spirochaetes and its Major Clades: Proposal for a Taxonomic Revision of the Phylum. Frontiers in Microbiology. 2013;

15. Toledo A, Anda P, Escudero R, Larsson C, Bergstrom S, Benach JL. Phylogenetic Analysis of a Virulent Borrelia Species Isolated from Patients with Relapsing Fever. Journal of Clinical Microbiology. 2010 Jul 1;48(7):2484–9.

16. Rudenko N, Golovchenko M, Grubhoffer L, Oliver JH. Updates on Borrelia burgdorferi sensu lato complex with respect to public health. Ticks and Tick-borne Diseases. 2011 Sep 1;2(3):123–8.

17. Postic D, Garnier M, Baranton G. Multilocus sequence analysis of atypical Borrelia burgdorferi sensu lato isolates – Description of Borrelia californiensis sp. nov., and genomospecies 1 and 2. International Journal of Medical Microbiology. 2007 Jul 2;297(4):263–71.

18. Mead PS. Epidemiology of Lyme Disease. Infectious Disease Clinics of North America. 2015 Jun;29(2):187–210.

19. Biesiada G, Czepiel J, Leśniak MR, Garlicki A, Mach T. Lyme disease: review. Arch Med Sci. 2012 Dec 20;8(6):978–82.

20. Steere AC, Coburn J, Glickstein L. The emergence of Lyme disease. J Clin Invest. 2004 Apr 15;113(8):1093–101.

21. Berger BW. Dermatologic Manifestations of Lyme Disease. Rev Infect Dis. 1989 Sep 1;11(Supplement_6):S1475–81.

22. Hyde JA. Borrelia burgdorferi Keeps Moving and Carries on: A Review of Borrelial Dissemination and Invasion. FRONTIERS IN IMMUNOLOGY. 2017 Feb 21;8.

23. Kenedy MR, Lenhart TR, Akins DR. The Role of Borrelia burgdorferi Outer Surface Proteins. FEMS Immunol Med Microbiol. 2012 Oct;66(1):1–19.

24. Steere AC. Lyme Disease. New England Journal of Medicine. 1989 Aug 31;321(9):586–96.

25. Steere AC, Sikand VK, Schoen RT, Nowakowski J. Asymptomatic Infection with Borrelia burgdorferi. Clinical Infectious Diseases. 2003 Aug 15;37(4):528–32.

26. Halperin JJ. Nervous system Lyme disease. J Neurol Sci. 1998 Jan 8;153(2):182–91.

27. Logigian EL, Kaplan RF, Steere AC. Chronic neurologic manifestations of Lyme disease. N Engl J Med. 1990 Nov 22;323(21):1438–44.

28. Oschmann P, Dorndorf W, Hornig C, Schäfer C, Wellensiek HJ, Pflughaupt KW. Stages and syndromes of neuroborreliosis. J Neurol. 1998 May;245(5):262–72.

29. Steere AC. The Clinical Evolution of Lyme Arthritis. Ann Intern Med. 1987 Nov 1;107(5):725.

30. Arvikar SL, Steere AC. 5. Diagnosis and Treatment of Lyme Arthritis. Infect Dis Clin North Am. 2015 Jun;29(2):269–80.

31. Ścieszka J, Dąbek J, Cieślik P. Post-Lyme disease syndrome. Reumatologia. 2015;53(1):46–8.

32. Shapiro ED. Borrelia burgdorferi (Lyme disease). Pediatr Rev. 2014 Dec;35(12):500–9.

33. Levi T, Kilpatrick AM, Mangel M, Wilmers CC. Deer, predators, and the emergence of Lyme disease. Proc Natl Acad Sci U S A. 2012 Jul 3;109(27):10942–7.

34. Fraser CM, Casjens S, Huang WM, Sutton GG, Clayton R, Lathigra R, et al. Genomic sequence of a Lyme disease spirochaete, Borrelia burgdorferi. Nature. 1997 Dec 11;390(6660):580–6.

35. Casjens S, Palmer N, van Vugt R, Huang WM, Stevenson B, Rosa P, et al. A bacterial genome in flux: the twelve linear and nine circular extrachromosomal DNAs in an infectious isolate of the Lyme disease spirochete Borrelia burgdorferi. Mol Microbiol. 2000 Feb;35(3):490–516.

36. Barbour AG, Garon CF. Linear Plasmids of the Bacterium Borrelia burgdferi Have Covalently Closed Ends. :4.

37. Di L, Pagan PE, Packer D, Martin CL, Akther S, Ramrattan G, et al. BorreliaBase: a phylogeny-centered browser of Borrelia genomes. BMC Bioinformatics. 2014 Jul 3;15:233.

38. Qiu W-G, Martin CL. Evolutionary Genomics of Borrelia burgdorferi sensu lato: Findings, Hypotheses, and the Rise of Hybrids. Infect Genet Evol. 2014 Oct;27:576–93.

39. Weening EH, Parveen N, Trzeciakowski JP, Leong JM, Höök M, Skare JT. Borrelia burgdorferi Lacking DbpBA Exhibits an Early Survival Defect during Experimental Infection. Infect Immun. 2008 Dec;76(12):5694–705.

40. Zhi H, Weening EH, Barbu EM, Hyde JA, Höök M, Skare JT. The BBA33 lipoprotein binds collagen and impacts Borrelia burgdorferi pathogenesis. Mol Microbiol. 2015 Apr;96(1):68–83.

41. Hyde JA, Weening EH, Chang M, Trzeciakowski JP, Höök M, Cirillo JD, et al. Bioluminescent imaging of Borrelia burgdorferi in vivo demonstrates that the fibronectin binding protein BBK32 is required for optimal infectivity. Mol Microbiol. 2011 Oct;82(1):99–113.

42. Barbour AG. Isolation and cultivation of Lyme disease spirochetes. Yale J Biol Med. 1984 Aug;57(4):521–5.

43. Posey JE, Gherardini FC. Lack of a role for iron in the Lyme disease pathogen. Science. 2000 Jun 2;288(5471):1651–3.

44. Radolf JD, Samuels DS. Borrelia: Molecular Biology, Host Interaction and Pathogenesis [Internet]. Caister Academic Press; 2010. Available from: https://books.google.com/books?id=1iHDrzSIcI0C

45. von Lackum K, Stevenson B. Carbohydrate utilization by the Lyme borreliosis spirochete, Borrelia burgdorferi. FEMS Microbiol Lett. 2005 Feb 1;243(1):173–9.

46. MOTALEB MA, LIU J, WOOTEN RM. Spirochetal motility and chemotaxis in the natural enzootic cycle and development of Lyme disease. Curr Opin Microbiol. 2015 Dec;28:106–13.

47. Barbour AG, Hayes SF. Biology of Borrelia species. Microbiol Rev. 1986 Dec 1;50(4):381–400.

48. Takayama K, Rothenberg RJ, Barbour AG. Absence of lipopolysaccharide in the Lyme disease spirochete, Borrelia burgdorferi. Infect Immun. 1987 Sep;55(9):2311–3.

49. Brooks CS, Vuppala SR, Jett AM, Akins DR. Identification of Borrelia burgdorferi Outer Surface Proteins. Infect Immun. 2006 Jan 1;74(1):296–304.

50. Wooten RM, Ma Y, Yoder RA, Brown JP, Weis JH, Zachary JF, et al. Toll-like receptor 2 is required for innate, but not acquired, host defense to Borrelia burgdorferi. J Immunol. 2002 Jan 1;168(1):348–55.

51. Bolz DD, Sundsbak RS, Ma Y, Akira S, Kirschning CJ, Zachary JF, et al. MyD88 Plays a Unique Role in Host Defense but Not Arthritis Development in Lyme Disease. The Journal of Immunology. 2004 Aug 1;173(3):2003–10.

52. Charon NW, Goldstein SF, Marko M, Hsieh C, Gebhardt LL, Motaleb MA, et al. The Flat-Ribbon Configuration of the Periplasmic Flagella of Borrelia burgdorferi and Its Relationship to Motility and Morphology. Journal of Bacteriology. 2009 Jan 15;191(2):600–7.

53. Motaleb MA, Corum L, Bono JL, Elias AF, Rosa P, Samuels DS, et al. Borrelia burgdorferi periplasmic flagella have both skeletal and motility functions. Proc Natl Acad Sci U S A. 2000 Sep 26;97(20):10899–904.

54. Dunham-Ems SM, Caimano MJ, Pal U, Wolgemuth CW, Eggers CH, Balic A, et al. Live imaging reveals a biphasic mode of dissemination of *Borrelia burgdorferi* within ticks. J Clin Invest. 2009 Dec 1;119(12):3652–65.

55. Lejal E, Moutailler S, Šimo L, Vayssier-Taussat M, Pollet T. Tick-borne pathogen detection in midgut and salivary glands of adult Ixodes ricinus. Parasites & Vectors. 2019 Apr 2;12(1):152.

56. Wormser GP. Hematogenous dissemination in early Lyme disease. Wien Klin Wochenschr. 2006 Nov 1;118(21):634–7.

57. Charon NW, Cockburn A, Li C, Liu J, Miller KA, Miller MR, et al. The unique paradigm of spirochete motility and chemotaxis. Annu Rev Microbiol. 2012;66:349–70.

58. Motaleb MA, Sultan SZ, Miller MR, Li C, Charon NW. CheY3 of Borrelia burgdorferi Is the Key Response Regulator Essential for Chemotaxis and Forms a Long-Lived Phosphorylated Intermediate. Journal of Bacteriology. 2011 Jul 1;193(13):3332–41.

59. Novak EA, Sekar P, Xu H, Moon KH, Manne A, Wooten RM, et al. The Borrelia burgdorferi CheY3 response regulator is essential for chemotaxis and completion of its natural infection cycle. Cellular Microbiology. 2016;18(12):1782–99.

60. Motaleb MA, Miller MR, Li C, Bakker RG, Goldstein SF, Silversmith RE, et al. CheX Is a Phosphorylated CheY Phosphatase Essential for Borrelia

burgdorferi Chemotaxis. Journal of Bacteriology. 2005 Dec 1;187(23):7963–9.

61. Moon KH, Hobbs G, Motaleb MA. Borrelia burgdorferi CheD Promotes Various Functions in Chemotaxis and the Pathogenic Life Cycle of the Spirochete. Infection and Immunity. 2016 Jun 1;84(6):1743–52.

62. Zhang K, Liu J, Charon NW, Li C. Hypothetical Protein BB0569 Is Essential for Chemotaxis of the Lyme Disease Spirochete Borrelia burgdorferi. Journal of Bacteriology. 2016 Feb 15;198(4):664–72.

63. Sze CW, Morado DR, Liu J, Charon NW, Xu H, Li C. Carbon storage regulator A (CsrA(Bb)) is a repressor of Borrelia burgdorferi flagellin protein FlaB. Mol Microbiol. 2011 Nov;82(4):851–64.

64. Sanjuan E, Esteve-Gassent MD, Maruskova M, Seshu J. Overexpression of CsrA (BB0184) alters the morphology and antigen profiles of Borrelia burgdorferi. Infect Immun. 2009 Nov;77(11):5149–62.

65. Iyer R, Caimano MJ, Luthra A, Axline D, Jr, Corona A, et al. Stage-Specific Global Alterations in the Transcriptomes of Lyme Disease Spirochetes During Tick Feeding and Following Mammalian Host-Adaptation. Molecular microbiology. 2015 Feb;95(3):509.

66. Brooks CS, Hefty PS, Jolliff SE, Akins DR. Global Analysis of Borrelia burgdorferi Genes Regulated by Mammalian Host-Specific Signals. Infect Immun. 2003 Jun;71(6):3371–83.

67. Akins DR, Bourell KW, Caimano MJ, Norgard MV, Radolf JD. A new animal model for studying Lyme disease spirochetes in a mammalian host-adapted state. J Clin Invest. 1998 May 15;101(10):2240–50.

68. Carroll JA, Garon CF, Schwan TG. Effects of environmental pH on membrane proteins in Borrelia burgdorferi. Infect Immun. 1999 Jul;67(7):3181–7.

69. Ojaimi C, Brooks C, Casjens S, Rosa P, Elias A, Barbour A, et al. Profiling of Temperature-Induced Changes in Borrelia burgdorferi Gene Expression by Using Whole Genome Arrays. Infect Immun. 2003 Apr;71(4):1689–705.

70. Revel AT, Talaat AM, Norgard MV. DNA microarray analysis of differential gene expression in Borrelia burgdorferi, the Lyme disease spirochete. PNAS. 2002 Feb 5;99(3):1562–7.

71. Stevenson B, Schwan TG, Rosa PA. Temperature-related differential expression of antigens in the Lyme disease spirochete, Borrelia burgdorferi. Infect Immun. 1995 Nov;63(11):4535–9.

72. Carroll JA, Cordova RM, Garon CF. Identification of 11 pH-regulated genes in Borrelia burgdorferi localizing to linear plasmids. Infect Immun. 2000 Dec;68(12):6677–84.

73. Hyde JA, Trzeciakowski JP, Skare JT. Borrelia burgdorferi Alters Its Gene Expression and Antigenic Profile in Response to CO2 Levels. J Bacteriol. 2007 Jan;189(2):437–45.

74. Seshu J, Boylan JA, Gherardini FC, Skare JT. Dissolved Oxygen Levels Alter Gene Expression and Antigen Profiles in Borrelia burgdorferi. Infection and Immunity. 2004 Mar;72(3):1580.

75. Tokarz R, Anderton JM, Katona LI, Benach JL. Combined Effects of Blood and Temperature Shift on Borrelia burgdorferi Gene Expression as Determined by Whole Genome DNA Array. Infect Immun. 2004 Sep;72(9):5419–32.

76. Stevenson B, Seshu J. Regulation of Gene and Protein Expression in the Lyme Disease Spirochete. In: Adler B, editor. Spirochete Biology: The Post Genomic Era [Internet]. Cham: Springer International Publishing; 2018 [cited 2019 Sep 24]. p. 83–112. (Current Topics in Microbiology and Immunology). Available from: https://doi.org/10.1007/82_2017_49

77. Burtnick MN, Downey JS, Brett PJ, Boylan JA, Frye JG, Hoover TR, et al. Insights into the complex regulation of rpoS in Borrelia burgdorferi. Mol Microbiol. 2007 Jul 1;65(2):277–93.

78. Caimano MJ, Iyer R, Eggers CH, Gonzalez C, Morton EA, Gilbert MA, et al. Analysis of the RpoS regulon in Borrelia burgdorferi in response to mammalian host signals provides insight into RpoS function during the enzootic cycle. Mol Microbiol. 2007 Sep;65(5):1193–217.

79. Yang XF, Alani SM, Norgard MV. The response regulator Rrp2 is essential for the expression of major membrane lipoproteins in Borrelia burgdorferi. Proc Natl Acad Sci U S A. 2003 Sep 16;100(19):11001–6.

80. Boardman BK, He M, Ouyang Z, Xu H, Pang X, Yang XF. Essential Role of the Response Regulator Rrp2 in the Infectious Cycle of Borrelia burgdorferi. Infect Immun. 2008 Sep;76(9):3844–53.

81. Blevins JS, Xu H, He M, Norgard MV, Reitzer L, Yang XF. Rrp2, a σ54-Dependent Transcriptional Activator of Borrelia burgdorferi, Activates rpoS in an Enhancer-Independent Manner. J Bacteriol. 2009 Apr;191(8):2902–5.

82. Ouyang Z, Blevins JS, Norgard MV. Transcriptional interplay among the regulators Rrp2, RpoN and RpoS in Borrelia burgdorferi. Microbiology (Reading, Engl). 2008 Sep;154(Pt 9):2641–58.

83. Yang XF, Alani SM, Norgard MV. The response regulator Rrp2 is essential for the expression of major membrane lipoproteins in Borrelia burgdorferi. Proc Natl Acad Sci U S A. 2003 Sep 16;100(19):11001–6.

84. Rogers EA, Terekhova D, Zhang H-M, Hovis KM, Schwartz I, Marconi RT. Rrp1, a cyclic-di-GMP-producing response regulator, is an important regulator of Borrelia burgdorferi core cellular functions. Mol Microbiol. 2009 Mar;71(6):1551–73.

85. Caimano MJ, Kenedy MR, Kairu T, Desrosiers DC, Harman M, Dunham-Ems S, et al. The Hybrid Histidine Kinase Hk1 Is Part of a Two-Component System That Is Essential for Survival of Borrelia burgdorferi in Feeding Ixodes scapularis Ticks ▿ . Infect Immun. 2011 Aug;79(8):3117–30.

86. Smith AH, Blevins JS, Bachlani GN, Yang XF, Norgard MV. Evidence that RpoS (σS) in Borrelia burgdorferi Is Controlled Directly by RpoN (σ54/σN). Journal of Bacteriology. 2007 Mar 1;189(5):2139–44.

87. Caimano MJ, Eggers CH, Hazlett KRO, Radolf JD. RpoS Is Not Central to the General Stress Response in Borrelia burgdorferi but Does Control Expression of One or More Essential Virulence Determinants. Infect Immun. 2004 Nov 1;72(11):6433–45.

88. Fisher MA, Grimm D, Henion AK, Elias AF, Stewart PE, Rosa PA, et al. Borrelia burgdorferi sigma54 is required for mammalian infection and vector transmission but not for tick colonization. Proc Natl Acad Sci USA. 2005 Apr 5;102(14):5162–7.

89. Hübner A, Yang X, Nolen DM, Popova TG, Cabello FC, Norgard MV. Expression of Borrelia burgdorferi OspC and DbpA is controlled by a RpoN–RpoS regulatory pathway. Proc Natl Acad Sci U S A. 2001 Oct 23;98(22):12724–9.

90. Samuels DS, Radolf JD. Who is the BosR around here anyway? Mol Microbiol. 2009 Dec;74(6):1295–9.

91. Miller CL, Karna SLR, Seshu J. Borrelia host adaptation Regulator (BadR) regulates rpoS to modulate host adaptation and virulence factors in Borrelia burgdorferi. Molecular Microbiology. 2013 Apr;88(1):105–24.

92. Ouyang Z, Zhou J. BadR (BB0693) controls growth phase-dependent induction of rpoS and bosR in Borrelia burgdorferi via recognizing TAAAATAT motifs. Molecular Microbiology. 2015 Dec;98(6):1147–67.

93. Seshu J, Esteve-Gassent MD, Labandeira-Rey M, Kim JH, Trzeciakowski JP, Höök M, et al. Inactivation of the fibronectin-binding adhesin gene bbk32 significantly attenuates the infectivity potential of Borrelia burgdorferi. Molecular Microbiology. 2006 Mar 1;59(5):1591–601.

94. Caimano MJ, Eggers CH, Gonzalez CA, Radolf JD. Alternate Sigma Factor RpoS Is Required for the In Vivo-Specific Repression of Borrelia burgdorferi Plasmid lp54-Borne ospA and lp6.6 Genes. J Bacteriol. 2005 Nov;187(22):7845–52.

95. He M, Boardman BK, Yan D, Yang XF. Regulation of Expression of the Fibronectin-Binding Protein BBK32 in Borrelia burgdorferi. J Bacteriol. 2007 Nov 15;189(22):8377–80.

96. Tilly K, Krum JG, Bestor A, Jewett MW, Grimm D, Bueschel D, et al. Borrelia burgdorferi OspC Protein Required Exclusively in a Crucial Early Stage of Mammalian Infection. Infect Immun. 2006 Jun;74(6):3554–64.

97. Grimm D, Tilly K, Byram R, Stewart PE, Krum JG, Bueschel DM, et al. Outer-surface protein C of the Lyme disease spirochete: a protein induced in ticks for infection of mammals. Proc Natl Acad Sci USA. 2004 Mar 2;101(9):3142–7.

98. Brown EL, Guo BP, O'Neal P, Höök M. Adherence of Borrelia burgdorferi IDENTIFICATION OF CRITICAL LYSINE RESIDUES IN DbpA REQUIRED FOR DECORIN BINDING. J Biol Chem. 1999 Sep 10;274(37):26272–8.

99. Guo BP, Brown EL, Dorward DW, Rosenberg LC, Höök M. Decorin-binding adhesins from Borrelia burgdorferi. Molecular Microbiology. 1998;30(4):711–23.

100. Probert WS, Johnson BJB. Identification of a 47 kDa fibronectin-binding protein expressed by Borrelia burgdorferi isolate B31. Molecular Microbiology. 1998;30(5):1003–15.

101. Kim JH, Singvall J, Schwarz-Linek U, Johnson BJB, Potts JR, Höök M. BBK32, a Fibronectin Binding MSCRAMM from Borrelia burgdorferi, Contains a Disordered Region That Undergoes a Conformational Change on Ligand Binding. J Biol Chem. 2004 Oct 1;279(40):41706–14.

102. Garcia BL, Zhi H, Wager B, Höök M, Skare JT. Borrelia burgdorferi BBK32 Inhibits the Classical Pathway by Blocking Activation of the C1 Complement Complex. PLOS Pathogens. 2016 Jan 25;12(1):e1005404.

103. Shi Y, Xu Q, McShan K, Liang FT. Both Decorin-Binding Proteins A and B Are Critical for the Overall Virulence of Borrelia burgdorferi. Infect Immun. 2008 Mar;76(3):1239–46.

104. Pal U, Yang X, Chen M, Bockenstedt LK, Anderson JF, Flavell RA, et al. OspC facilitates Borrelia burgdorferi invasion of Ixodes scapularis salivary glands. J Clin Invest. 2004 Jan 15;113(2):220–30.

105. Yang XF, Pal U, Alani SM, Fikrig E, Norgard MV. Essential Role for OspA/B in the Life Cycle of the Lyme Disease Spirochete. J Exp Med. 2004 Mar 1;199(5):641–8.

106. Schwan TG, Piesman J, Golde WT, Dolan MC, Rosa PA. Induction of an outer surface protein on Borrelia burgdorferi during tick feeding. Proc Natl Acad Sci USA. 1995 Mar 28;92(7):2909–13.

107. Pal U, Li X, Wang T, Montgomery RR, Ramamoorthi N, Desilva AM, et al. TROSPA, an Ixodes scapularis receptor for Borrelia burgdorferi. Cell. 2004 Nov 12;119(4):457–68.

108. Pal U, de Silva AM, Montgomery RR, Fish D, Anguita J, Anderson JF, et al. Attachment of Borrelia burgdorferi within Ixodes scapularis mediated by outer surface protein A. J Clin Invest. 2000 Aug 15;106(4):561–9.

109. Novak EA, Sultan SZ, Motaleb MA. The cyclic-di-GMP signaling pathway in the Lyme disease spirochete, Borrelia burgdorferi. Front Cell Infect Microbiol. 2014;4:56.

110. Ryjenkov DA, Tarutina M, Moskvin OV, Gomelsky M. Cyclic Diguanylate Is a Ubiquitous Signaling Molecule in Bacteria: Insights into Biochemistry of the GGDEF Protein Domain. J Bacteriol. 2005 Mar;187(5):1792–8.

111. Kostick JL, Szkotnicki LT, Rogers EA, Bocci P, Raffaelli N, Marconi RT. The diguanylate cyclase, Rrp1, regulates critical steps in the enzootic cycle of the Lyme disease spirochetes. Molecular Microbiology. 2011;81(1):219–31.

112. He M, Ouyang Z, Troxell B, Xu H, Moh A, Piesman J, et al. Cyclic di-GMP is Essential for the Survival of the Lyme Disease Spirochete in Ticks. PLOS Pathogens. 2011 Jun 30;7(6):e1002133.

113. Caimano MJ, Dunham-Ems S, Allard AM, Cassera MB, Kenedy M, Radolf JD. Cyclic di-GMP Modulates Gene Expression in Lyme Disease Spirochetes at the Tick-Mammal Interface To Promote Spirochete Survival during the Blood

Meal and Tick-to-Mammal Transmission. Infection and Immunity. 2015 Aug 1;83(8):3043–60.

114. Pappas CJ, Iyer R, Petzke MM, Caimano MJ, Radolf JD, Schwartz I. Borrelia burgdorferi Requires Glycerol for Maximum Fitness During The Tick Phase of the Enzootic Cycle. PLOS Pathogens. 2011 Jul 7;7(7):e1002102.

115. Sze CW, Smith A, Choi YH, Yang X, Pal U, Yu A, et al. Study of the Response Regulator Rrp1 Reveals Its Regulatory Role in Chitobiose Utilization and Virulence of Borrelia burgdorferi. Infection and Immunity. 2013 May 1;81(5):1775–87.

116. Rhodes RG, Atoyan JA, Nelson DR. The chitobiose transporter, chbC, is required for chitin utilization in Borrelia burgdorferi. BMC Microbiol. 2010 Jan 26;10:21.

117. Tilly K, Elias AF, Errett J, Fischer E, Iyer R, Schwartz I, et al. Genetics and Regulation of Chitobiose Utilization in Borrelia burgdorferi. J Bacteriol. 2001 Oct;183(19):5544–53.

118. Sultan SZ, Pitzer JE, Boquoi T, Hobbs G, Miller MR, Motaleb MA. Analysis of the HD-GYP Domain Cyclic Dimeric GMP Phosphodiesterase Reveals a Role in Motility and the Enzootic Life Cycle of Borrelia burgdorferi ▿. Infect Immun. 2011 Aug;79(8):3273–83.

119. Sultan SZ, Pitzer JE, Miller MR, Motaleb MdA. Analysis of a Borrelia burgdorferi phosphodiesterase demonstrates a role for cyclic-di-GMP in motility and virulence. Mol Microbiol. 2010 Jul 1;77(1):128–42.

120. Zhang J-J, Chen T, Yang Y, Du J, Li H, Troxell B, et al. Positive and Negative Regulation of Glycerol Utilization by the c-di-GMP Binding Protein PlzA in Borrelia burgdorferi. Journal of Bacteriology. 2018 Nov 15;200(22):e00243-18.

121. Pitzer JE, Sultan SZ, Hayakawa Y, Hobbs G, Miller MR, Motaleb MA. Analysis of the Borrelia burgdorferi Cyclic-di-GMP-Binding Protein PlzA Reveals a Role in Motility and Virulence ▿. Infect Immun. 2011 May;79(5):1815–25.

122. Kostick-Dunn JL, Izac JR, Freedman JC, Szkotnicki LT, Oliver LD, Marconi RT. The Borrelia burgdorferi c-di-GMP Binding Receptors, PlzA and PlzB, Are Functionally Distinct. Front Cell Infect Microbiol. 2018 Jul 11;8:213.

123. He M, Zhang J-J, Ye M, Lou Y, Yang XF. Cyclic Di-GMP Receptor PlzA Controls Virulence Gene Expression through RpoS in Borrelia burgdorferi. Infect Immun. 2014 Jan;82(1):445–52.

124. Freedman JC, Rogers EA, Kostick JL, Zhang H, Iyer R, Schwartz I, et al. Identification and molecular characterization of a cyclic-di-GMP effector protein, PlzA (BB0733): additional evidence for the existence of a functional cyclic-di-GMP regulatory network in the Lyme disease spirochete, Borrelia burgdorferi. FEMS Immunol Med Microbiol. 2010 Mar;58(2):285–94.

125. Bugrysheva J, Dobrikova EY, Godfrey HP, Sartakova ML, Cabello FC. Modulation of Borrelia burgdorferi Stringent Response and Gene Expression during Extracellular Growth with Tick Cells. Infection and Immunity. 2002 Jun 1;70(6):3061–7.

126. Bugrysheva J, Dobrikova EY, Sartakova ML, Caimano MJ, Daniels TJ, Radolf JD, et al. Characterization of the stringent response and rel(Bbu) expression in Borrelia burgdorferi. J Bacteriol. 2003 Feb;185(3):957–65.

127. Bugrysheva JV, Bryksin AV, Godfrey HP, Cabello FC. Borrelia burgdorferi rel is responsible for generation of guanosine-3'-diphosphate-5'-triphosphate and growth control. Infect Immun. 2005 Aug;73(8):4972–81.

128. Drecktrah D, Lybecker M, Popitsch N, Rescheneder P, Hall LS, Samuels DS. The Borrelia burgdorferi RelA/SpoT Homolog and Stringent Response Regulate Survival in the Tick Vector and Global Gene Expression during Starvation. PLOS Pathogens. 2015 Sep 15;11(9):e1005160.

129. Dulebohn DP, Hayes BM, Rosa PA. Global Repression of Host-Associated Genes of the Lyme Disease Spirochete through Post-Transcriptional Modulation of the Alternative Sigma Factor RpoS. PLOS ONE. 2014 Mar 26;9(3):e93141.

130. Hayes BM, Dulebohn DP, Sarkar A, Tilly K, Bestor A, Ambroggio X, et al. Regulatory Protein BBD18 of the Lyme Disease Spirochete: Essential Role During Tick Acquisition? mBio. 2014 May 1;5(2):e01017-14.

131. Sarkar A, Hayes BM, Dulebohn DP, Rosa PA. Regulation of the virulence determinant OspC by bbd18 on linear plasmid lp17 of Borrelia burgdorferi. J Bacteriol. 2011 Oct;193(19):5365–73.

132. Vakulskas CA, Potts AH, Babitzke P, Ahmer BMM, Romeo T. Regulation of Bacterial Virulence by Csr (Rsm) Systems. Microbiol Mol Biol Rev. 2015 Jun 1;79(2):193–224.

133. Karna SLR, Prabhu RG, Lin Y-H, Miller CL, Seshu J. Contributions of Environmental Signals and Conserved Residues to the Functions of Carbon Storage Regulator A of Borrelia burgdorferi. Infection and Immunity. 2013 Aug 1;81(8):2972–85.

134. Sze CW, Li C. Inactivation of bb0184, which encodes carbon storage regulator A, represses the infectivity of Borrelia burgdorferi. Infect Immun. 2011 Mar;79(3):1270–9.

135. Ouyang Z, Zhou J, Norgard MV. CsrA (BB0184) Is Not Involved in Activation of the RpoN-RpoS Regulatory Pathway in Borrelia burgdorferi. Infection and Immunity. 2014 Apr;82(4):1511.

136. Liu MY, Gui G, Wei B, Preston JF, Oakford L, Yüksel Ü, et al. The RNA Molecule CsrB Binds to the Global Regulatory Protein CsrA and Antagonizes Its Activity in Escherichia coli. J Biol Chem. 1997 Jul 11;272(28):17502–10.

137. Jutras BL, Jones GS, Verma A, Brown NA, Antonicello AD, Chenail AM, et al. Posttranscriptional self-regulation by the Lyme disease bacterium's BpuR DNA/RNA-binding protein. J Bacteriol. 2013 Nov;195(21):4915–23.

138. Graebsch A, Roche S, Niessing D. X-ray structure of Pur-α reveals a Whirly-like fold and an unusual nucleic-acid binding surface. PNAS. 2009 Nov 3;106(44):18521–6.

139. Jutras BL, Savage CR, Arnold WK, Lethbridge KG, Carroll DW, Tilly K, et al. The Lyme disease spirochete's BpuR DNA/RNA-binding protein is differentially expressed during the mammal–tick infectious cycle, which affects translation of the SodA superoxide dismutase. Molecular Microbiology. 2019;112(3):973–91.

140. Savage CR, Jutras BL, Bestor A, Tilly K, Rosa PA, Tourand Y, et al. Borrelia burgdorferi SpoVG DNA- and RNA-Binding Protein Modulates the Physiology of the Lyme Disease Spirochete. Journal of Bacteriology. 2018 Jun 15;200(12):e00033-18.

141. Jankowsky E. RNA Helicases at work: binding and rearranging. Trends Biochem Sci. 2011 Jan;36(1):19–29.

142. Khemici V, Linder P. RNA helicases in bacteria. Current Opinion in Microbiology. 2016 Apr 1;30:58–66.

143. Redder P, Hausmann S, Khemici V, Yasrebi H, Linder P. Bacterial versatility requires DEAD-box RNA helicases. FEMS Microbiology Reviews. 2015 May 1;39(3):392–412.

144. Salman-Dilgimen A, Hardy P-O, Dresser AR, Chaconas G. HrpA, a DEAH-box RNA helicase, is involved in global gene regulation in the Lyme disease spirochete. PLoS ONE. 2011;6(7):e22168.

145. Salman-Dilgimen A, Hardy P-O, Radolf JD, Caimano MJ, Chaconas G. HrpA, an RNA Helicase Involved in RNA Processing, Is Required for Mouse

Infectivity and Tick Transmission of the Lyme Disease Spirochete. PLOS Pathogens. 2013 Dec 19;9(12):e1003841.

146. Dutta T, Srivastava S. Small RNA-mediated regulation in bacteria: A growing palette of diverse mechanisms. Gene. 2018 May 20;656:60–72.

147. Barquist L, Vogel J. Accelerating Discovery and Functional Analysis of Small RNAs with New Technologies. Annual Review of Genetics. 2015;49(1):367–94.

148. Nitzan M, Rehani R, Margalit H. Integration of Bacterial Small RNAs in Regulatory Networks. Annu Rev Biophys. 2017 May 22;46(1):131–48.

149. Beisel CL, Storz G. Base pairing small RNAs and their roles in global regulatory networks. FEMS Microbiol Rev. 2010 Sep;34(5):866–82.

150. Storz G, Vogel J, Wassarman KM. Regulation by small RNAs in bacteria: expanding frontiers. Mol Cell. 2011 Sep 16;43(6):880–91.

151. Dutcher HA, Raghavan R. Origin, Evolution, and Loss of Bacterial Small RNAs. Microbiol Spectr. 2018 Apr;6(2):UNSP RWR-0004-2017.

152. Updegrove TB, Shabalina SA, Storz G. How do base-pairing small RNAs evolve? FEMS Microbiol Rev. 2015 May;39(3):379–91.

153. Gottesman S, Storz G. Bacterial Small RNA Regulators: Versatile Roles and Rapidly Evolving Variations. Cold Spring Harb Perspect Biol. 2011 Dec 1;3(12):a003798.

154. Beisel CL, Storz G. The base pairing RNA Spot 42 participates in a multi-output feedforward loop to help enact catabolite repression in Escherichia coli. Mol Cell. 2011 Feb 4;41(3):286–97.

155. Durand S, Storz G. Reprogramming of Anaerobic Metabolism by the FnrS Small RNA. Mol Microbiol. 2010 Mar;75(5):1215–31.

156. Carrier M-C, Lalaouna D, Massé E. Broadening the Definition of Bacterial Small RNAs: Characteristics and Mechanisms of Action. Annual Review of Microbiology. 2018;72(1):141–61.

157. Santiago-Frangos A, Woodson SA. Hfq chaperone brings speed dating to bacterial sRNA. Wiley Interdiscip Rev RNA. 2018;9(4):e1475.

158. Kavita K, de Mets F, Gottesman S. New aspects of RNA-based regulation by Hfq and its partner sRNAs. Curr Opin Microbiol. 2017 Nov 7;42:53–61.

159. Waters LS, Storz G. Regulatory RNAs in Bacteria. Cell. 2009 Feb 20;136(4):615–28.

160. Georg J, Hess WR. cis-Antisense RNA, Another Level of Gene Regulation in Bacteria. Microbiol Mol Biol Rev. 2011 Jun 1;75(2):286–300.

161. Popitsch N, Bilusic I, Rescheneder P, Schroeder R, Lybecker M. Temperature-dependent sRNA transcriptome of the Lyme disease spirochete. BMC Genomics. 2017;18:28.

162. Bilusic I, Popitsch N, Rescheneder P, Schroeder R, Lybecker M. Revisiting the coding potential of the E. coli genome through Hfq co-immunoprecipitation. RNA Biology. 2014 May 1;11(5):641–54.

163. Breaker RR. Riboswitches: from ancient gene-control systems to modern drug targets. Future Microbiology. 2009 Sep 1;4(7):771–3.

164. Serganov A, Nudler E. A Decade of Riboswitches. Cell. 2013 Jan 17;152(1):17–24.

165. Kortmann J, Narberhaus F. Bacterial RNA thermometers: molecular zippers and switches. Nature Reviews Microbiology. 2012 Apr;10(4):255–65.

166. Loh E, Righetti F, Eichner H, Twittenhoff C, Narberhaus F. RNA Thermometers in Bacterial Pathogens. Microbiology Spectrum. 2018 Apr;6(2).

167. Li W, Ying X, Lu Q, Chen L. Predicting sRNAs and Their Targets in Bacteria. Genomics, Proteomics & Bioinformatics. 2012 Oct;10(5):276–84.

168. Tsai C-H, Liao R, Chou B, Palumbo M, Contreras LM. Genome-Wide Analyses in Bacteria Show Small-RNA Enrichment for Long and Conserved Intergenic Regions. J Bacteriol. 2015 Jan 1;197(1):40–50.

169. Lybecker MC, Samuels DS. Temperature-induced regulation of RpoS by a small RNA in Borrelia burgdorferi. Molecular Microbiology. 2007;64(4):1075–89.

170. Lybecker MC, Abel CA, Feig AL, Samuels DS. Identification and function of the RNA chaperone Hfq in the Lyme disease spirochete Borrelia burgdorferi. Mol Microbiol. 2010 Nov;78(3):622–35.

171. Obana N, Nakamura K, Nomura N. Role of RNase Y in Clostridium perfringens mRNA Decay and Processing. J Bacteriol. 2017 Jan;199(2):UNSP e00703.

172. Bruce HA, Du D, Matak-Vinkovic D, Bandyra KJ, Broadhurst RW, Martin E, et al. Analysis of the natively unstructured RNA/protein-recognition core in the

Escherichia coli RNA degradosome and its interactions with regulatory RNA/Hfq complexes. Nucleic Acids Research. 2018 Jan 9;46(1):387–402.

173. Hui MP, Foley PL, Belasco JG. Messenger RNA Degradation in Bacterial Cells. Annu Rev Genet. 2014;48:537–59.

174. Arraiano CM, Andrade JM, Domingues S, Guinote IB, Malecki M, Matos RG, et al. The critical role of RNA processing and degradation in the control of gene expression. FEMS Microbiol Rev. 2010 Sep 1;34(5):883–923.

175. Archambault L, Borchert JS, Bergeron J, Snow S, Schlax PJ. Measurements of mRNA Degradation in Borrelia burgdorferi. J Bacteriol. 2013 Nov 1;195(21):4879–87.

176. Mattsson JG, Svärd SG, Kirsebom LA. Characterization of the Borrelia burgdorferi RNase P RNA gene reveals a novel tertiary interaction. J Mol Biol. 1994 Aug 5;241(1):1–6.

177. Anacker ML, Drecktrah D, LeCoultre RD, Lybecker M, Samuels DS. RNase III Processing of rRNA in the Lyme Disease Spirochete Borrelia burgdorferi. Journal of Bacteriology. 2018 Jul 1;200(13):e00035-18.

178. Arnold WK, Savage CR, Brissette CA, Seshu J, Livny J, Stevenson B. RNA-Seq of Borrelia burgdorferi in Multiple Phases of Growth Reveals Insights into the Dynamics of Gene Expression, Transcriptome Architecture, and Noncoding RNAs. PLOS ONE. 2016 Oct 5;11(10):e0164165.

179. Casselli T, Tourand Y, Bankhead T. Altered Murine Tissue Colonization by Borrelia burgdorferi following Targeted Deletion of Linear Plasmid 17-Carried Genes. Infect Immun. 2012 May;80(5):1773–82.

180. Radolf JD, Caimano MJ, Stevenson B, Hu LT. Of ticks, mice and men: understanding the dual-host lifestyle of Lyme disease spirochaetes. Nat Rev Microbiol. 2012 Jan 9;10(2):87–99.

181. Labandeira-Rey M, Skare JT. Decreased Infectivity in Borrelia burgdorferi Strain B31 Is Associated with Loss of Linear Plasmid 25 or 28-1. Infect Immun. 2001 Jan;69(1):446–55.

182. Zhang J-R, Hardham JM, Barbour AG, Norris SJ. Antigenic Variation in Lyme Disease Borreliae by Promiscuous Recombination of VMP-like Sequence Cassettes. Cell. 1997 Apr 18;89(2):275–85.

183. Purser JE, Lawrenz MB, Caimano MJ, Howell JK, Radolf JD, Norris SJ. A plasmid-encoded nicotinamidase (PncA) is essential for infectivity of Borrelia burgdorferi in a mammalian host. Molecular Microbiology. 2003 May 1;48(3):753–64.

184. Sadziene A, Thomas DD, Bundoc VG, Holt SC, Barbour AG. A flagella-less mutant of Borrelia burgdorferi. Structural, molecular, and in vitro functional characterization. J Clin Invest. 1991 Jul;88(1):82–92.

185. Samuels DS, Marconi RT, Huang WM, Garon CF. gyrB mutations in coumermycin A1-resistant Borrelia burgdorferi. J Bacteriol. 1994 May;176(10):3072–5.

186. Hyde JA, Weening EH, Skare JT. Genetic Manipulation of Borrelia burgdorferi. Curr Protoc Microbiol. 2011 Feb;CHAPTER:Unit-12C.4.

187. Antibody-resistant mutants of Borrelia burgdorferi: in vitro selection and characterization. J Exp Med. 1992 Sep 1;176(3):799–809.

188. Pal U Editor, Buyuktanir O Editor, Scott Samuels D, Drecktrah D, Hall LS, Walker JM Series editor. Genetic Transformation and Complementation. Borrelia burgdorferi : Methods and Protocols. 2017;183.

189. Lin T, Gao L, Zhang C, Odeh E, Jacobs MB, Coutte L, et al. Analysis of an Ordered, Comprehensive STM Mutant Library in Infectious Borrelia burgdorferi: Insights into the Genes Required for Mouse Infectivity. PLOS ONE. 2012 Oct 25;7(10):e47532.

190. Tao eLin, Erin B Troy, Linden T Hu, Lihui eGao, Steven J Norris. Transposon mutagenesis as an approach to improved understanding of Borrelia pathogenesis and biology. Frontiers in Cellular and Infection Microbiology. 2014;

191. Muñoz-López M, García-Pérez JL. DNA Transposons: Nature and Applications in Genomics. Curr Genomics. 2010 Apr;11(2):115–28.

192. Chao MC, Abel S, Davis BM, Waldor MK. The Design and Analysis of Transposon-Insertion Sequencing Experiments. Nat Rev Microbiol. 2016 Feb;14(2):119–28.

193. Judson N, Mekalanos JJ. Transposon-based approaches to identify essential bacterial genes. Trends in Microbiology. 2000 Nov 1;8(11):521–6.

194. Lampe DJ, Akerley BJ, Rubin EJ, Mekalanos JJ, Robertson HM. Hyperactive transposase mutants of the Himar1 mariner transposon. PNAS. 1999 Sep 28;96(20):11428–33.

195. Stewart PE, Hoff J, Fischer E, Krum JG, Rosa PA. Genome-Wide Transposon Mutagenesis of Borrelia burgdorferi for Identification of Phenotypic Mutants. Appl Environ Microbiol. 2004 Oct;70(10):5973–9.

196. Botkin DJ, Abbott AN, Stewart PE, Rosa PA, Kawabata H, Watanabe H, et al. Identification of Potential Virulence Determinants by Himar1 Transposition of Infectious Borrelia burgdorferi B31. Infect Immun. 2006 Dec;74(12):6690–9.

197. Morozova OV, Dubytska LP, Ivanova LB, Moreno CX, Bryksin AV, Sartakova ML, et al. Genetic and physiological characterization of 23S rRNA and ftsJ mutants of Borrelia burgdorferi isolated by mariner transposition. Gene. 2005 Aug 29;357(1):63–72.

198. Troy EB, Lin T, Gao L, Lazinski DW, Camilli A, Norris SJ, et al. Understanding Barriers to Borrelia burgdorferi Dissemination during Infection Using Massively Parallel Sequencing. Infection and Immunity. 2013 Jul 1;81(7):2347–57.

199. van Opijnen T, Bodi KL, Camilli A. Tn-seq; high-throughput parallel sequencing for fitness and genetic interaction studies in microorganisms. Nat Methods. 2009 Oct;6(10):767–72.

200. Troy EB, Lin T, Gao L, Lazinski DW, Lundt M, Camilli A, et al. Global Tn-seq Analysis of Carbohydrate Utilization and Vertebrate Infectivity of Borrelia burgdorferi. Mol Microbiol. 2016 Sep;101(6):1003–23.

201. Ramsey ME, Hyde JA, Medina-Perez DN, Lin T, Gao L, Lundt ME, et al. A high-throughput genetic screen identifies previously uncharacterized Borrelia burgdorferi genes important for resistance against reactive oxygen and nitrogen species. PLOS Pathogens. 2017 Feb 17;13(2):e1006225.

202. Phelan JP, Kern A, Ramsey ME, Lundt ME, Sharma B, Lin T, et al. Genome-wide screen identifies novel genes required for Borrelia burgdorferi survival in its Ixodes tick vector. PLoS Pathogens. 2019 May 14;15(5):1–27.

203. Ahmed W, Hafeez MA, Mahmood S. Identification and functional characterization of bacterial small non-coding RNAs and their target: A review. Gene Reports. 2018 Mar 1;10:167–76.

204. Wager B, Shaw DK, Groshong AM, Blevins JS, Skare JT. BB0744 Affects Tissue Tropism and Spatial Distribution of Borrelia burgdorferi. Infect Immun. 2015 Sep;83(9):3693–703.

205. Hyde JA, Shaw DK, Smith R, Trzeciakowski JP, Skare JT. The BosR regulatory protein of Borrelia burgdorferi interfaces with the RpoS regulatory pathway and modulates both the oxidative stress response and pathogenic properties of the Lyme disease spirochete. Mol Microbiol. 2009 Dec;74(6):1344–55.

206. Frank KL, Bundle SF, Kresge ME, Eggers CH, Samuels DS. aadA Confers Streptomycin Resistance in Borrelia burgdorferi. Journal of Bacteriology. 2003 Nov 15;185(22):6723–7.

207. Goodhead I, Darby AC. Taking the pseudo out of pseudogenes. Current Opinion in Microbiology. 2015 Feb 1;23:102–9.

208. Williams DL, Slayden RA, Amin A, Martinez AN, Pittman TL, Mira A, et al. Implications of high level pseudogene transcription in Mycobacterium leprae. BMC Genomics. 2009 Aug 25;10(1):397.

209. Kawabata H, Norris SJ, Watanabe H. BBE02 Disruption Mutants of Borrelia burgdorferi B31 Have a Highly Transformable, Infectious Phenotype. Infect Immun. 2004 Dec;72(12):7147–54.

210. Jacobs MB, Norris SJ, Phillippi-Falkenstein KM, Philipp MT. Infectivity of the Highly Transformable BBE02− lp56− Mutant of Borrelia burgdorferi, the Lyme Disease Spirochete, via Ticks. Infection and Immunity. 2006 Jun 1;74(6):3678–81.

211. Dulebohn DP, Bestor A, Rego ROM, Stewart PE, Rosa PA. Borrelia burgdorferi Linear Plasmid 38 Is Dispensable for Completion of the Mouse-Tick Infectious Cycle ▿. Infect Immun. 2011 Sep;79(9):3510–7.

212. Casselli T, Crowley MA, Highland MA, Tourand Y, Bankhead T. A small intergenic region of lp17 is required for evasion of adaptive immunity and induction of pathology by the Lyme disease spirochete. Cellular Microbiology. 2019;21(7):e13029.

213. Site-directed mutagenesis by overlap extension using the polymerase chain reaction. Gene. 1989 Apr 15;77(1):51–9.

214. Horton RM, Hunt HD, Ho SN, Pullen JK, Pease LR. Engineering hybrid genes without the use of restriction enzymes: gene splicing by overlap extension. Gene. 1989 Apr 15;77(1):61–8.

215. Karna SLR, Sanjuan E, Esteve-Gassent MD, Miller CL, Maruskova M, Seshu J. CsrA Modulates Levels of Lipoproteins and Key Regulators of Gene Expression Critical for Pathogenic Mechanisms of Borrelia burgdorferi. Infection and Immunity. 2011 Feb 1;79(2):732–44.

216. Bugrysheva J, Dobrikova EY, Godfrey HP, Sartakova ML, Cabello FC. Modulation of Borrelia burgdorferi Stringent Response and Gene Expression during Extracellular Growth with Tick Cells. Infect Immun. 2002 Jun;70(6):3061–7.

217. Ouyang Z, Deka RK, Norgard MV. BosR (BB0647) controls the RpoN-RpoS regulatory pathway and virulence expression in Borrelia burgdorferi by a novel DNA-binding mechanism. Plos Pathogens. 2011 Feb 10;7(2):e1001272–e1001272.

218. Caimano MJ, Iyer R, Eggers CH, Gonzalez C, Morton EA, Gilbert MA, et al. Analysis of the RpoS regulon in Borrelia burgdorferi in response to mammalian host signals provides insight into RpoS function during the enzootic cycle. Mol Microbiol. 2007 Sep;65(5):1193–217.

219. Östberg Y, Bunikis I, Bergström S, Johansson J. The Etiological Agent of Lyme Disease, Borrelia burgdorferi, Appears To Contain Only a Few Small RNA Molecules. J Bacteriol. 2004 Dec 15;186(24):8472–7.

220. Papenfort K, Vogel J. Regulatory RNA in bacterial pathogens. Cell Host Microbe. 2010 Jul 22;8(1):116–27.

221. Pitman S, Cho KH. The Mechanisms of Virulence Regulation by Small Noncoding RNAs in Low GC Gram-Positive Pathogens. Int J Mol Sci. 2015 Dec 14;16(12):29797–814.

222. Michaux C, Verneuil N, Hartke A, Giard J-C. Physiological roles of small RNA molecules. Microbiology. 2014;160(6):1007–19.

223. Barik A, Das S. A comparative study of sequence- and structure-based features of small RNAs and other RNAs of bacteria. RNA Biol. 2017 Nov 3;1–9.

224. Melamed S, Peer A, Faigenbaum-Romm R, Gatt YE, Reiss N, Bar A, et al. Global Mapping of Small RNA-Target Interactions in Bacteria. Molecular Cell. 2016 Sep 1;63(5):884–97.

225. Zhi H, Weening EH, Barbu EM, Hyde JA, Höök M, Skare JT. The BBA33 lipoprotein binds collagen and impacts Borrelia burgdorferi pathogenesis. Mol Microbiol. 2015 Apr;96(1):68–83.

226. Labandeira-Rey M, Seshu J, Skare JT. The Absence of Linear Plasmid 25 or 28-1 of Borrelia burgdorferi Dramatically Alters the Kinetics of Experimental Infection via Distinct Mechanisms. Infection and Immunity. 2003 Aug 1;71(8):4608–13.

227. Labandeira-Rey M, Baker EA, Skare JT. VraA (BBI16) Protein of Borrelia burgdorferi Is a Surface-Exposed Antigen with a Repetitive Motif That Confers Partial Protection against Experimental Lyme Borreliosis. Infect Immun. 2001 Mar 1;69(3):1409–19.

228. Patton TG, Brandt KS, Nolder C, Clifton DR, Carroll JA, Gilmore RD. Borrelia burgdorferi bba66 Gene Inactivation Results in Attenuated Mouse Infection by Tick Transmission. Infection and Immunity. 2013 Jul 1;81(7):2488–98.

229. Gilmore RD, Howison RR, Schmit VL, Nowalk AJ, Clifton DR, Nolder C, et al. Temporal Expression Analysis of the Borrelia burgdorferi Paralogous Gene Family 54 Genes BBA64, BBA65, and BBA66 during Persistent Infection in Mice. Infection and Immunity. 2007 Jun 1;75(6):2753–64.

230. Lybecker MC, Samuels DS. Small RNAs of Borrelia burgdorferi: Characterizing Functional Regulators in a Sea of sRNAs. Yale J Biol Med. 2017 Jun 23;90(2):317–23.

231. Caldelari I, Chao Y, Romby P, Vogel J. RNA-Mediated Regulation in Pathogenic Bacteria. Cold Spring Harb Perspect Med. 2013 Sep;3(9):a010298.

232. Gilmore RD, Howison RR, Schmit VL, Carroll JA. Borrelia burgdorferi expression of the bba64, bba65, bba66, and bba73 genes in tissues during persistent infection in mice. Microb Pathog. 2008 Dec;45(5–6):355–60.

233. Liang FT, Nelson FK, Fikrig E. Molecular adaptation of Borrelia burgdorferi in the murine host. J Exp Med. 2002 Jul 15;196(2):275–80.

234. Stewart PE, Bestor A, Cullen JN, Rosa PA. A Tightly Regulated Surface Protein of Borrelia burgdorferi Is Not Essential to the Mouse-Tick Infectious Cycle. Infect Immun. 2008 May;76(5):1970–8.

235. Mulay VB, Caimano MJ, Iyer R, Dunham-Ems S, Liveris D, Petzke MM, et al. Borrelia burgdorferi bba74 Is Expressed Exclusively during Tick Feeding and Is Regulated by Both Arthropod- and Mammalian Host-Specific Signals. J Bacteriol. 2009 Apr;191(8):2783–94.

236. Ouyang Z, Narasimhan S, Neelakanta G, Kumar M, Pal U, Fikrig E, et al. Activation of the RpoN-RpoS regulatory pathway during the enzootic life cycle of Borrelia burgdorferi. BMC Microbiology. 2012;12:44.

237. Williams SK, Weiner ZP, Gilmore RD. Human neuroglial cells internalize Borrelia burgdorferi by coiling phagocytosis mediated by Daam1. PLOS ONE. 2018 May 10;13(5):e0197413.

238. Liu W, Sato A, Khadka D, Bharti R, Diaz H, Runnels LW, et al. Mechanism of activation of the Formin protein Daam1. PNAS. 2008 Jan 8;105(1):210–5.

239. Hoffmann A-K, Naj X, Linder S. Daam1 is a regulator of filopodia formation and phagocytic uptake of Borrelia burgdorferi by primary human macrophages. The FASEB Journal. 2014 Apr 2;28(7):3075–89.

240. Liu T, Zhang K, Xu S, Wang Z, Fu H, Tian B, et al. Detecting RNA-RNA interactions in E. coli using a modified CLASH method. BMC Genomics. 2017 May 3;18(1):343.

241. Kudla G, Granneman S, Hahn D, Beggs JD, Tollervey D. Cross-linking, ligation, and sequencing of hybrids reveals RNA–RNA interactions in yeast. PNAS. 2011 Jun 14;108(24):10010–5.

242. Han K, Tjaden B, Lory S. GRIL-seq provides a method for identifying direct targets of bacterial small regulatory RNA by *in vivo* proximity ligation. Nature Microbiology. 2016 Dec 22;2(3):nmicrobiol2016239.

243. Ternan N. Small regulatory RNA molecules in bacteria. 2013;8.

244. Elias AF, Bono JL, Kupko JJ, Stewart PE, Krum JG, Rosa PA. New antibiotic resistance cassettes suitable for genetic studies in Borrelia burgdorferi. J Mol Microbiol Biotechnol. 2003;6(1):29–40.

245. Liveris D, Wang G, Girao G, Byrne DW, Nowakowski J, McKenna D, et al. Quantitative Detection of Borrelia burgdorferi in 2-Millimeter Skin Samples of Erythema Migrans Lesions: Correlation of Results with Clinical and Laboratory Findings. J Clin Microbiol. 2002 Apr;40(4):1249–53.

246. Pal U, Wang P, Bao F, Yang X, Samanta S, Schoen R, et al. Borrelia burgdorferi basic membrane proteins A and B participate in the genesis of Lyme arthritis. Journal of Experimental Medicine. 2008 Jan 21;205(1):133–41.

247. Tokarz R, Anderton JM, Katona LI, Benach JL. Combined effects of blood and temperature shift on Borrelia burgdorferi gene expression as determined by whole genome DNA array. Infect Immun. 2004 Sep;72(9):5419–32.

248. Lybecker M, Zimmermann B, Bilusic I, Tukhtubaeva N, Schroeder R. The double-stranded transcriptome of Escherichia coli. PNAS. 2014 Feb 25;111(8):3134–9.

249. Seshu J, Boylan JA, Hyde JA, Swingle KL, Gherardini FC, Skare JT. A conservative amino acid change alters the function of BosR, the redox regulator of Borrelia burgdorferi. Molecular Microbiology. 2004;54(5):1352–63.

250. Busch A, Richter AS, Backofen R. IntaRNA: efficient prediction of bacterial sRNA targets incorporating target site accessibility and seed regions. Bioinformatics. 2008 Dec 15;24(24):2849–56.

251. Papenfort K, Vanderpool CK. Target activation by regulatory RNAs in bacteria. FEMS Microbiol Rev. 2015 May;39(3):362–78.

252. The role of RNases in the regulation of small RNAs. Current Opinion in Microbiology. 2014 Apr 1;18:105–15.

253. Pappesch R, Warnke P, Mikkat S, Normann J, Wisniewska-Kucper A, Huschka F, et al. The Regulatory Small RNA MarS Supports Virulence of Streptococcus pyogenes. Sci Rep. 2017 Sep 25;7(1):1–15.

254. Montgomery RR, Nathanson MH, Malawista SE. The fate of Borrelia burgdorferi, the agent for Lyme disease, in mouse macrophages. Destruction, survival, recovery. The Journal of Immunology. 1993 Feb 1;150(3):909–15.

255. Montgomery RR, Booth CJ, Wang X, Blaho VA, Malawista SE, Brown CR. Recruitment of Macrophages and Polymorphonuclear Leukocytes in Lyme Carditis. Infection and Immunity. 2007 Feb 1;75(2):613–20.